

# The spatial, temporal and structural composition of water quality of the Great Barrier Reef, and indicators of water quality and mapping risk

Glenn De'ath

Australian Institute of Marine Science, Townsville



**Australian Government**



**AUSTRALIAN INSTITUTE  
OF MARINE SCIENCE**



**Australian Government**

**Department of the Environment  
and Water Resources**

Funded through the Australian Government's  
Marine and Tropical Sciences Research Facility  
Project 1.1.5 Great Barrier Reef data synthesis and development of  
the Great Barrier Reef component of the Integrated Report Card

© Australian Institute of Marine Science

This report should be cited as:

De'ath, G. (2007) *The spatial, temporal and structural composition of water quality of the Great Barrier Reef, and indicators of water quality and mapping risk*. Unpublished report to the Marine and Tropical Sciences Research Facility. Reef and Rainforest Research Centre Limited, Cairns (71pp.).

Made available online by the Reef and Rainforest Research Centre Limited for the Australian Government's Marine and Tropical Sciences Research Facility.

The Marine and Tropical Sciences Research Facility (MTSRF) is part of the Australian Government's Commonwealth Environment Research Facilities programme. The MTSRF is represented in North Queensland by the Reef and Rainforest Research Centre Limited (RRRC). The aim of the MTSRF is to ensure the health of North Queensland's public environmental assets – particularly the Great Barrier Reef and its catchments, tropical rainforests including the Wet Tropics World Heritage Area, and the Torres Strait – through the generation and transfer of world class research and knowledge sharing.

This publication is copyright. The Copyright Act 1968 permits fair dealing for study, research, information or educational purposes subject to inclusion of a sufficient acknowledgement of the source.

The views and opinions expressed in this publication are those of the authors and do not necessarily reflect those of the Australian Government or the Minister for the Environment and Water Resources.

While reasonable effort has been made to ensure that the contents of this publication are factually correct, the Commonwealth does not accept responsibility for the accuracy or completeness of the contents, and shall not be liable for any loss or damage that may be occasioned directly or indirectly through the use of, or reliance on, the contents of this publication.

This report is available for download from the Reef and Rainforest Research Centre Limited website:  
[http://www.rrrc.org.au/mtsr/theme\\_1/project\\_1\\_1\\_5.html](http://www.rrrc.org.au/mtsr/theme_1/project_1_1_5.html)



May 2007

# Contents

List of Figures.....	ii
List of Tables.....	iv
Acknowledgements.....	iv
<b>Executive Summary.....</b>	<b>5</b>
Analyses of Water Quality on the Great Barrier Reef.....	5
Indicators and Mapping Risk.....	5
Risk Assessment and Management of the Great Barrier Reef.....	6
<b>Introduction.....</b>	<b>9</b>
<b>The Data Sets.....</b>	<b>9</b>
<b>Statistical Modeling.....</b>	<b>9</b>
<b>Data Analysis.....</b>	<b>10</b>
Lagoon Water Quality.....	10
Long-term Chlorophyll.....	13
Secchi Depth.....	13
<b>Results.....</b>	<b>16</b>
Lagoon Water Quality.....	16
Chlorophyll and Phaeophytin Long-Term Monitoring Data.....	27
The Structure of Water Quality Parameters.....	33
Indicators and Mapping Risk.....	38
Risk Assessment and Management of the Great Barrier Reef.....	43
Summary.....	50
<b>References.....</b>	<b>52</b>
<b>Appendix One.....</b>	<b>53</b>
<b>Appendix Two.....</b>	<b>57</b>
Spatial distributions of the WQ Parameters.....	57

## List of Figures

<b>Figure ES.1.</b> An example of risk maps with associated uncertainty.....	8
<b>Figure 1.</b> Locations of sampling 4067 sites for the lagoon water quality data, 97 sites for the chlorophyll long-term data and 2058 secchi sites .....	14
<b>Figure 2.</b> Distribution of lagoon sites with latitude and relative distance across the reef.....	15
<b>Figure 3.</b> Boxplots showing concentrations of water quality parameters on the log base 2 scale .....	15
<b>Figure 4.</b> Estimated spatial trends of chlorophyll, phaeophytin and nitrite .....	19
<b>Figure 5.</b> Estimated spatial trends of nitrate, ammonia and total dissolved nitrogen.....	20
<b>Figure 6.</b> Estimated spatial trends of particulate nitrogen, dissolved inorganic phosphorous and total dissolved phosphorous.....	21
<b>Figure 7.</b> Estimated spatial trends of particulate phosphorous, silicate and suspended solids .....	22
<b>Figure 8.</b> Partial effects of relative distance across the reef (0 = Coast; 1 = Edge of Outer Reef) on the 12 water quality parameters together with approximate 95% confidence intervals .....	23
<b>Figure 9.</b> Partial effects of relative distance along the reef (0 = South; 1 = North) on the 12 water quality parameters together with approximate 95% confidence intervals .....	24
<b>Figure 10.</b> Partial effects plots of months (1=Jan, 2=Feb, etc) for the 12 water quality parameters together with approximate 95% confidence intervals.....	25
<b>Figure 11.</b> Partial effects plots of years for the 12 water quality parameters together with approximate 95% confidence intervals.....	26
<b>Figure 12.</b> Estimated spatial patterns of chlorophyll and phaeophytin from the long-term monitoring.....	29
<b>Figure 13.</b> Partial effects plots of relative distance across the reef (0 = Coast; 1 = Edge of Outer Reef) on chlorophyll and phaeophytin from long-term monitoring together with approximate 95% confidence intervals.....	30
<b>Figure 14.</b> Partial effects plots of relative distance along the reef (0 = South; 1 = North) on chlorophyll and phaeophytin from long-term monitoring together with approximate 95% confidence intervals .....	30
<b>Figure 15.</b> Partial effects plots of months (1=Jan, 2=Feb, etc) on chlorophyll and phaeophytin from long-term monitoring together with approximate 95% confidence intervals .....	31
<b>Figure 16.</b> Partial effects plots of years on chlorophyll and phaeophytin from long-term monitoring together with approximate 95% confidence intervals .....	31
<b>Figure 17.</b> Estimated spatial trends of secchi disk visibility for the northern and southern sections of the GBR.....	32
<b>Figure 18.</b> Principal components biplot of the 12 water quality variables .....	33
<b>Figure 19.</b> Cluster analysis of the 12 water quality variables .....	34
<b>Figure 20.</b> Redundancy analysis showing how structure of the WQ parameters varies with pre-post 1998, seasons, across and along .....	35
<b>Figure 21.</b> Generalised procrustes analysis of quality variables shown how the configurations vary with distance along and across the reef, and over time (months and years).....	36
<b>Figure 22.</b> Risk regions for three potential WQ indicators: the ZZ = the summed z-scores across all 12 WQ parameters.....	39
<b>Figure 23.</b> Risk regions for three potential WQ indicators.....	40
<b>Figure 24.</b> Estimated spatial trends of secchi disk visibility and pooled chlorophyll data .....	41
<b>Figure 25.</b> An example of risk maps with associated uncertainty.....	42

**Figure 26.** Left: the zoning of the GBRWHA. Centre: the risk map for water clarity (secchi). Right: The zones of the GBRWHA assigned to high, moderate and low risk from the risk map .....45

**Figure 27.** Enlargement of Figure 26 showing finer detail of zonings, reef risk map, and assignment of zones to high, moderate and low risk categories.....46

**Figure 28.** Outline of Marine National Park (green), Habitat Protection (dark blue) and General Use (light blue) zones .....47

**Figure 29.** Enlarged version of Figure 28 showing inshore Marine National Park (green), Habitat Protection (dark blue) and General Use (light blue) zones.....48

**Figure 30.** Risk for combined chlorophyll and water clarity (secchi) data .....49

**Figure A1.1.** Demonstration of how a rescaling of one axis relative to the other can change the fitted surface and the degree of model fit (e.g. R2).....53

**Figure A.1.2.** Estimated spatial trends of chlorophyll based on across-along (A-A left) coordinates and latitude-longitude (L-L right).....54

**Figure A.1.3.** Estimated spatial trends of suspended solids based on across-along (A-A left) coordinates and latitude-longitude (L-L right).....55

**Figure A2.1.** The three panels show (left to right): (1) the distribution of sites where chlorophyll was sampled. The dot sizes are proportional to the relative values of chlorophyll, (2) the spatially smoothed trend adjusted for temporal (month and year) effects, and (3) the precision (SE) of the smoothed surface .....58

**Figure A2.2.** The three panels show (left to right): (1) the distribution of sites where phaeophytin was sampled. The dot sizes are proportional to the relative observed values, (2) the spatially smoothed trend adjusted for temporal (month and year) effects, and (3) the precision (SE) of the smoothed surface .....59

**Figure A2.3.** The three panels show (left to right): (1) the distribution of sites where nitrite was sampled. The dot sizes are proportional to the relative observed values, (2) the spatially smoothed trend adjusted for temporal (month and year) effects, and (3) the precision (SE) of the smoothed surface .....60

**Figure A2.4.** The three panels show (left to right): (1) the distribution of sites where nitrate was sampled. The dot sizes are proportional to the relative observed values, (2) the spatially smoothed trend adjusted for temporal (month and year) effects, and (3) the precision (SE) of the smoothed surface .....61

**Figure A2.5.** The three panels show (left to right): (1) the distribution of sites where ammonia was sampled. The dot sizes are proportional to the relative observed values, (2) the spatially smoothed trend adjusted for temporal (month and year) effects, and (3) the precision (SE) of the smoothed surface .....62

**Figure A2.6.** The three panels show (left to right): (1) the distribution of sites where total dissolved nitrogen was sampled. The dot sizes are proportional to the relative observed values, (2) the spatially smoothed trend adjusted for temporal (month and year) effects, and (3) the precision (SE) of the smoothed surface.....63

**Figure A2.7.** The three panels show (left to right): (1) the distribution of sites where particulate nitrate was sampled. The dot sizes are proportional to the relative observed values, (2) the spatially smoothed trend adjusted for temporal (month and year) effects, and (3) the precision (SE) of the smoothed surface .....64

**Figure A2.8.** The three panels show (left to right): (1) the distribution of sites where dissolve inorganic phosphorous was sampled. The dot sizes are proportional to the relative observed values, (2) the spatially smoothed trend adjusted for temporal (month and year) effects, and (3) the precision (SE) of the smoothed surface .....65

**Figure A2.9.** The three panels show (left to right): (1) the distribution of sites where total dissolved phosphorous was sampled. The dot sizes are proportional to the relative observed values, (2) the spatially smoothed trend adjusted for temporal (month and year) effects, and (3) the precision (SE) of the smoothed surface .....66

**Figure A2.10.** The three panels show (left to right): (1) the distribution of sites where particulate phosphorous was sampled. The dot sizes are proportional to the relative observed values, (2) the spatially smoothed trend adjusted for temporal (month and year) effects, and (3) the precision (SE) of the smoothed surface .....67

**Figure A2.11.** The three panels show (left to right): (1) the distribution of sites where silicate was sampled. The dot sizes are proportional to the relative observed values, (2) the spatially smoothed trend adjusted for temporal (month and year) effects, and (3) the precision (SE) of the smoothed surface .....68

**Figure A2.12.** The three panels show (left to right): (1) the distribution of sites where suspended solids was sampled. The dot sizes are proportional to the relative observed values, (2) the spatially smoothed trend adjusted for temporal (month and year) effects, and (3) the precision (SE) of the smoothed surface .....69

## List of Tables

**Table 1.** The numbers of depth-averaged data for each WQ parameter and the number of zero values replaced by the estimated minimum detectable level .....10

**Table 2.** Summary of exploratory analyses of variance for the 12 WQ parameters with spatial, temporal and trip variables as explanatory variables .....16

**Table 3.** Comparison of across-along and latitude-longitude as spatial explanatory variables for 12 WQ parameters .....18

**Table 4.** Comparison of the percentage prediction error for the full spatial-temporal model S+M+Y (S =across-along, M=months, Y=years) and reduced models S+M and S .....18

**Table 5.** Summary of exploratory analyses of variance for chlorophyll and phaeophytin with spatial, temporal and trip variables as explanatory variables .....27

**Table 6.** Comparison of across-along and latitude-longitude as spatial explanatory variables chlorophyll and phaeophytin .....28

**Table 7.** Comparison of the percentage prediction error for the full spatial-temporal model S+M+Y (S =across-along, M=months, Y=years) and reduced models S+M and S .....28

**Table 8.** Generalised Procrustes analyses of the 12 WQ parameter lagoon data ..... 37

## Acknowledgements

Contributions to this work including the Australian Institute of Marine Science through the extensive knowledge of its scientists and its extensive data sets, Miles Furnas and co-workers (AIMS) for the water quality data, Rob Coles (DPIF) and Katharina Fabricius and co-workers (AIMS) for secchi data and Dr Bill Venables (CSIRO) for his statistical knowledge and enthusiasm. This research was conducted with the support of funding from the Australian Government's Marine and Tropical Sciences Research Facility.

## Executive Summary

This work comprises two components. First, three major data sets from broadscale water quality (WQ) sampling programs on the Great Barrier Reef (GBR) are analysed and spatial patterns and temporal change are presented and discussed. Second, the use of these data as potential indicators of WQ is explored. Five potential indicators are calculated and mapped. Problems of estimating risk and relative risk are discussed, an exemplary risk scale is proposed, and risk regions are mapped for the whole of the GBR. Uncertainty levels of risk are estimated and displayed jointly with risk on single maps. These maps and the methods on which they are based represent a useful prototype for future risk mapping programs.

### *Analyses of Water Quality on the Great Barrier Reef*

The three data sets analysed were: (1) lagoon water quality data comprising measures of 12 WQ parameters (1976-2006), (2) long-term chlorophyll monitoring data (1992-2006), and (3) a composite data set on water clarity based on secchi disks.

The principal findings were:

- Spatial-temporal models are poor predictors of WQ parameters. Between 0% and 40% of the variation in WQ parameters is typically predictable, with chlorophyll and suspended solids being well predicted and derivatives of nitrogen being very poorly predicted.
- Concentrations of all WQ parameters decrease by 50-80% from the coast to a distance 15-20% across the Reef. From 20% across the Reef to the outer Reef they typically decrease by an additional 0-20%. This inner coastal strip should be the focus of future monitoring with fixed sites and automated logging of a few selected parameters; perhaps water clarity and chlorophyll. This cross-shelf pattern of strong decline in the near-shore varies along the coast for many WQ parameters, and is typically much steeper in the central third of the GBR and much flatter in the far north.
- Synchronised cyclical seasonal variation occurs for most of the WQ parameters. Nutrients typically peak in March-April and are 10-50% lower in August-September. This seasonal variation must be accounted for in sampling programs.
- Despite having collected extensive data on WQ for over 30 years for the 12 WQ parameters and 15 years for chlorophyll, we cannot make definitive statements about long-term trends in WQ on the GBR. For most of the dissolved WQ parameters the variation is such that further collection of such data should be highly questionable. The temporal trends are poorly estimated due to: (a) high variability of WQ between sampling trips and sampling locations, and (b) low precision and (likely) systematic bias of WQ measures.
- Water clarity is highly predictable spatially (~75%) and is very high compared to the WQ parameters analysed previously. This statistical property, together with its known links to biotic function and ease of measurement, suggest water clarity could be a very useful indicator of WQ, but additional work is needed to assess temporal variation.

### *Indicators and Mapping Risk*

Potential indicators of risk and exemplary risk maps based on values that determine *relative risk* at levels of “high”, “moderate” and “low” were developed. It is important to discriminate between *relative risk* and *absolute risk*; the former is relatively easy to predict compared to the latter. Few would argue that increased pollutants leads to increased risk, however specifying a level of exposure that leads to adverse effects is a considerable challenge for a system as complex as the GBR, and is unlikely to be achieved in other than a few restricted instances.

Five potential indicators of relative risk were developed together with measures of risk uncertainty. The measures included both individual and composite measures of WQ, and risk maps based on plausible values that determine high, moderate and low risk regions were generated and interpreted. Of the five indicators; three are derived from the multivariate lagoon WQ data, and of remaining two, one was based on chlorophyll data pooled across lagoon and long-term chlorophyll surveys, and the second was based on water clarity drawn from three data sources.

Regions of relative risk are mapped for the five indicators using the "60-30-10 rule". This rule is a tentative suggestion for defining levels of relative risk that may be suitable for ecosystem management in the absence of known critical exposure levels. Predicted values lower than the 60<sup>th</sup> percentile of the *observed* data are declared "low risk", the 60<sup>th</sup>ile-90<sup>th</sup>ile are "moderate", and >90<sup>th</sup>ile are high risk. Having a small "high risk" band is attractive since (a) this focuses attention exclusively on the highest risk areas, and (b) the relatively small size may make risk-reduction through action more feasible. For simplicity and ease of interpretation, red, orange and green coloring is used to indicate high, moderate and low risk regions respectively. Additionally the certainty of the predictions are estimated and represented by colour saturation with strong shades indicating low uncertainty, and pale shades indicating high uncertainty. Although classification of relative risk into these three categories can be a useful summary for non-technical presentation, it does constitute a substantial loss of information, and is not recommended for all purposes. In particular, small areas of extreme risk may be missed, and for management to be effective we require systems that can quantitatively combine and display multiple sources of risk at high spatial and temporal resolution, for example through contour and trend plots.

The risk maps for the three indicators based on the lagoon WQ data are very similar. The most striking feature is a narrow coastal band of high risk that extends from just south of the Whitsunday Islands to Port Douglas in the North. The risk maps for the composite chlorophyll data and the water clarity also show strong patterns (Figure ES.1). The chlorophyll risk map shows strong similarities to the first three indicators in that the narrow coastal band of high risk also extends from just south of the Whitsunday Islands to Port Douglas in the North, but it also shows high, though more uncertain risk, in the Pompeys. The water clarity maps again show the coastal high risk strip, together with a moderate risk strip, but the high risk extends further north and south. In the case of the northern extension this can be explained as high sediments discharging from far northern rivers but containing lower level nutrients than the more southerly rivers.

This initial exercise in mapping risk shows promise and the work can be further developed in many ways. There are many issues related to validation against field and laboratory experiments, temporal and spatial scales of the effectiveness, cost and ease of implementation, and new technologies, such as automated sensors and remote sensing that can more efficiently gather the data necessary to assess risk. Additional work is proceeding in order to identify indicators that can be used in the field, based on additional empirical analyses. A major focus of the additional work is validation in the sense that biotic measures can be shown to correlate to the indicator values.

## ***Risk Assessment and Management of the Great Barrier Reef***

The Marine Park Rezoning Plan is fundamental to GBRWHA management. The mosaic of individual zones determines access and activities for the whole of the GBRWHA. Risk maps can provide crucial information necessary for effective management of the GBRWHA, and various ways of using risk information as a management tool are investigated in this section.

Several issues will require collaborative efforts between science and management in order to effectively use risk information (such as the WQ predictions and maps in this Report) in order to better manage the GBRWHA.

Some central issues are:

1. Geographical scale is the crucial factor, with sizes of zones varying three orders of magnitude.
2. Classifying individual zones can be misleading due to their highly variable sizes.
3. Interactive visual quantitative methods, based on best science, need to be developed in conjunction with management agencies.

An example of combining risk maps based on scientific knowledge using chlorophyll and water clarity data is presented. However, this simple method used ignores the the possibilities of establishing functional relationships between pollutants and biotic responses. By establishing such environmental-biotic relationships, the effectiveness of risk maps to management could be greatly improved. For example, it would provide us with the possibility of predicting biotic responses to environmental change. Such work is in progress.

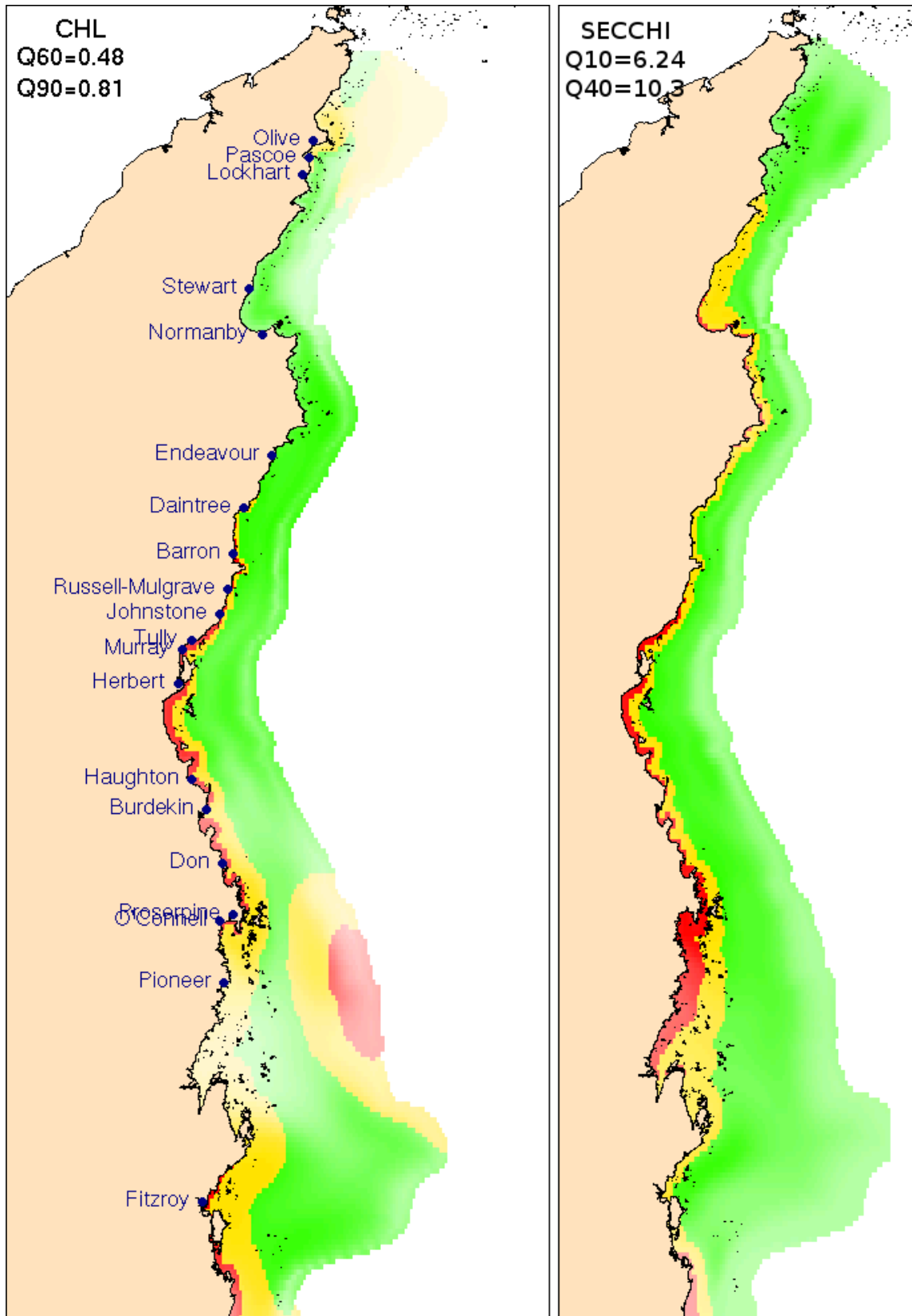


**Figure ES.1.** An example of risk maps with associated uncertainty. The left panel show the risk map for chlorophyll, and the right panel the risk for water clarity as measured by secchi disk. The red, orange and green regions indicate high, moderate and low risk regions formed by the 90% and 60th percentile breaks respectively. The strong-pale shades indicate regions of low-high uncertainty of the risk respectively.

## Introduction

This work comprises two components. First, analyses of three major data sets from broadscale water quality (WQ) sampling programs on the Great Barrier Reef (GBR) are presented. The analyses show spatial patterns and temporal change for both single WQ parameters and structural WQ (i.e. multivariate patterns and change). One of these data sets, the lagoon water quality, comprising over 30 years of data, has not been previously analysed. Findings are synthesised across the data sets, discussed, and observations on the efficiency and effectiveness of sampling strategies are discussed.

Second, the use of these data as potential indicators is explored. Five potential indicators are calculated and mapped. Of the five, two are derived from single WQ parameters, namely chlorophyll and water clarity based on secchi disk visibility, and the remaining three are composite indicators based on multivariate structures extracted from the lagoon data. An exemplary risk scale is proposed and risk regions are mapped for the whole of the GBR. Uncertainty levels are estimated for all points on the maps and joint displays of risk and the uncertainty of that risk are displayed. These single maps represent a useful prototype for future risk mapping programs.

## The Data Sets

Three data sets were used for this Report:

1. Lagoon water quality (WQ) data comprising 12 measures of WQ, physical conditions and location and collected by AIMS (Miles Furnas and co-workers) from 1976-2006.
2. Long-term chlorophyll monitoring data collected by GBRMPA and AIMS over the period 1992-2006.
3. A composite data set on water clarity based on secchi disks. These data are mainly composed of DPI seagrass monitoring data (Rob Coles), but also include contributions from AIMS (Katharina Fabricius and Miles Furnas).

## Statistical Modeling

The data were analysed in three ways:

1. Univariate analyses were used to model each of the 12 WQ parameters in the lagoon data, and chlorophyll and phaeophytin from the long-term chlorophyll data, as functions of space and time. Secchi depth was analysed for spatial patterns only. Generalised mixed models (GLMMs: Breslow and Clayton 1993, Bates and Saikat 2004) were used to analyse for all univariate analyses.
2. Multivariate analyses that modeled the interrelationships between the 12 WQ parameters of the lagoon data to determine the structure of WQ and how it varied with space and time. Principal components analysis, generalised procrustes analysis (Gower 1976, Goodall 1990) and cluster analysis were used for these tasks.
3. From the univariate and multivariate analyses a set of candidate indicators of “water quality risk” were identified. These were analysed spatially and categorised into levels of high, moderate and low risk. Spatial maps showing the risk levels together with the uncertainty of the estimated risk were then produced.

In all analyses the spatial component of the models was based on relative distance across and along the Reef rather than the usual latitude-longitude. Relative distance across and along the Reef takes advantage of the natural boundaries of the GBR that affect many of the bio-physical processes of the Reef, and thus one might expect that many spatial distributions

of observed data would be best explained (and best predicted) in this coordinate system. This has been shown to be the case in numerous data analyses (unpublished data). The across-along coordinates are also particularly useful for graphical presentations of change and can be interpreted in more scientifically meaningful ways than latitude-longitude. Relative distance across and along the reef are also more informative in the case of models that do not include interactions between across and along, having a particularly simple interpretation, whereas the equivalent latitude-longitude interactions have no simple interpretation.

An additional consideration that can be introduced into the across-along spatial models is the relative scaling of across and along. The value of this meta-parameter can be selected to maximise the degree of fit or the predictive performance of the model. The relative scaling does, in many instances, reflect the relative rates of change in the in two principal directions.

A comparison of the across-along models with the usual latitude-longitude models based on predictive error was also made for the lagoon WQ data.

## Data Analysis

### *Lagoon Water Quality*

Data on 12 WQ parameters collected over 30 years on the Great Barrier Reef Lagoon were analysed individually for spatial and temporal patterns, and collectively to assess their multivariate structure and how that varied in space and time. The WQ parameters were chlorophyll (CHL), phaeophytin (PHA), nitrite (NO<sub>2</sub>), nitrate (NO<sub>3</sub>), ammonia (NH<sub>4</sub>), total dissolved nitrogen (TDN), particulate nitrogen (PN), dissolved inorganic phosphorous (DIP), total dissolved phosphorous (DOP), particulate phosphorous (PP), silicate (SI) and suspended solids (SS). For each WQ parameter between 10,221 and 19,327 samples were recorded at varying depths at 5561 sites (Figure 1). The data were depth averaged since additional depth information from CTD casts were not yet available. The number of samples forming the averages were used as weights in the statistical analyses. The depth-averaged data (n=5561) were inspected and exploratory analyses show a number of observations with value zero (Table 1). For each WQ parameter, these were replaced by half the the minimum non-zero value observed (an estimate of the minimum detectable level). The resulting data showed high variance with many extreme high and low values that is typical for WQ data. Plotting the data by year revealed seemingly abnormally high values of the nitrogen-based parameters from the years 1976-1987 with typical values >10 times typical values of the later years. Since many other variables had no data for this period, the data for all parameters was restricted to the period 1988 to 2006.

**Table 1.** The numbers of depth-averaged data for each WQ parameter and the number of zero values replaced by the estimated minimum detectable level.

	CHL	PHA	NO <sub>2</sub>	NO <sub>3</sub>	NH <sub>4</sub>	TDN	PN	DIP	TDP	PP	SI	SS
<b>N</b>	4924	4688	4680	5025	4311	3456	2402	4713	3326	2461	4538	3411
<b>N "0s"</b>	0	0	1222	637	162	0	2	276	9	0	36	7

These data are difficult to analyse for several reasons:

1. The sampling over space and time (months and years) was strongly unbalanced. This results in substantial information loss and makes it difficult to disentangle spatial and temporal effects, as well as effects on varying scales within space and time. It is even more difficult to assess interactions between spatial and temporal effects. In such situations we need to adjust each set of effects for all others, and are often limited to analyses comprising only main effects.
2. The Great Barrier Reef has a structure that challenges any spatial analysis – long, narrow with winding borders and a width that increases with distance from the equator. The boundaries of the coastline and the dramatic shift in conditions at the outer edge of the Reef require any analysis to take into account the likely effects of such an unusual structure. Water typically flows along the Reef and depth increases across the Reef. Also the reef structures typically lie along the Reef. Contrarily, latitude and longitude vary at  $\sim 45^\circ$  to the main reef structure and this spatial coordinate system is eminently unsuitable to capture the Reef's physical structure. An alternative, previously used in Fabricius & De'ath (2004) is to spatially model GBR processes in terms of relative distance across and along the Reef. Distance across is defined for each location as its distance to the coast divided by the sum of the distances to the coast and to the outer edge of the Reef. Similarly, distance along is defined as distance from the southern end of the Reef divided by the sum of the distances to the southern and northern ends of the Reef. The area of the Reef is thus mapped into a unit square. For many spatial analyses of Reef data the effects of across and along are independent (i.e. the model is additive in across and along) and this leads to a simple interpretation not possible with the latitude-longitude system. However, if the spatial model based on across-along is not additive in across and along (thin plate splines: Wood 2003), then this approach can be extended by optimising the scale of across relative to along (see Appendix One). In the data analyses of this Report, the comparison between the two spatial coordinate systems was made, and demonstrated that the across-along system gave better predictions and was more interpretable than latitude-longitude. Additional discussion and examples are shown in Appendix One.
3. There was substantial missing information (Table 1), and this is problematic. First, it is difficult to comment with certainty on differences in spatial and temporal patterns of the various WQ parameters, since any conclusions are based on different sets of explanatory data. These problems are magnified when we wish to simultaneously analyse the 12 WQ parameters to see how they co-vary with and jointly relate to space and time. For these data, reducing the data set to the cases with no missing values results in a substantial loss of cases; in this instance from 4067 to 1531. The alternative of first using imputation to estimate the missing data is impractical for these data given (1) the large proportion of missing cases, and (2) the weak relationships on which any imputation may be made.
4. The data observed on the WQ parameters have extremely skew distributions. The often-used approach of transforming to a more even distribution (e.g using logarithmic or power transformations) is useful for comparing patterns in the data, but leads to negatively biased estimates of effects (i.e. patterns and differences). In this instance we wish to obtain unbiased estimates since it is possible that data such as these may be used to inform the process of setting targets for the RWQPP. Generalised linear models (GLMs) can be used to overcome the bias and were used for the data analyses.
5. The spatial and temporal effects were non-linear and smooth terms were used in all models. The GLMs are thus replaced by generalised additive models (GAMs; Wood ) with smooth terms for both individual predictors but also for joint predictors such as across-along.

6. The data were collected in trips that were non-systematically allocated in space and time. The nature of WQ processes, and initial exploratory analyses suggested that this likely lead to substantial inter-trip variation that needs to be accounted for in the modelling process. This would usually be done by introducing additional random effects into the models, thus extending the GAM to a generalised additive mixed model (GAMM). However the non-systematic nature of the trips does detract from the quality of analyses since it introduces variation that inflates the variance of parameter estimates.
7. There are substantial numbers of outliers in the data. Reliable determination of outliers or down-weighting of such is difficult for such complex data sets. Given the complexities of the data encountered so far, the chosen technique was to fit a model, drop the cases with extreme residuals, and then refit the model to the reduced data.

## Univariate Analyses

The focus of this study was spatial patterns and, to a lesser degree, inter-annual change. The long term trends were seen to be of secondary importance since (1) the inter-annual spatial variation in site locations was difficult to control for, and (2) preliminary analyses suggested implausible magnitudes and patterns of temporal change for some parameters.

The data were sampled at several depths at each site. The number of samples was primarily, but not always dependent on the bottom-depth. Depth was not a factor of primary interest in these analysis and hence data were depth averaged for each site. This reduced the number of cases from 22298 to 5256, the latter representing individual sites. The data collection years ranged from 1976 to 2006, but the number of sites in the early years were relatively few and initial data QC checks suggested that the years up and including to 1987 should be discarded. This reduced the number of sites to 4067.

Generalised linear mixed models (GLMMs: Breslow and Clayton 1993, Bates Saikat 2004) were used to analyse each of the 12 WQ parameters. The explanatory variables were across, along, months and years each of which was treated as a numeric variable. Smooth terms were fitted using thin-plate splines for the spatial variables, a cyclic periodic smoother form months and a smooth term for years. Trip was included as a random effect and given the timing and duration of trips was confounded with the month-year interaction. No interaction terms, other than the spatial smooths, were considered due to (1) the primary focus was on spatial patterns, and (2) the difficulties due to the sampling structure.

The smoothness of the spatial and temporal terms was treated differently. For months and years the smoothness was fixed at 5-df and 3-df respectively, since the objective was to control for this variation and optimising the degree of smoothing was a secondary consideration. For spatial patterns however, the objective was to determine the spatial patterns as accurately as possible. For GLMMs, the degree of smoothing can be obtained by generalised cross-validation (Wood 2004), however this approach lead to implausibly complex spatial fits, seemingly due to a lack of independence that was not easily modeled. A more robust approach was therefore adopted, based on the prediction error of the candidate models. The prediction error (PE) of a model is defined as the sum of squared prediction errors divided by the sum of squared observations about the overall mean. It can also be expressed as a percentage (PE%) and can vary from 0% (perfect prediction) to >100% (no predictive capacity). The predictive capacity can be expressed as 100-PE% and is somewhat similar to  $R^2$  (a measure of variation *explained* by a model) that most readers will be more familiar with.

Estimating prediction error involved choosing a set of values for the smoothness of the spatial surfaces and fitting models using 5-fold cross-validation for each level of smoothness. The groups used for the cross-validation were based on trips and hence each trip was predicted from other trips. The smoothness corresponding to the minimum prediction error

(based on the leave-out samples) was selected for a final fitting of the model. Models with similar smooth effects were used to compare the effectiveness of the across-along and latitude-longitude coordinate systems, and also the across-along model with and without spatial interaction.

### **Multivariate Analyses**

For these data, only cases that have no missing values were used. This resulted in a substantial loss of cases, from 4067 to 1531, but imputation of missing values, or pairwise calculations, were not used due to the large fraction of missing data. The 1531 were deemed sufficient to extract meaningful multivariate structure. Principal components analyses were used to assess the correlational structure of the 12 WQ parameters (standardised) together with cluster analysis. The variation of the structure was explored using generalised procrustes analysis (Gower 1975, Goodall 1991).

### **Statistical Software**

All analyses were done using the R statistical software system (R Development Core Team 2007).

### ***Long-term Chlorophyll***

Additional data were available for chlorophyll and phaeophytin from long-term transect surveys. These surveys cover the period 1992-2006 and have been reported elsewhere (Brodie et al, 2007). These data were sampled at 97 sites within 9 broad transects along the GBR. The transects were visited within the period 1992-2006 though in recent years there has been more dropping of sites and addition of new sites. The data are well-balanced and have been cleaned and analysed on several previous occasions, and hence many of the problems associated with the lagoon WQ data were not present.

### **Analyses**

The analysis of these data in this Report differed from that of Brodie et al (2007) where transects were used as regions within which trends were explored. Instead, we followed the methods outlined above for the univariate lagoon analyses. The only difference was that sampling units that were visits (random effects) in the lagoon analyses, were replaced by sites in this analysis.

### ***Secchi Depth***

These data comprised 2058 secchi readings; 1371 from DPI seagrass surveys, 394 from the lagoon data and 293 from inshore surveys. The extensive and systematic coverage (Figure 1) makes them ideal to determine spatial patterns.

### **Analyses**

There are no higher-level sampling units in these data as was the case with the lagoon data and the chlorophyll long-term data, however one might expect spatial correlation between sites and this was investigated. The temporal data values were highly confounded with spatial locations, precluding investigations of the former. Addressing the issue of temporal change in water clarity should be a priority for future work.

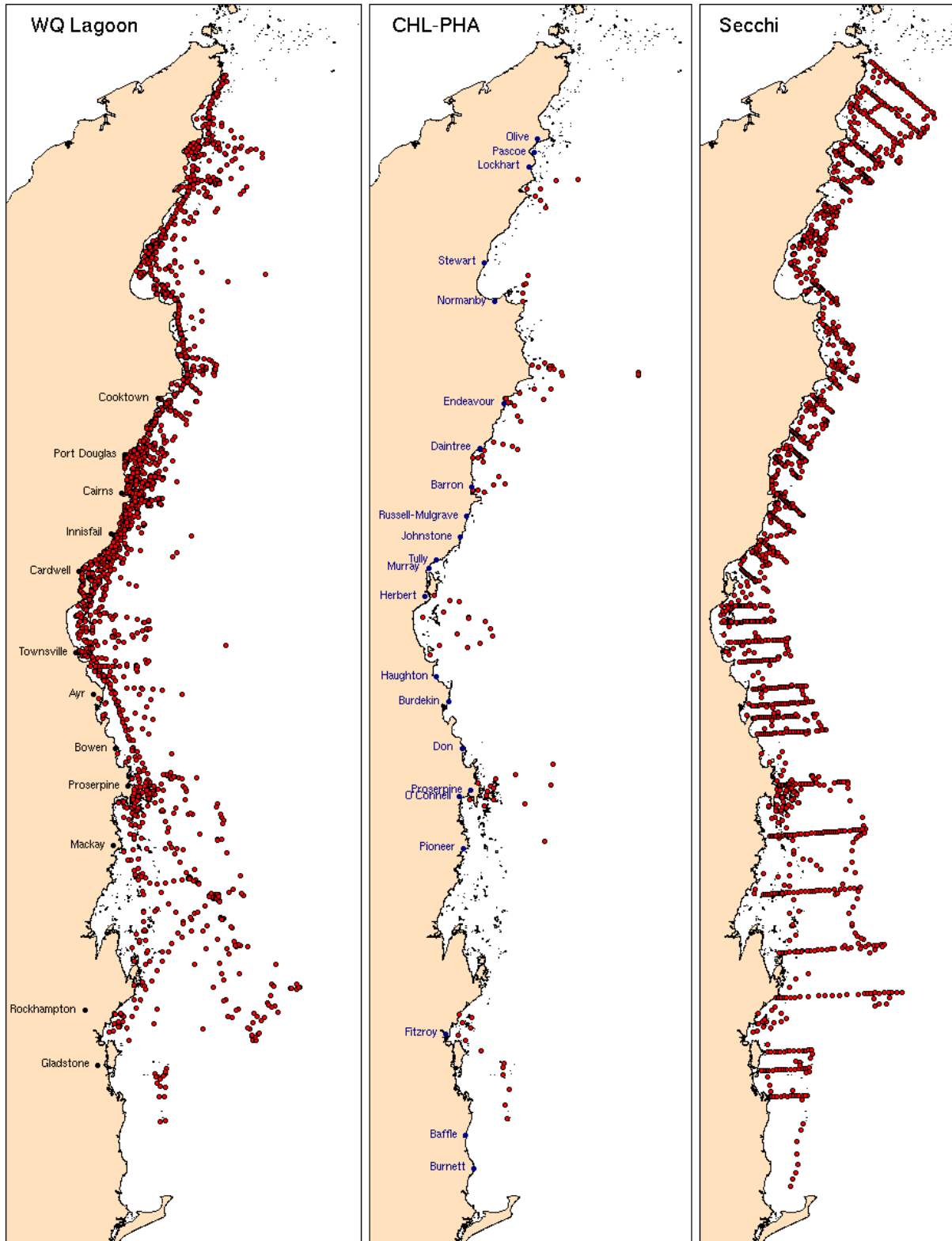


**Figure 1.** Locations of sampling 4067 sites for the lagoon water quality data, 97 sites for the chlorophyll long-term data and 2058 secchi sites. Coastal towns and rivers are shown in the first two graphics respectively.

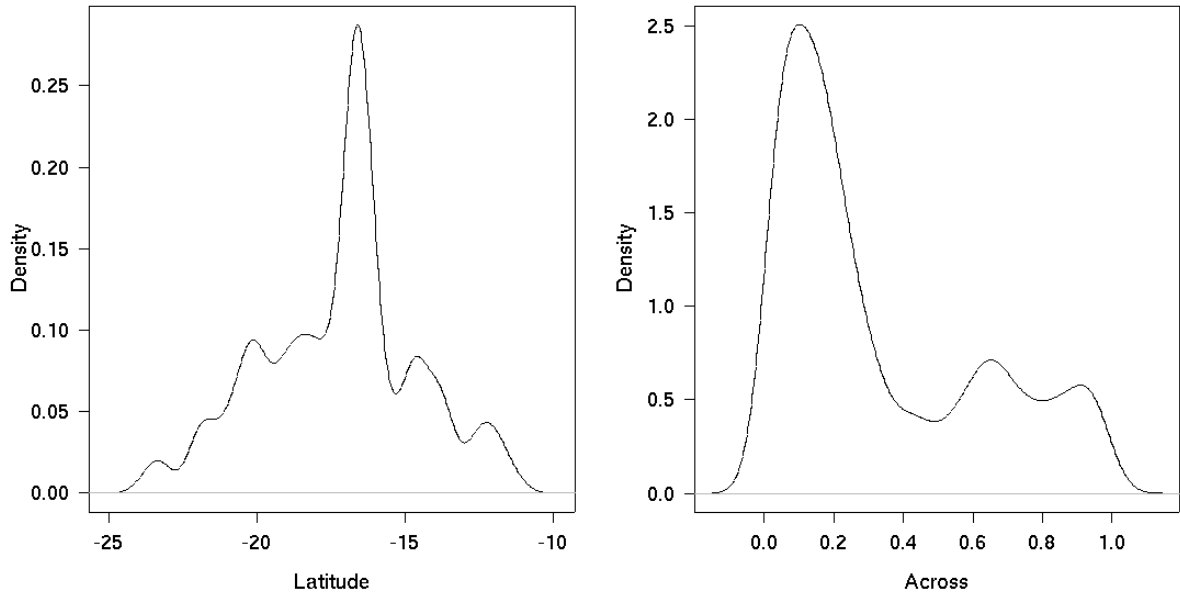


**Figure 2.** Distribution of lagoon sites with latitude and relative distance across the reef. The majority of sites lie within 14 to 17OS and less than 30% across the shelf.

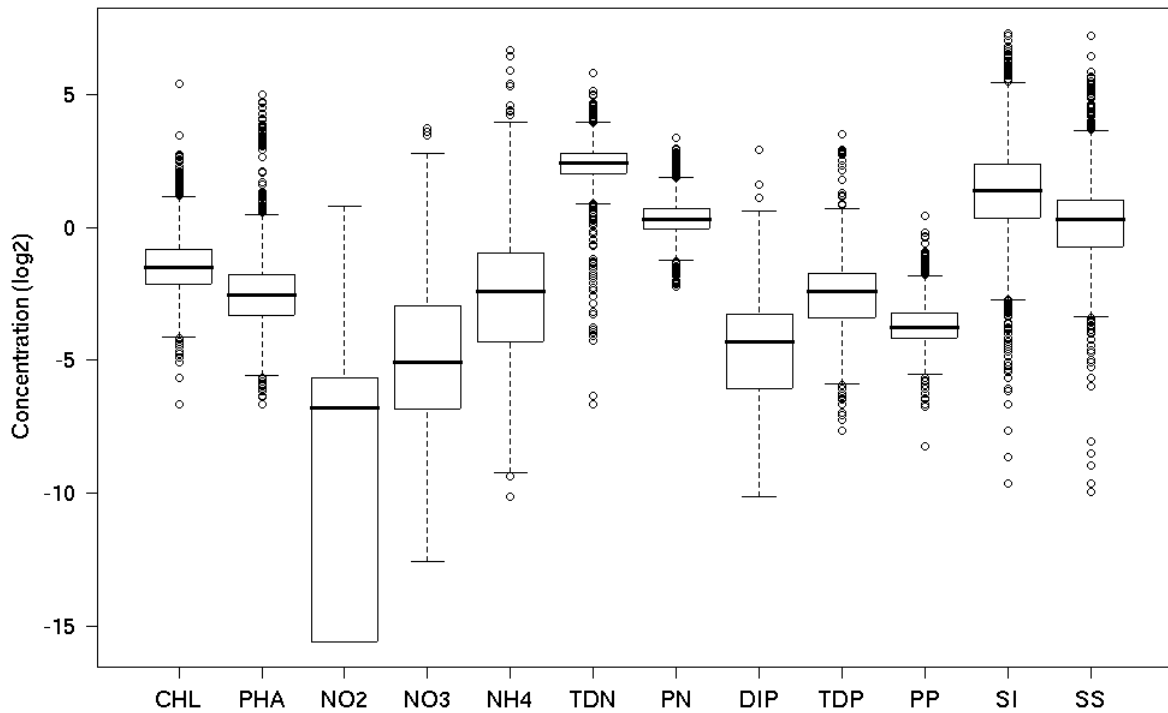


**Figure 3.** Boxplots showing concentrations of water quality parameters on the log base 2 scale.

## Results

### *Lagoon Water Quality*

An exploratory analysis of variance was used to obtain some simple approximations to the magnitudes and likely importance of sources of variation in the GLMM models subsequently used for inference. The results of this exploration (Table 2) show substantial variation due to trip; the F-ratio of trip mean sums of square (MSS) against residual sums of squares varied from 9-50, and trip accounted for 13-45% of all SS. Spatial and temporal variation was substantial, but was consistently higher for the “solid” WQ parameters (CHL, PHA, PN, PP, SS) than the “dissolved” parameters.

**Table 2.** Summary of exploratory analyses of variance for the 12 WQ parameters with spatial, temporal and trip variables as explanatory variables. Degrees of freedom for the sources of variation are shown in brackets.

WQ	F-ratios				% SS			
	Across (7)	Along (7)	Month (4)	Year (5)	Trip	Space-Time (23)	Trip	Error
CHL	118	73	113	122	16	35	19	46
PHA	93	56	65	126	17	29	23	49
NO2	2	13	34	81	28	10	37	53
NO3	22	16	28	93	17	13	26	61
NH4	13	56	87	174	50	19	45	36
TDN	23	31	37	61	22	15	31	53
PN	92	70	53	20	23	30	31	39
DIP	22	77	71	441	22	32	24	44
TDP	47	47	89	303	30	30	32	38
PP	118	12	34	41	9	31	16	53
SI	182	46	37	44	14	31	19	49
SS	448	34	17	118	12	48	13	39

### Results from the GLMM Models

The strategy for modelling the spatial-temporal effects of the lagoon data was as follows. First find the best spatial model whilst at the same time including the temporal effects. The spatial components considered were (1) smooth terms in across and along including interactions between them, (2) an smooth additive model in across and along (i.e. no interaction), and (3) smooth terms in latitude and longitude including interactions. All 2-dimensional terms were based on tensor-splines (Wood 2007) and all 1-dimensional terms used natural splines or, in the case of months cyclic splines so that the transition from December to January was continuous and smooth.

The results of fitting the GLMM models are shown in Tables 3-4 and Figures 4-12. Tables 3-4 show how well the models predict each of the 12 WQ parameters and how those

predictions depend of the individual spatial and temporal predictors. CHL, DIP, SI and SS are the best, but not well, predicted (PE < 70%), whereas PHA and NO<sub>2</sub> are the least well predicted (PE > 80%) together with NH<sub>4</sub> which is totally unpredictable (PE = 98.8%). The spatial interactions vary in strength from no interaction to moderate interactions that account for ~3% of prediction error. The latitude-longitude models had prediction error ~0-3% greater than across-along. Dropping years and months from the models lead increases in prediction error of ~0 – 15% and years were the greatest contribution of these two predictors.

The variation due to trips was high (Tables 2 and 4) and is one of the major factors for the relatively poor predictability of WQ parameters. Trip variation includes many factors, but primarily accounts for non-systematic changes (i.e. unaccounted variation) in the body of sampled water on the scales of weeks – months. Thus a large number of observations are likely to contain less information than fewer, but regularly placed, observations in space and time.

The spatial maps (Figures 4-7) vary considerably but typically show strong gradients (close isoclines) close to the coast in the central third of the GBR. For some regions of the GBR where data were sparse, the spatial patterns are estimated poorly, and maps with the precision of the estimated patterns are presented in Appendix 2. Although for several of the WQ parameters there were substantial spatial interactions (Table 3), for the other parameters, the averaged across and along effects can be informative (Figures 7-8). For all the WQ parameters there is an ~50% reduction in concentrations from the coast to ~20% across the shelf, In the central section of the GBR this reduction is considerably higher where there are spatial interactions (e.g. CHL, PP, PN and SI), and correspondingly lower in the far north and, for some, in the south. For some WQ parameters, patterns along the Reef vary considerably without any clear interpretation.

The temporal variation was decomposed into cyclic effects for months and trends across years (Figures 10-11). Nine of the 12 WQ parameters show strong cyclical effects that peak around March-April and trough around August-September. The reduction in amplitudes of the peaks varied from around 65% for NO<sub>2</sub> to 30% for PP and PN. The trends across years show some significant effects (e.g. CHL, NO<sub>3</sub>, DIP and TDP), but the patterns defy any obvious explanation. Long term drift and variation in sampling and analytical procedures cannot be discounted, and these apparent trends should not be over-interpreted.

**Table 3.** Comparison of across-along and latitude-longitude as spatial explanatory variables for 12 WQ parameters. The percentage prediction error (%) is shown for the spatial-temporal model including (from left to right in the table) across-along, across-along as an additive model and latitude-longitude, with the increase in prediction error relative to the across-along model is shown in parentheses.

WQ parameter	Prediction error (%)		
	Across-Along	Across-Along-Additive	Latitude-Longitude
CHL	67.8	70.2 (2.4)	70.3 (2.5)
PHA	81.4	83.1 (1.7)	82.3 (0.9)
NO2	85.4	85.9 (0.5)	85.2 (-0.2)
NO3	74.1	76.8 (2.7)	73.9 (-0.2)
NH4	77.4	79.4 (2.4)	78.3 (0.9)
TDN	98.8	98.7 (-0.1)	99.7 (0.9)
PN	74.1	76.1 (2.0)	76.9 (2.8)
DIP	56.0	57.9 (1.9)	57.4 (1.4)
TDP	70.8	70.8 (0.0)	73.2 (2.4)
PP	75.6	78.5 (2.9)	75.9 (0.3)
SI	60.8	63.8 (3.0)	62.9 (2.1)
SS	59.4	61.0 (1.6)	61.3 (1.9)

**Table 4.** Comparison of the percentage prediction error for the full spatial-temporal model S+M+Y (S =across-along, M=months, Y=years) and reduced models S+M and S. The increase in prediction error are also shown (from left to right in the table) by dropping year (-Y) and month (-M). The estimates of the variance components for trip and pure error are also shown.

WQ parameter	Prediction error (%)					Trip variance	Error variance
	S+M+Y	-Y	S+M	-M	S		
CHL	67.8	3.2	71.0	7.3	78.3	0.74	0.38
PHA	81.4	2.7	84.1	1.2	85.3	0.52	0.49
NO2	85.4	-0.4	85.0	2.3	87.3	1.47	0.18
NO3	74.1	8.8	82.9	-1.5	81.4	0.83	0.49
NH4	77.4	-1.9	75.5	0.5	76.0	1.32	0.67
TDN	98.8	3.5	102.3	-2.0	100.3	0.30	0.85
PN	74.1	-2.7	71.4	1.6	73.0	0.31	0.45
DIP	56.0	13.0	69.0	2.2	71.2	0.49	0.32
TDP	70.8	11.9	82.7	0.9	83.6	0.87	0.37
PP	75.6	2.0	77.6	0.4	78.0	0.28	0.15
SI	60.8	1.1	61.9	2.1	64.0	0.40	1.54
SS	59.4	5.2	64.6	-2.2	62.4	0.50	1.02

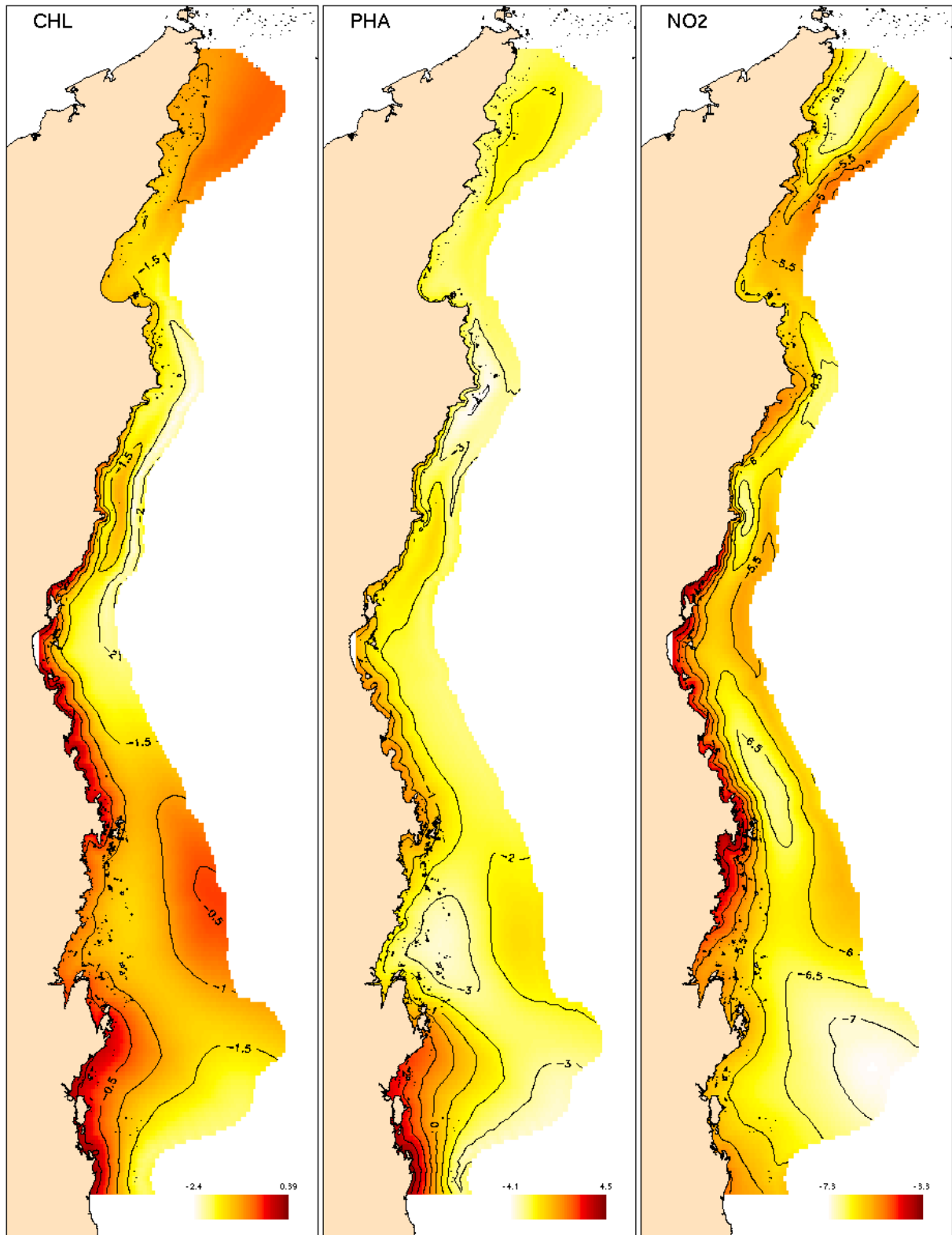


**Figure 4.** Estimated spatial trends of chlorophyll, phaeophytin and nitrite. All spatial plots are on a log<sub>2</sub> scale, and thus a change of one unit represents a doubling or halving.

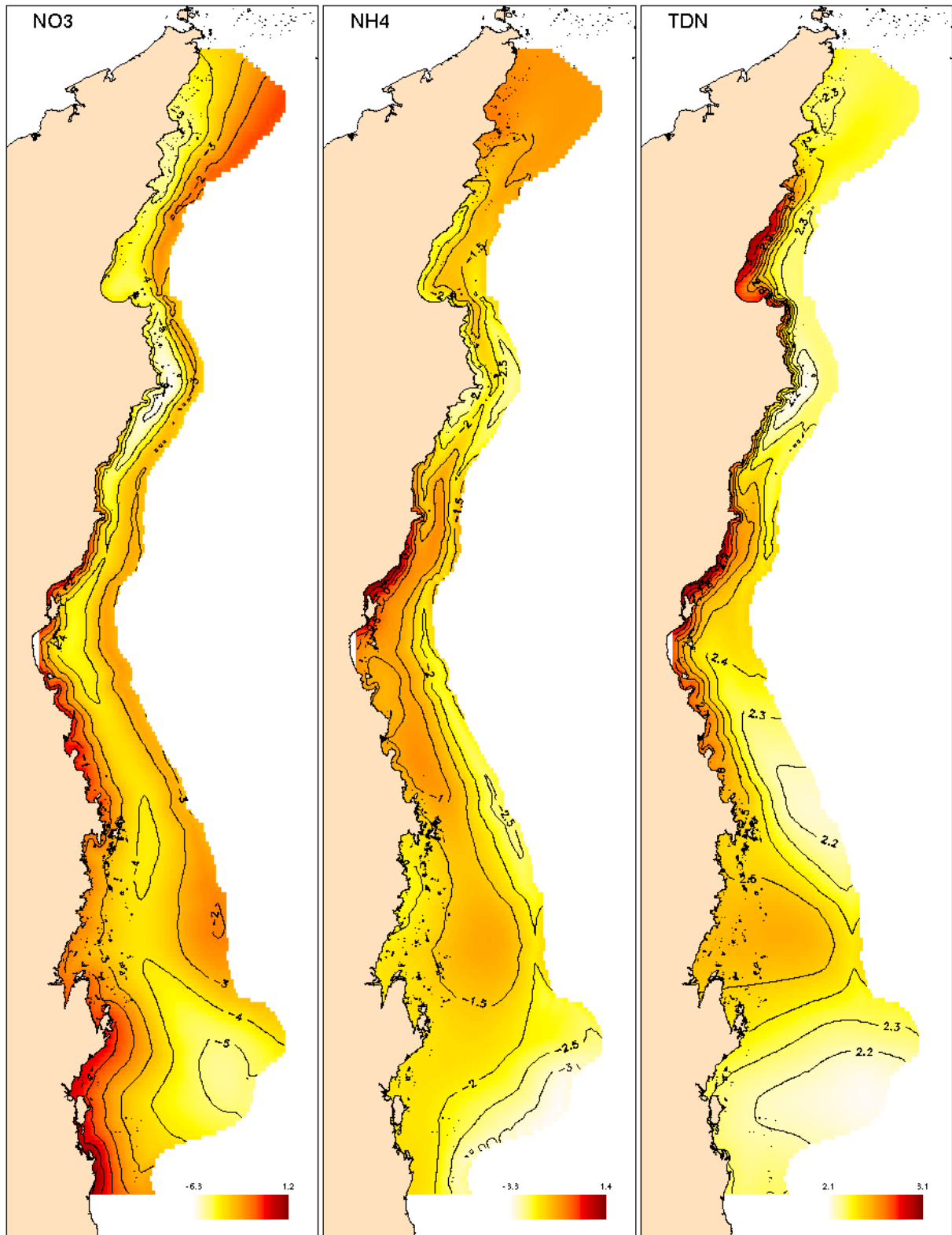


**Figure 5.** Estimated spatial trends of nitrate, ammonia and total dissolved nitrogen. All spatial plots are on a log<sub>2</sub> scale, and thus a change of one unit represents a doubling or halving.

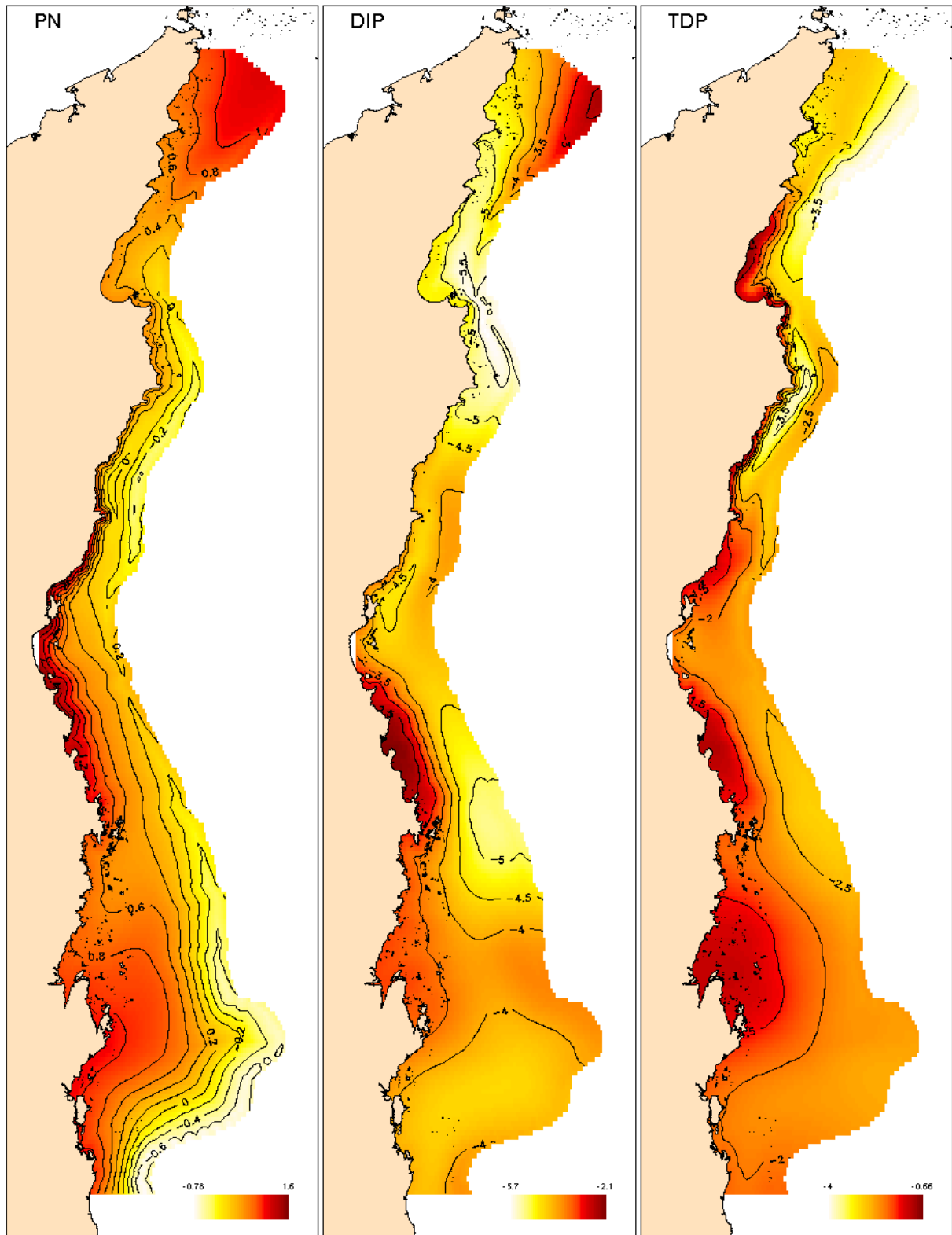


**Figure 6.** Estimated spatial trends of particulate nitrogen, dissolved inorganic phosphorous and total dissolved phosphorous. All spatial plots are on a log<sub>2</sub> scale, and thus a change of one unit represents a doubling or halving.

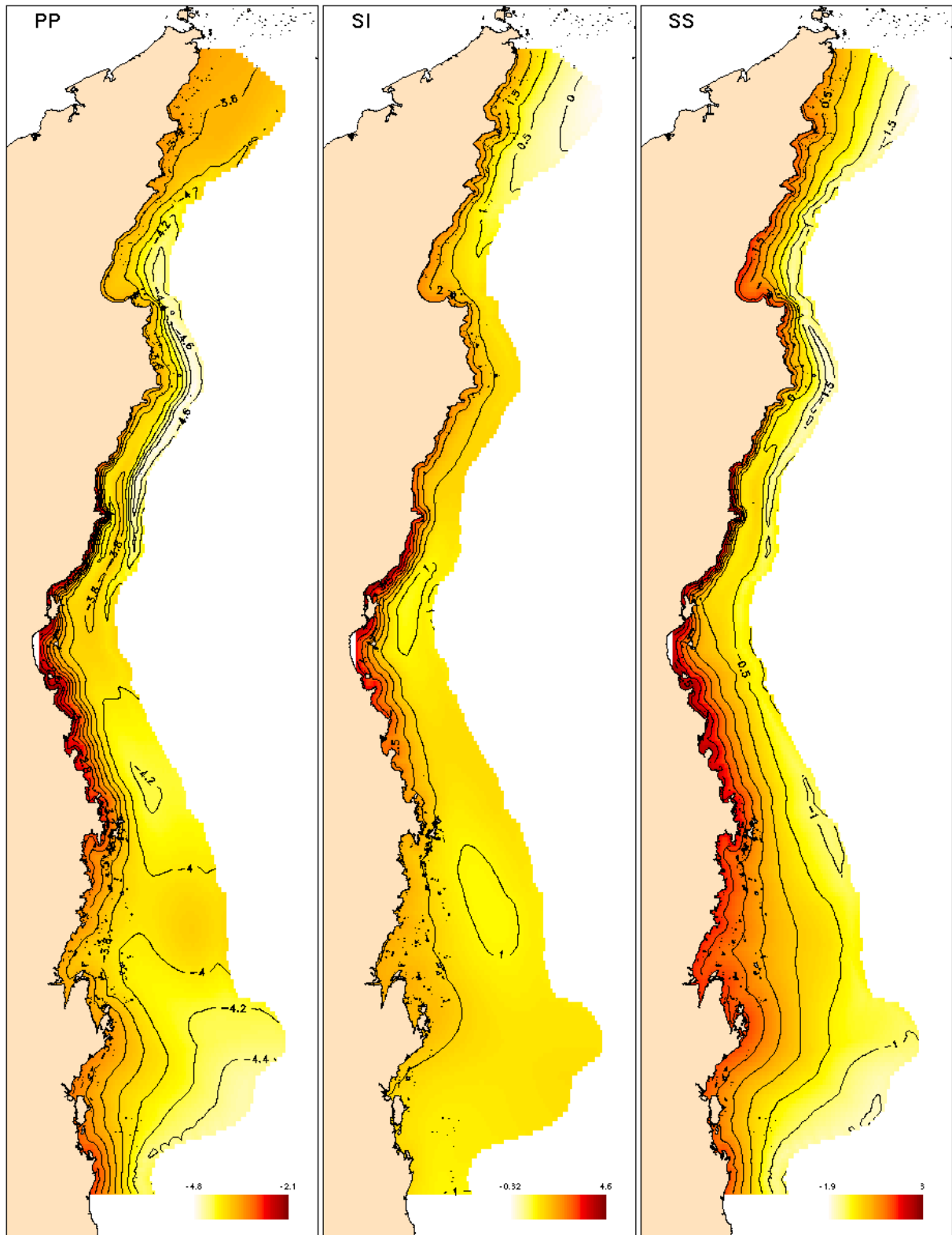


**Figure 7.** Estimated spatial trends of particulate phosphorous, silicate and suspended solids. All spatial plots are on a log<sub>2</sub> scale, and thus a change of one unit represents a doubling or halving.

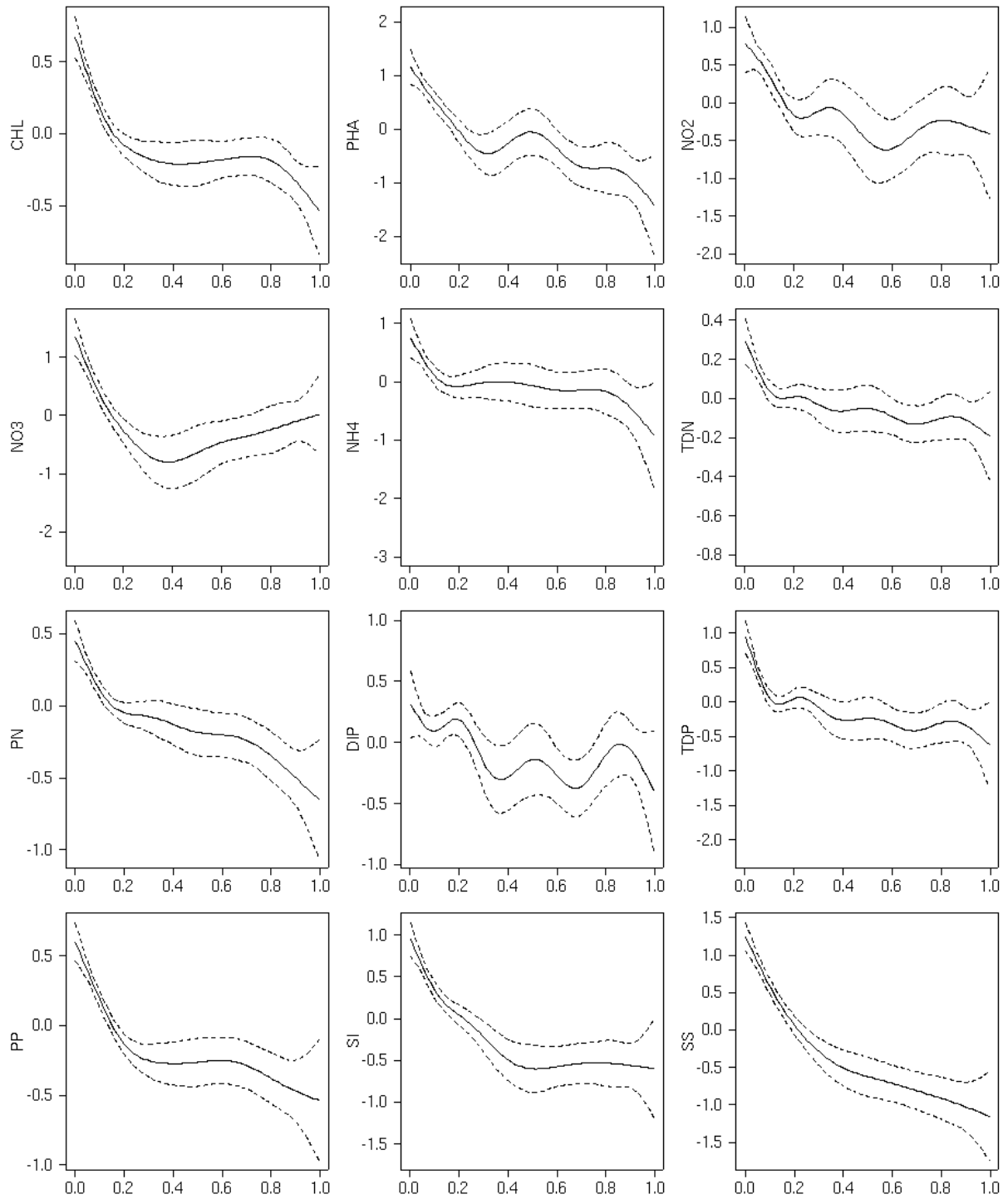


**Figure 8.** Partial effects of relative distance across the reef (0 = Coast; 1 = Edge of Outer Reef) on the 12 water quality parameters together with approximate 95% confidence intervals. All effects plots are on a log2 scale, and thus a change of one unit represents a doubling or halving.

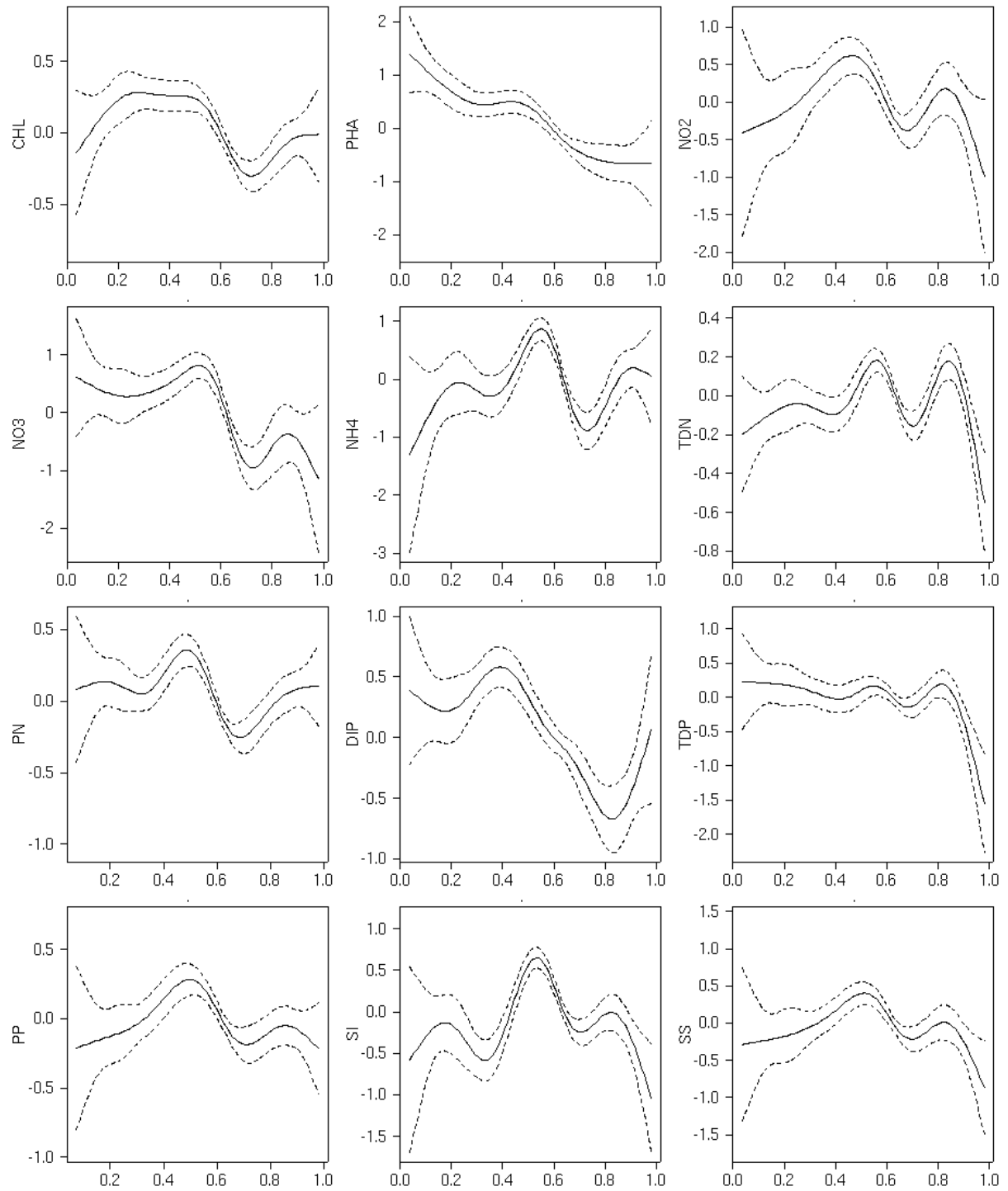


**Figure 9.** Partial effects of relative distance along the reef (0 = South; 1 = North) on the 12 water quality parameters together with approximate 95% confidence intervals.

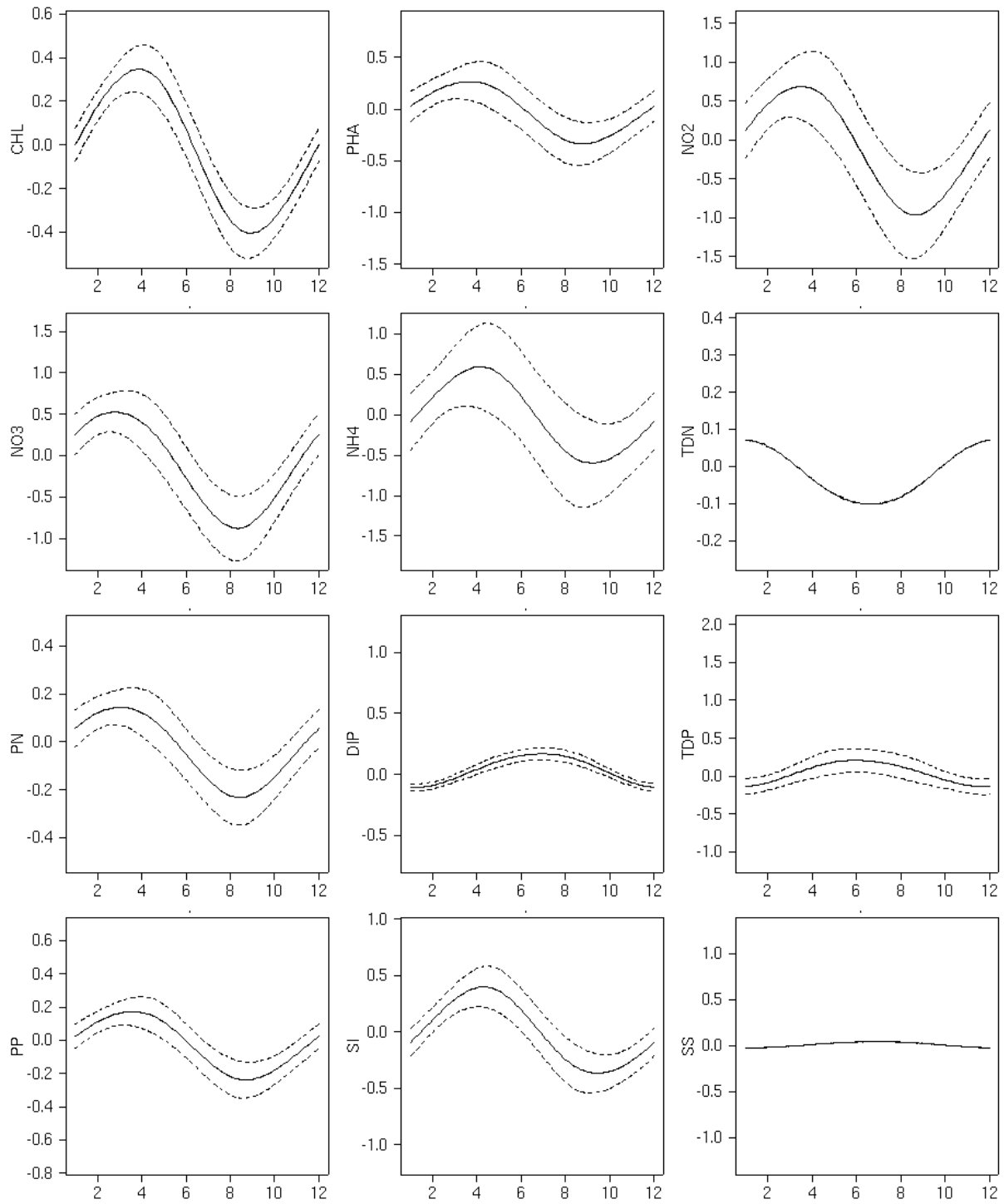


**Figure 10.** Partial effects plots of months (1=Jan, 2=Feb, etc) for the 12 water quality parameters together with approximate 95% confidence intervals. Confidence intervals were not estimable for TDN & SS.

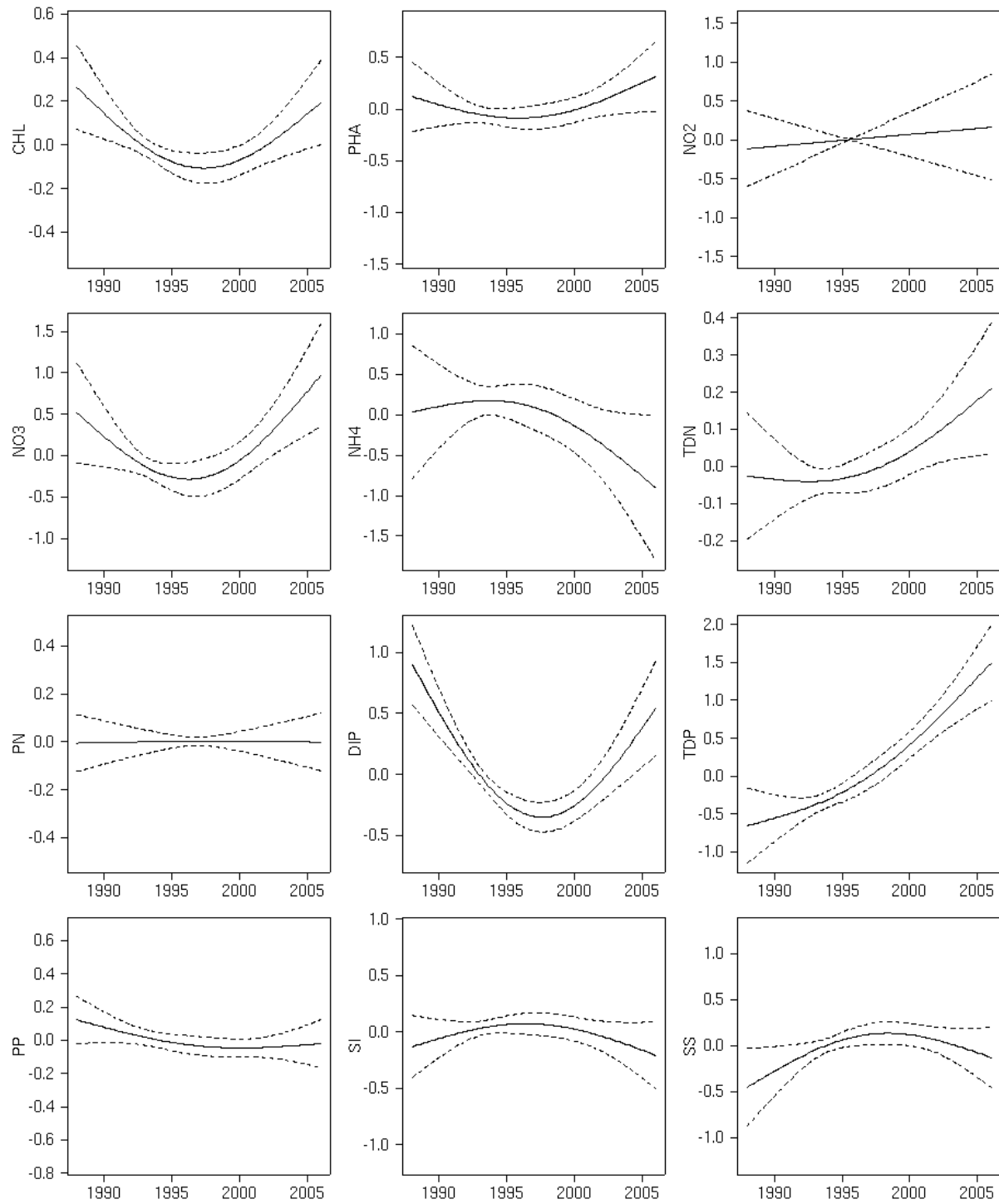


**Figure 11.** Partial effects plots of years for the 12 water quality parameters together with approximate 95% confidence intervals.

## *Chlorophyll and Phaeophytin Long-Term Monitoring Data*

The chlorophyll (CHL) and phaeophytin (PHA) long-term monitoring data differ from the lagoon data in that the data collection was designed to assess change and spatial differences between the regions. Thus the sites were revisited consistently over the years. Sites were not sampled at fixed times throughout years, but the spatial and temporal effects are less confounded than for the lagoon data. Also the random effects of site, which in the statistical analysis is equivalent to trip in the lagoon data, are smaller than trip effects, since the sites variation comprises only spatial variation, whereas the trip variation includes temporal variation. Thus despite there being only 25-50% as many observations in the long-term monitoring data set, the estimates of effects are more precise and patterns are clearer than for the lagoon data (Tables 5-7 and Figure 12).

### **Spatial Effects**

The spatial patterns are similar for CHL and PHA. Both show declines across the shelf and increases from north to south. The across patterns are however not consistent along the Reef, with no cross-shelf decline in the far north and very steep declines in the central Reef as indicated by the closely spaced isoclines (Figure 12). Similarly, the decline from south to north is stronger in the inshore than the offshore.

Averaged across the shelf, for both CHL and PHA there is an linear increase from north to south; CHL increases by ~100% and PHA by ~70%. Both CHL and PHA show strong declines across the shelf with a rapid decline in the inner 20% of the shelf followed by a flat period and then a further decline on the outer shelf

### **Temporal Effects**

The temporal patterns for both CHL and PHA show cyclic variation across the year with CHL peaking in March and the PHA cycle follows approximately one month later. The cyclical variation is about 40% for CHL and 30% for PHA. The trends across years are moderate with CHL showing a decline and subsequent increase, whereas PHA increases from a plateau in the later years. The variation over years for CHL is about 10% and for PHA is about 25%.

**Table 5.** Summary of exploratory analyses of variance for chlorophyll and phaeophytin with spatial, temporal and trip variables as explanatory variables. Degrees of freedom for the sources of variation are shown in brackets.

WQ	F-ratios					% SS		
	Across (7)	Along (7)	Month (4)	Year (5)	Location	Space- Time (23)	Location	Error
CHL	251	53	45	41	7	37	8	55
PHA	235	28	40	50	11	30	12	58

**Table 6.** Comparison of across-along and latitude-longitude as spatial explanatory variables chlorophyll and phaeophytin. The percentage prediction error is shown for the spatial-temporal model including (from left to right in the table) across-along, across-along as an additive model and latitude-longitude, with the increase in prediction error relative to the across-along model is shown in parentheses.

WQ parameter	Prediction error		
	Across-Along	Across-Along-Additive	Latitude-Longitude
CHL	68.1	71.6 (3.5)	69.6 (1.4)
PHA	74.3	77.4 (3.1)	75.9 (1.6)

**Table 7.** Comparison of the percentage prediction error for the full spatial-temporal model S+M+Y (S =across-along, M=months, Y=years) and reduced models S+M and S. The increase in prediction error are also shown (from left to right in the table) by dropping year (-Y) and month (-M). The estimates of the variance components for trip and pure error are also shown.

WQ parameter	Prediction error (%)					Site variance	Error variance
	S+M+Y	-Y	S+M	-M	S		
CHL	68.1	1.2	69.3	10.5	79.8	0.24	0.59
PHA	74.3	-0.3	74.0	9.4	83.4	0.27	0.44

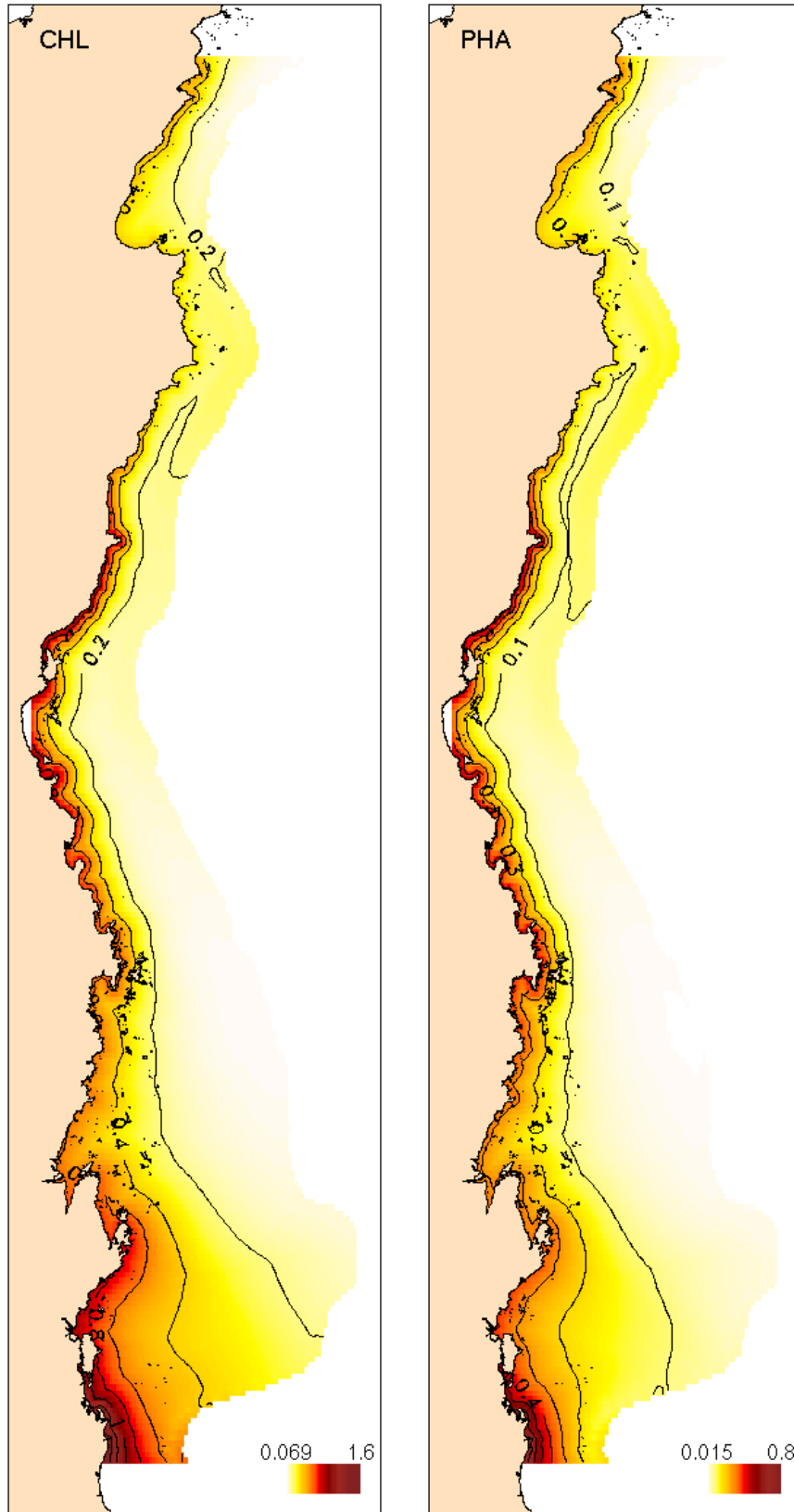


**Figure 12.** Estimated spatial patterns of chlorophyll and phaeophytin from the long-term monitoring.

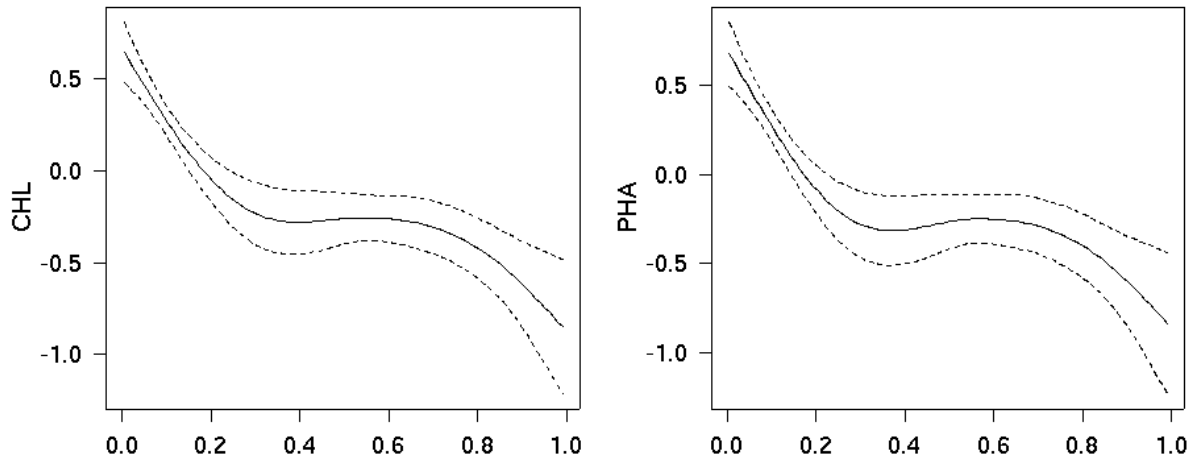


**Figure 13.** Partial effects plots of relative distance across the reef (0 = Coast; 1 = Edge of Outer Reef) on chlorophyll and phaeophytin from long-term monitoring together with approximate 95% confidence intervals. All effects plots are on a log<sub>2</sub> scale, and thus a change of one unit represents a doubling or halving.

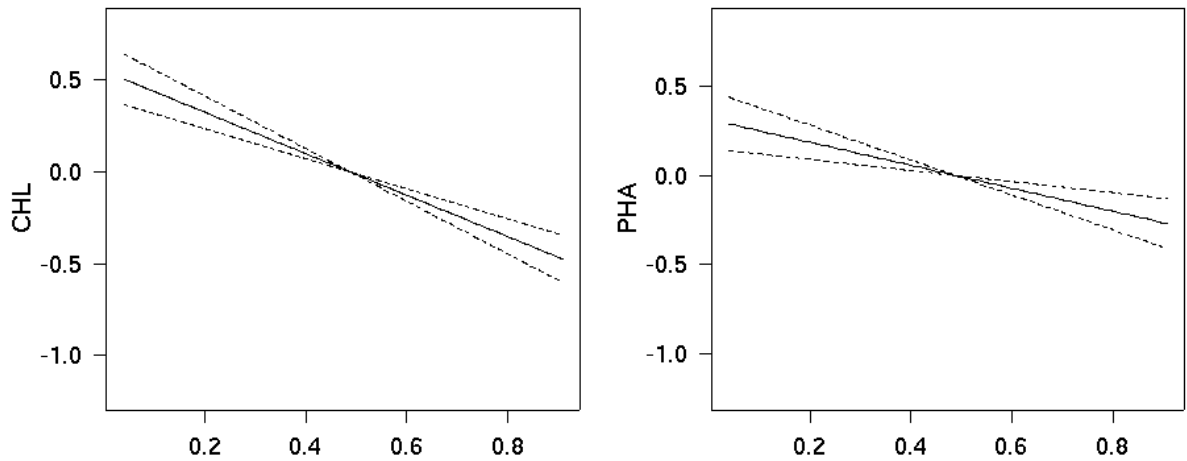


**Figure 14.** Partial effects plots of relative distance along the reef (0 = South; 1 = North) on chlorophyll and phaeophytin from long-term monitoring together with approximate 95% confidence intervals.

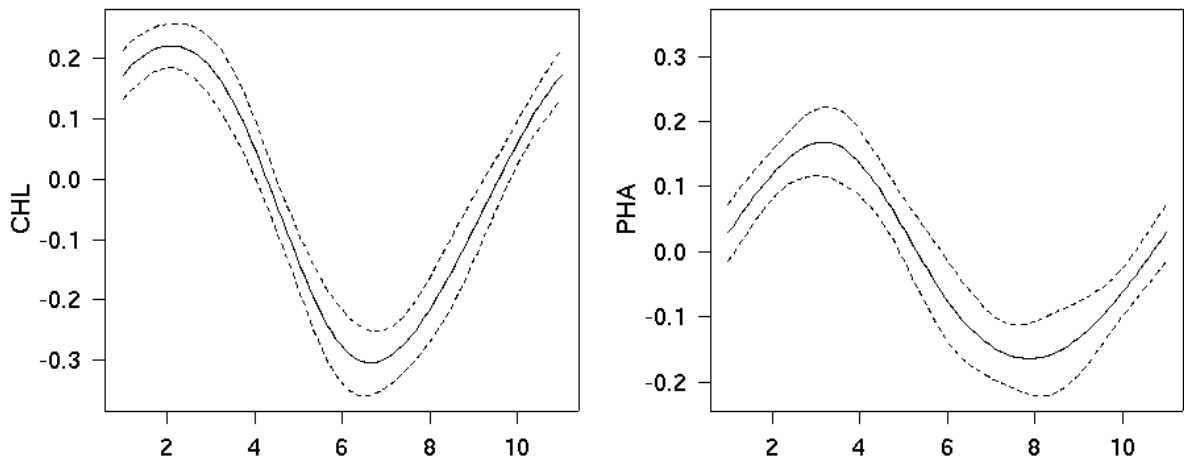


**Figure 15.** Partial effects plots of months (1=Jan, 2=Feb, etc) on chlorophyll and phaeophytin from long-term monitoring together with approximate 95% confidence intervals.

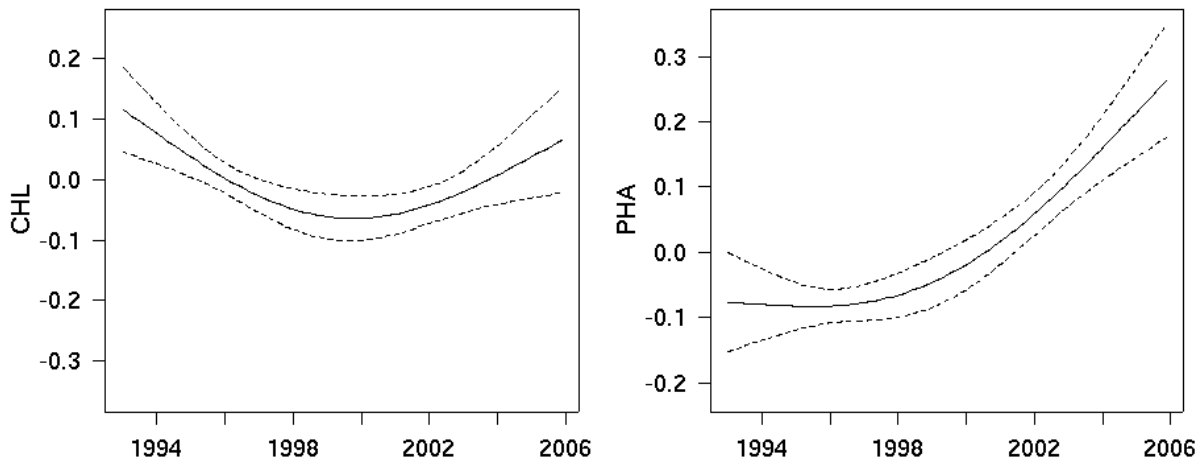


**Figure 16.** Partial effects plots of years on chlorophyll and phaeophytin from long-term monitoring together with approximate 95% confidence intervals.

**Water Clarity (Secchi) Data**

The spatial patterns in water clarity (secchi) were very strong (Figure 17). The prediction error (24.5%) was very low compared the the WQ parameters analysed previously. This statistical property, together with its known links to biotic function, suggest water clarity could be a very useful indicator of WQ.

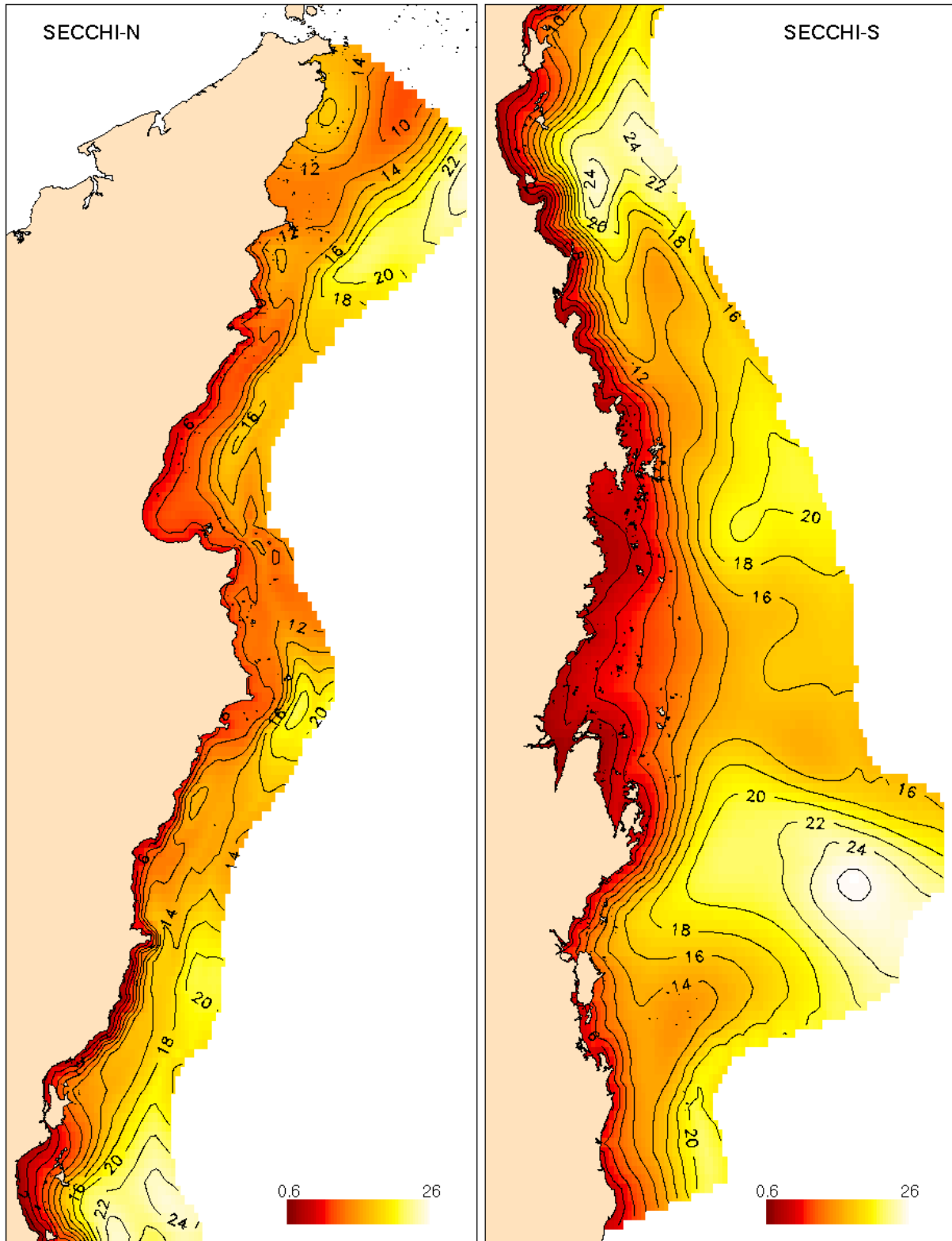


**Figure 17.** Estimated spatial trends of secchi disk visibility for the northern and southern sections of the GBR.

### *The Structure of Water Quality Parameters*

Principal components analyses were used to assess the correlational structure of the 12 WQ parameters (each standardised to mean zero and standard deviation one). The percentages of variance explained by the leading components was not particularly high with 20.2% and 14.6% for the 1<sup>st</sup> and 2<sup>nd</sup> components respectively. The principal components biplot (Figure 18) shows strong structure however with CHL, PHA, PP, PN and SS (the “solids”) strongly correlated and the remaining 7 WQ parameters less highly correlated but nonetheless forming a second group.

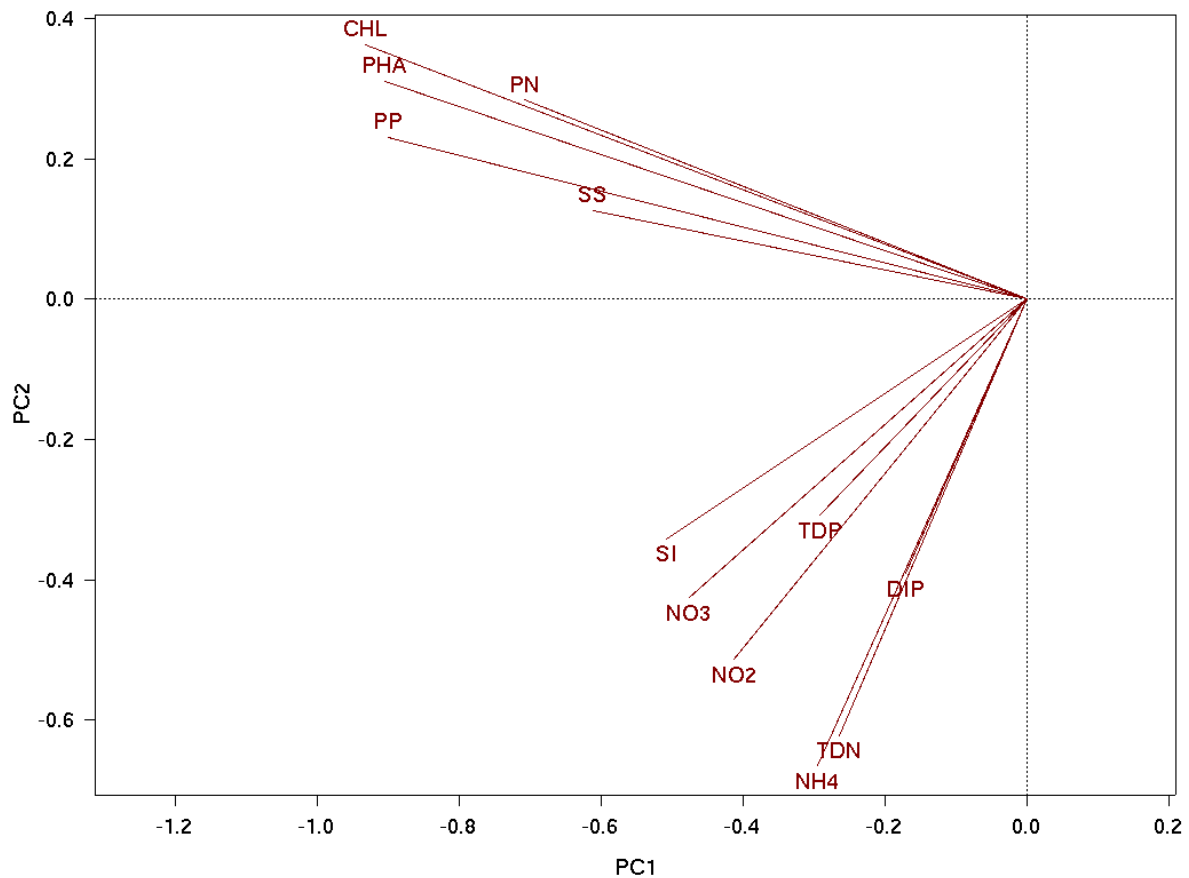


**Figure 18.** Principal components biplot of the 12 water quality variables. All variables were standardised to a mean of one and standard deviation of one prior to analysis. The solid and dissolved parameters are well-separated. The first two components explained 34.8% of the total variance.

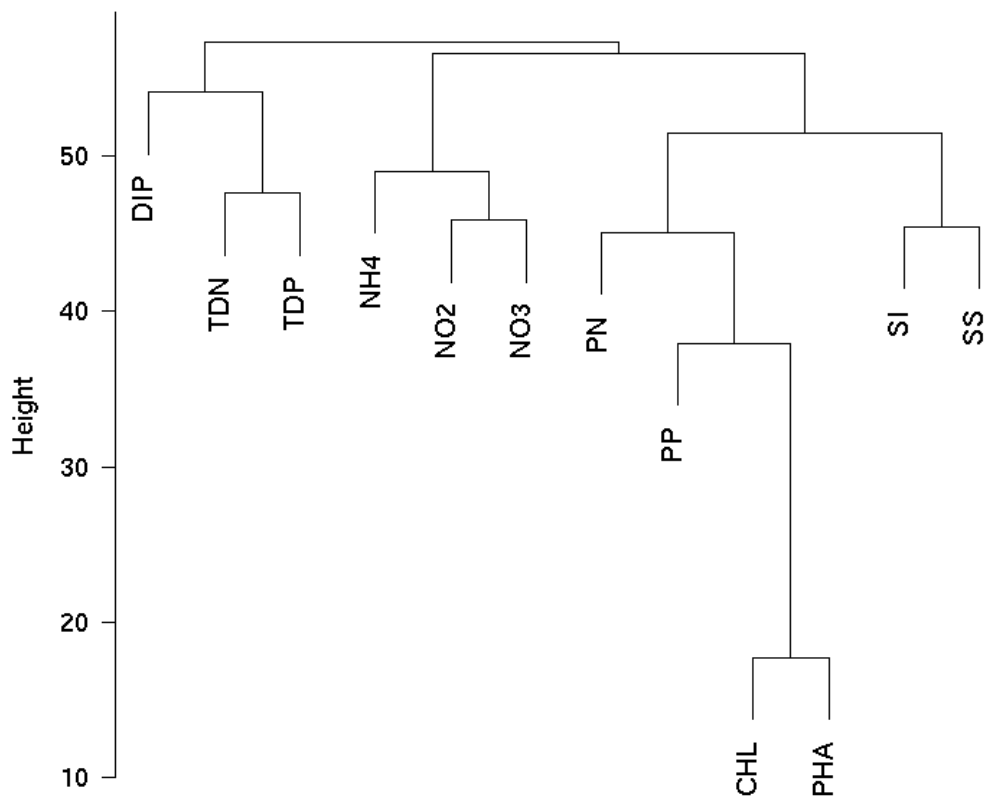


**Figure 19.** Cluster analysis of the 12 water quality variables. All variables were standardised to a mean of zero and standard deviation of one prior to analysis. The clusterings based on Euclidean distance and complete linkage show strong differences between solid and dissolved parameters are well-separated, as shown in the principal components biplot above, but also suggest a weaker separation between species of phosphorous and nitrogen.

A cluster analysis based on the WQ parameters also reflected the strong grouping between the solids (CHL, PHA, PP, PN), but also showed distinct, but much weaker groupings, between two groups of dissolved nutrients, one being nitrogen components (NH<sub>4</sub>, NO<sub>2</sub>, NO<sub>3</sub>), and the second (TDN, TDP, DIP) was a mix of the dissolved phosphorous components and TDN.

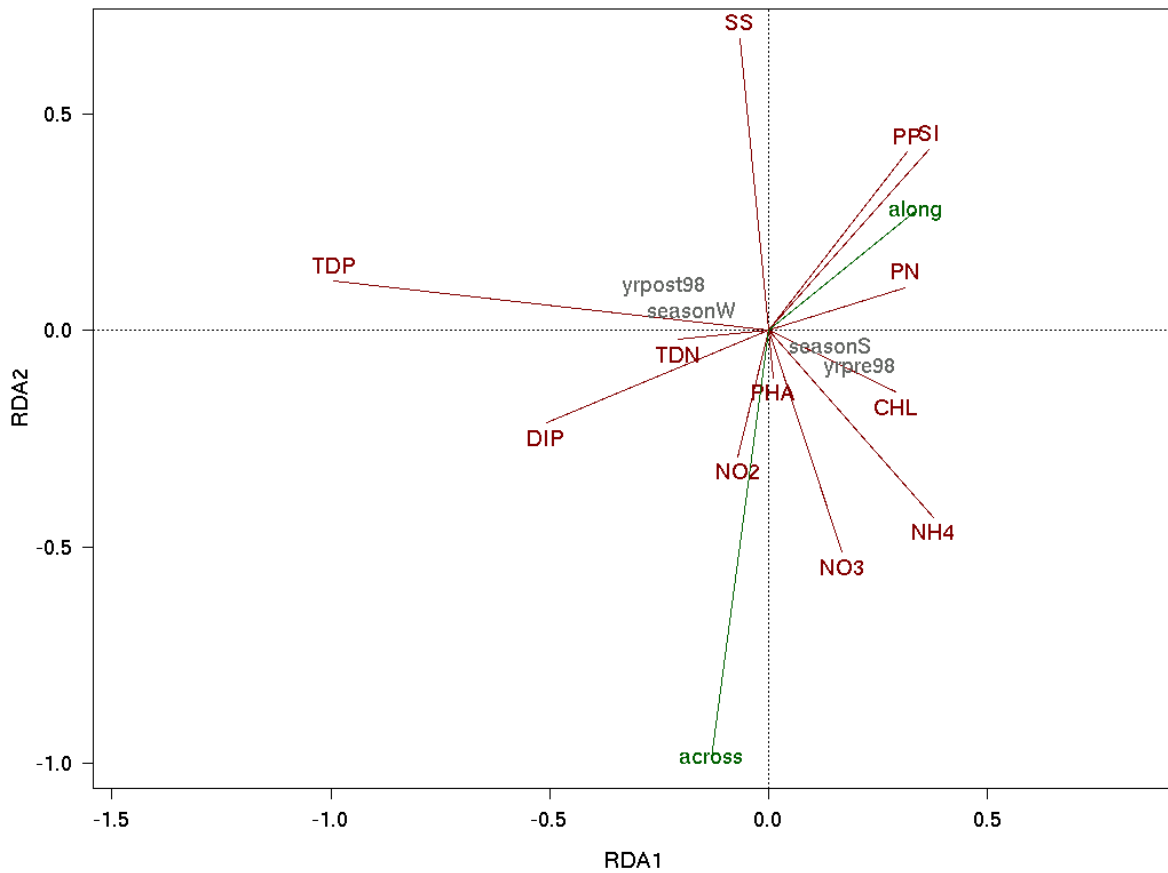


**Figure 20.** Redundancy analysis showing how structure of the WQ parameters varies with pre-post 1998, seasons, across and along.

The redundancy analysis explained 16.6% of the variation of the WQ parameters. A sequential analysis with the best explanatory variables added the model first. The variance accounted for by the explanatory variables was 8.2% (across), 4.7% (season W-S), 4.5% (pre-post 1998) and 1.8% (along) respectively. All explanatory variables were highly significant. The solids parameters identified as highly correlated in the PCA all declined most rapidly across the shelf. TDP and DIP tended to be relatively high in the wet season and post 1998, whereas NO<sub>3</sub> and NH<sub>4</sub> were low.

To quantify and explore the spatial and temporal structure in greater detail, a generalised procrustes analyses (GPA) was used. GPA is a method of aligning two or more spatial configurations and displaying them in low-dimensional spaces. This is achieved by rotating and expanding or contracting each configuration isotropically to minimise the sum of squared deviations (SSD) from each other. GPA also estimates the SSD between the groupings and this can be compared to the SSD between the centroids of each group. This partitions the variation into consensus SS (C: the SS of the averaged configuration about the overall centroid) and the residual SS (R: the SS of the aligned individual configurations about the averaged configuration). We can also estimate the error SS due to sampling (E) by resampling the data within the 4 groups. R can be compared to E, and a large R/E ratio indicates that the differences between the configurations are systematic.

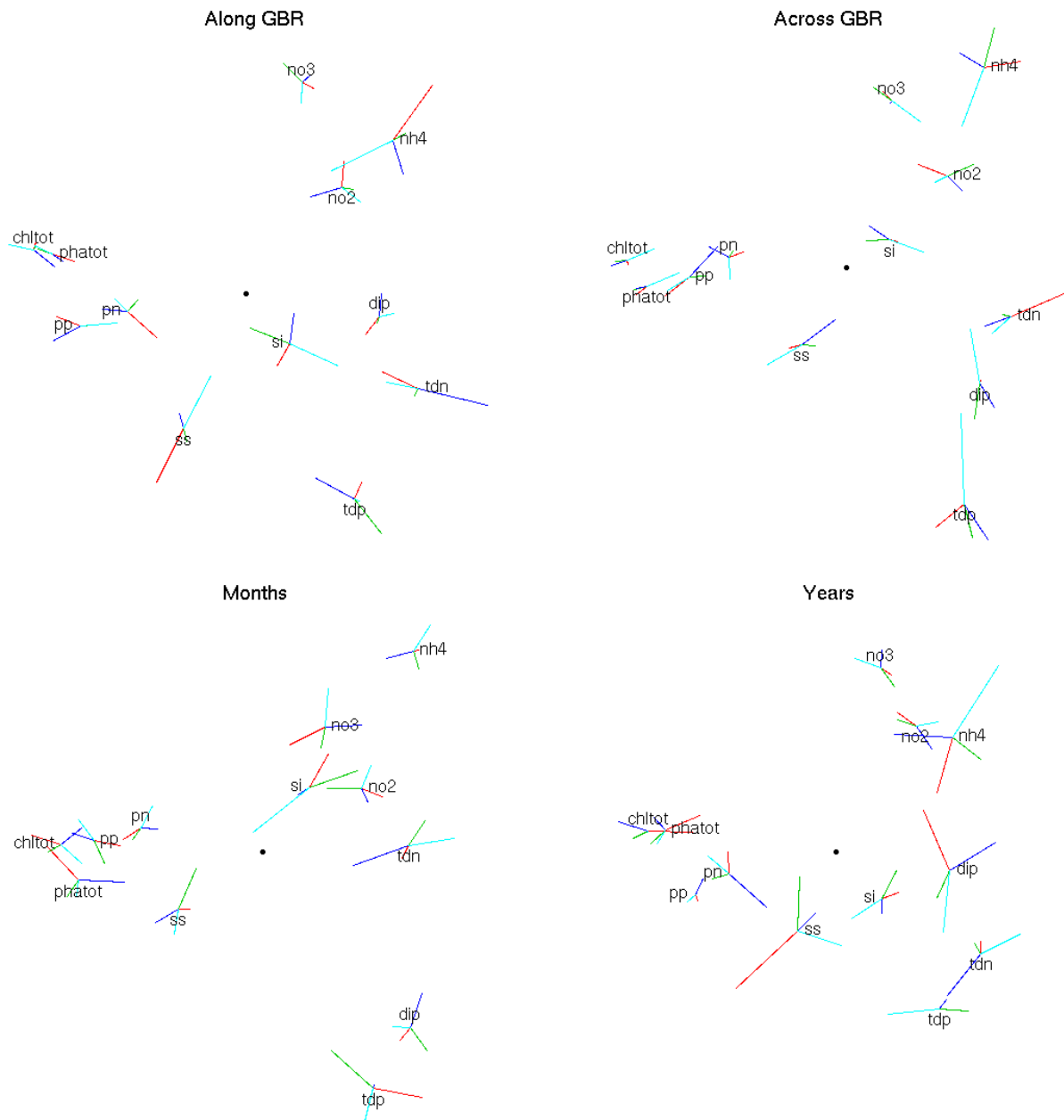


**Figure 21.** Generalised procrustes analysis of quality variables shown how the configuration vary with distance along and across the reef, and over time (months and years). In each of the 4 analyses the data were split into 4 groups according to the spatial or temporal variable. For each group, principal components configurations were calculated. The generalised procrustes analysis then rotates and expands or contracts each configuration isotropically to minimise the sum of squared deviations from each other. For each plot, each variable is represented by a star with 4 points; the end points represent the location of the variable relative to the centroid. The lengths of the deviations are very small compared to the distances between the variables suggesting patterns across each the 4 spatial and temporal variables do not vary greatly.

**Table 8.** Generalised Procrustes analyses of the 12 WQ parameter lagoon data. For each of four spatial and temporal groups (along, across, year, month), the consensus (C), residual (R) and total (E) sums of squares are shown.

WQ	Along			Across			Year			Month		
	C	R	E	C	R	E	C	R	E	C	R	E
CHL	<b>250</b>	<b>4</b>	<b>0.7</b>	<b>254</b>	<b>7</b>	<b>0.6</b>	<b>242</b>	<b>9</b>	<b>0.9</b>	<b>251</b>	<b>11</b>	<b>1.2</b>
PHA	<b>251</b>	<b>5</b>	<b>0.4</b>	<b>255</b>	<b>6</b>	<b>0.7</b>	<b>249</b>	<b>9</b>	<b>0.5</b>	<b>250</b>	<b>12</b>	<b>0.9</b>
NO2	342	8	0.8	345	9	0.9	327	11	0.7	332	12	1.2
NO3	334	7	0.9	333	8	1.1	311	16	1.1	329	11	1.3
NH4	362	16	1.2	379	14	1.5	373	13	1.3	345	50	1.1
TDN	374	22	0.9	369	17	1.4	327	29	1.2	362	17	0.9
PN	311	12	1.3	303	11	1.2	287	19	0.9	301	29	1.3
DIP	389	16	1.4	404	20	1.5	417	12	1.4	372	55	1.5
TDP	370	13	0.8	380	8	1.1	382	15	1.1	346	34	1.6
PP	<b>248</b>	<b>9</b>	<b>1.1</b>	<b>244</b>	<b>16</b>	<b>1.2</b>	<b>243</b>	<b>12</b>	<b>1.3</b>	<b>245</b>	<b>8</b>	<b>1.3</b>
SI	314	13	1.2	305	14	1.4	309	28	1.3	309	21	1.5
SS	314	16	1.5	272	30	1.7	333	28	1.4	243	54	1.7
	322	12	1.0	320	13	1.2	317	17	1.1	307	26	1.3

For each of across, along, years and months four equal-sized groups were formed (from low to high values) and a GPA analysis was run. The results are displayed in Figure 21 and Table 8. Due to their strong structure, four of the WQ parameters (CHL, PHA, PP and SS – all solids) show lower (bold) total sums of squares (T) than the expected average of 0.333. Those with lower trip variation (see earlier univariate analyses – Table 6), also have lower (italics) residual sums of squares (R) than average.

The residual SS are small compared to the consensus SS (Table 8), indicating that variation in correlation structure due to spatial and temporal effects is small compared the overall structure. However, the sampling error variation is in turn far smaller than the residual variation suggesting that the spatial and temporal effects, though small, are consistent.

Thus, we can conclude that there is strong structure in the WQ data. It is dominated by a cluster of five WQ parameters (solids) and two weaker groupings (mainly dissolved). The solids vary most strongly with relative distance across the Reef, this being the best predictor of the correlational structure. The correlational structure varies systematically with the spatial and temporal covariates, but not greatly compared to the overall structure.

## *Indicators and Mapping Risk*

This section explores some potential indicators of risk and shows likely risk maps based on plausible (but not definitive) values that determine *relative risk* at levels of “high”, “moderate” and “low”. It should be emphasised that *relative risk* and *absolute risk* are very different concepts. Determining the former is relatively easy compare to the latter. Few would argue with the view that increased pollutants leads to increased risk, but specifying a level of exposure at which an organism or ecosystem is likely to be adversely affected is a considerable challenge – one that for a system as complex as the GBR, is unlikely to be achieved in other than a few restricted instances.

It should also be emphasised that scale is an important issue. The analyses in this Report map WQ parameters on a scale of 10s-100s of kms. It would be unwise draw inferences at smaller scales.

The choice of WQ indicators is based on earlier and current work of Fabricius, De'ath *et al* that has shown links between various measures of WQ and possible biotic responses. These include reductions in species richness in levels of “poor” WQ and possible links of crown-of-thorns outbreaks to enhance levels of chlorophyll. Some of these indicators shown in this section, and/or variants of them, will be assessed in subsequent analytical work and reports. For example, various benthic data will be related to the spatial distributions mapped in this Report.

In this section we examine five possible indicators; three are derived from the multivariate lagoon WQ data (n=1531), and of the remaining two, the first is based on chlorophyll data from the pooled lagoon and long-term chlorophyll data (n=8238), and the second is a measure of water clarity, namely secchi disk depths (n=2058), drawn from three data sources: DPI seagrass surveys, the WQ lagoon data and inshore surveys (Fabricius).

Regions of relative risk are mapped for the five indicators using the “60-30-10 rule” (known as M10). Mapped (i.e. predicted) values lower than the 60<sup>th</sup> percentile of the *observed* data are declared “low risk”, the 60<sup>th</sup>ile-90<sup>th</sup>ile are “moderate”, and >90<sup>th</sup>ile are high risk. The regions are coloured red, orange and green indicating high, moderate and low risk regions respectively. Additionally the certainty (precision) of the predictions at each spatial points can be represented by their standard errors. These are used to vary the colour saturation with strong shades indicating regions of low uncertainty, and pale shades indicating regions of high uncertainty (e.g. Figure 23).

First we look at three potential indicators that are based on the analysis of WQ structure outlined earlier in this Report. They are not, at this stage, proposed the the best indicators, but nonetheless do illustrate plausible risk regions, and they are strongly similar to each other. This latter property is likely to pertain to many broad-scale indicators of WQ risk.

The first indicator, ZZ, is the sum of z-scores of the 12 WQ parameters, the second, PC1, is the 1<sup>st</sup> principal component of the standardised WQ parameters, and the third, PCS, is the 1<sup>st</sup> principal component of the five standardised “solids” WQ parameters, namely CHL, PHA, SS, PN and PP, that were shown to be highly correlated. The spatial distribution of the three indicators is shown in Figure 21, and they are strikingly similar. All three show very high levels in the inshore central and southern-central section of the Reef. These high levels extend ~20% across the Reef. The values of PC1 are somewhat higher in the far north due to high estimates of nitrogen components, but estimates in this region are imprecise and should be treated with caution (see Appendix 2).

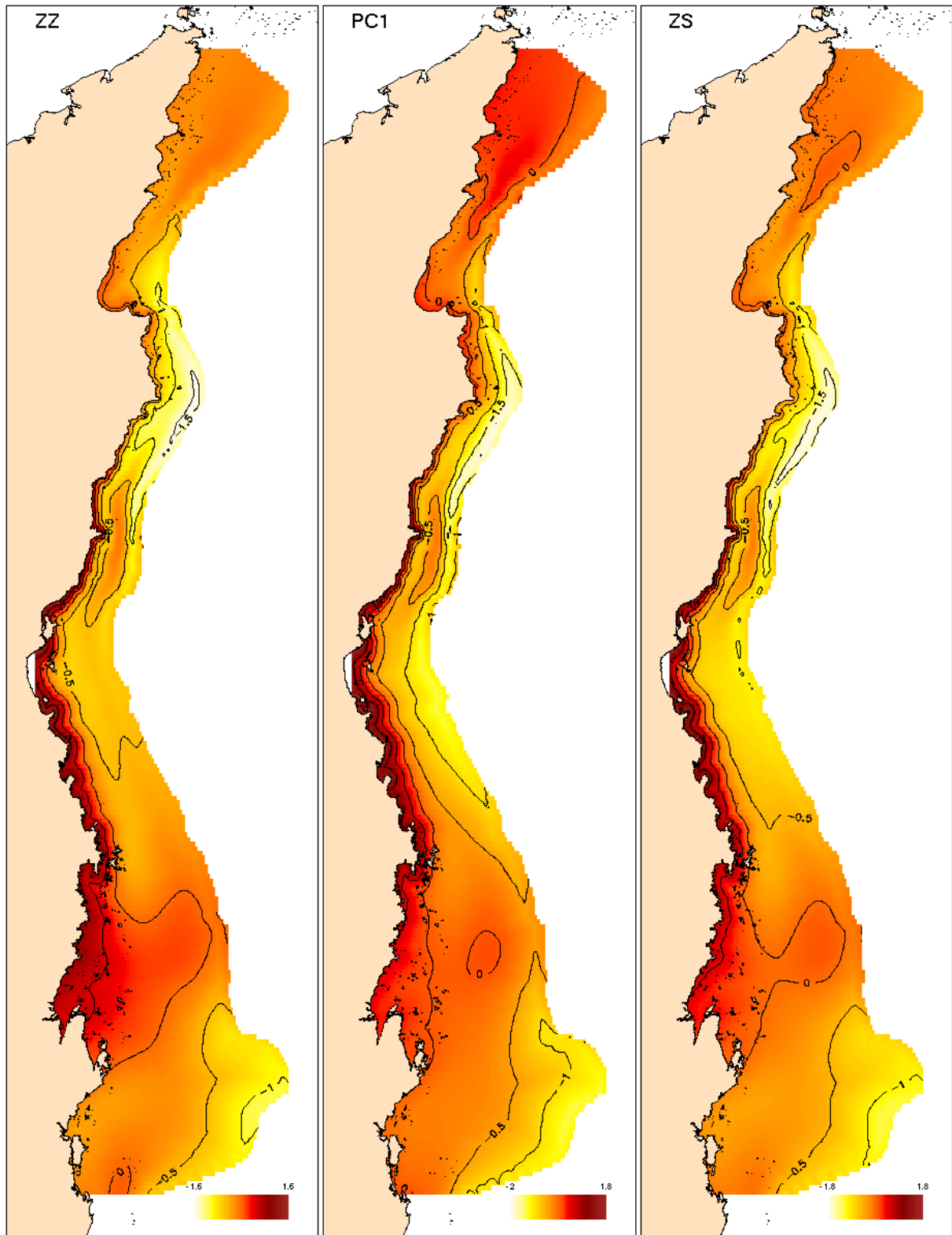


**Figure 22.** Risk regions for three potential WQ indicators: the ZZ = the summed z-scores across all 12 WQ parameters, PC1 = the 1st principal component, and ZS = the summed z-scores of the “solids” -- CHL, PHA, SS, PN and PP.

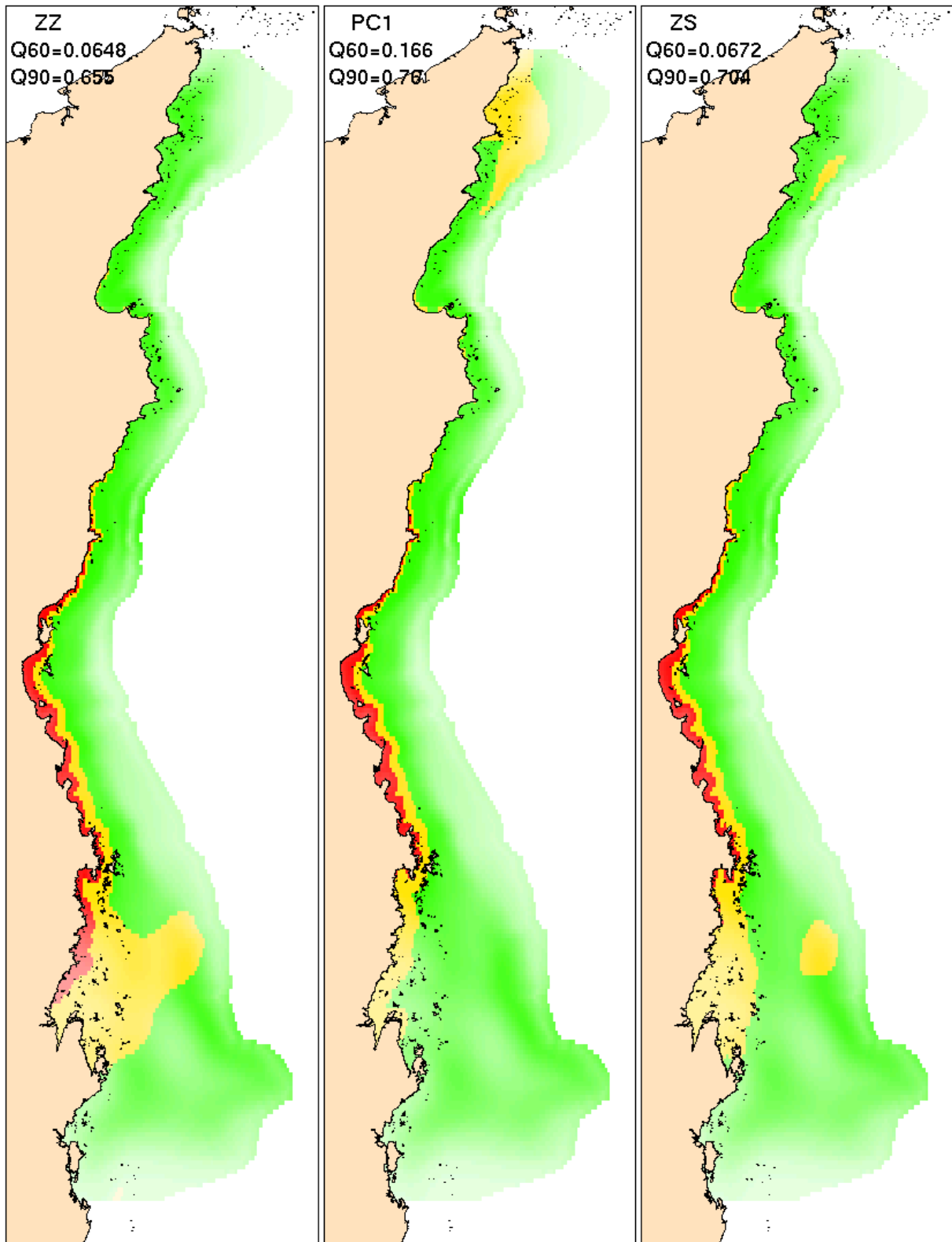


**Figure 23.** Risk regions for three potential WQ indicators: ZZ, PC1 and ZS (see Figure 22). The red, orange and green indicate high, moderate and low risk regions formed by the 90% and 60th percentile breaks of the data respectively. The strong – pale shades indicate regions of low -- high uncertainty of the risk.

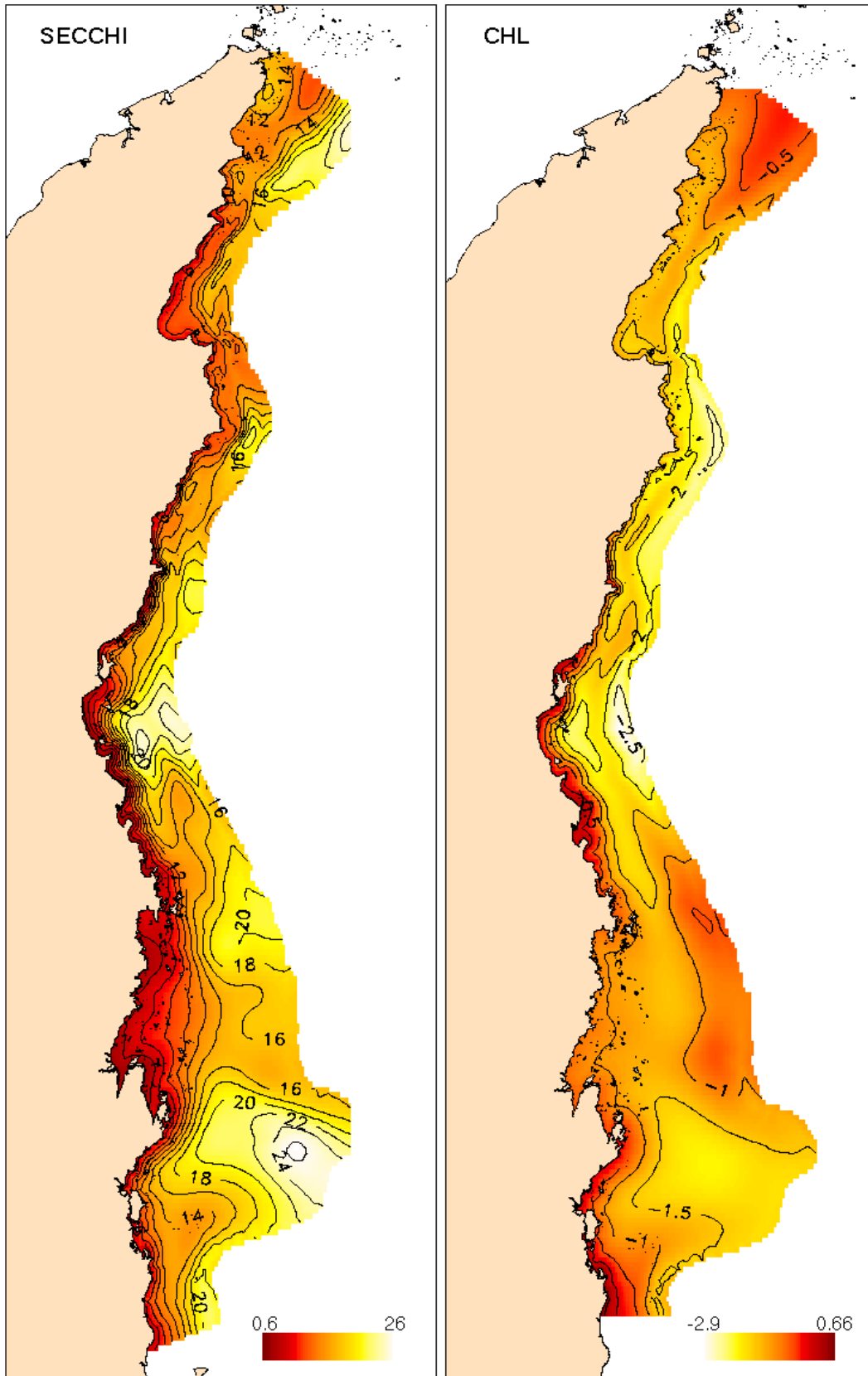


**Figure 24.** Estimated spatial trends of secchi disk visibility and pooled chlorophyll data (log base 2). For spatial plots on a log<sub>2</sub> scale a change of one unit represents a doubling or halving.

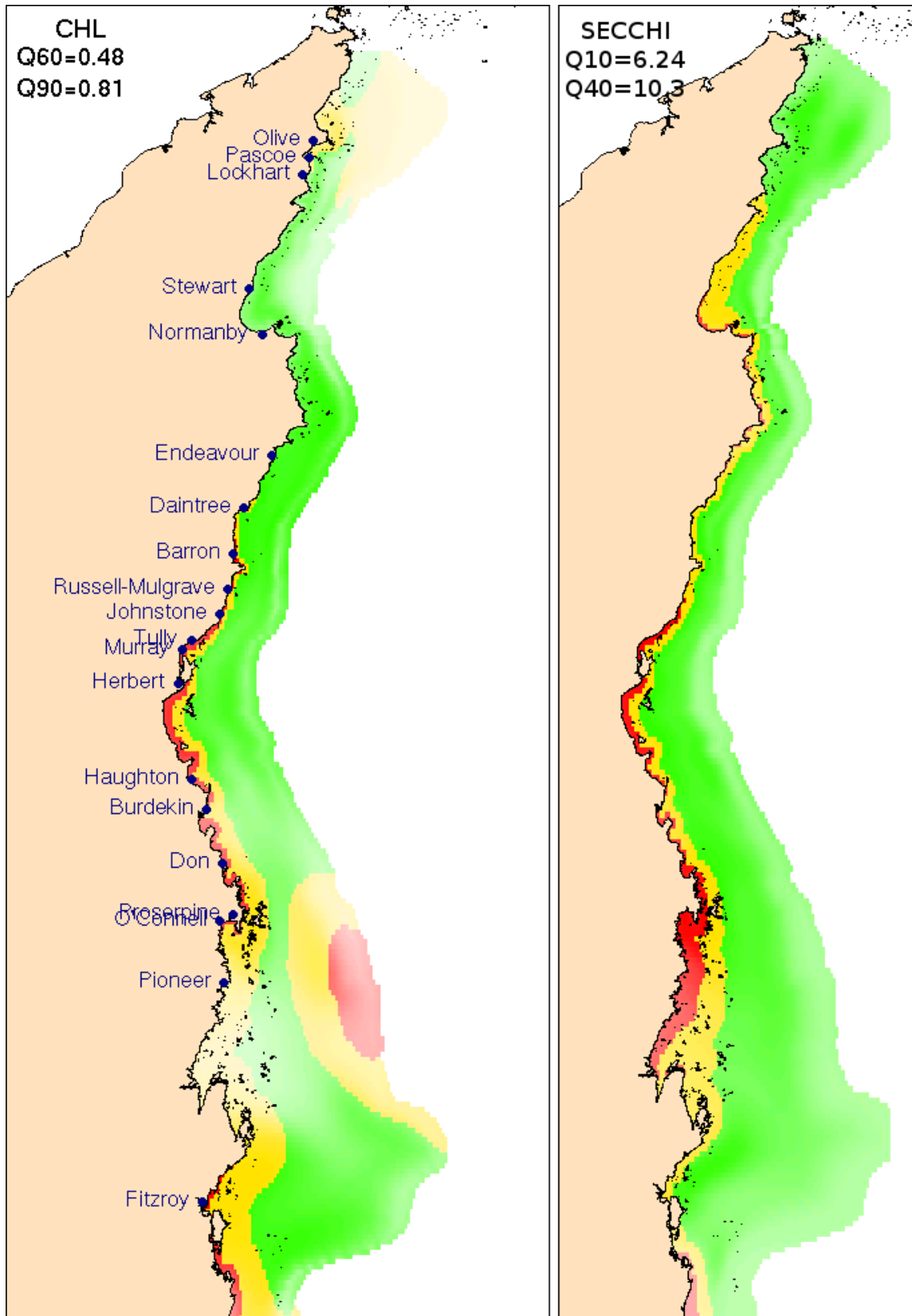


**Figure 25.** An example of risk maps with associated uncertainty. The left panel show the risk map for chlorophyll, and the right panel the risk map for water clarity as measured by secchi disk. The red, orange and green indicate high, moderate and low risk regions formed by the 90% and 60th percentile breaks of the data respectively. The strong-pale shades indicate regions of low-high uncertainty of the risk.

The most striking feature is the narrow coastal band of high risk that extends from just south of the Whitsunday Islands to Port Douglas in the North. Given (1) the evidence presented earlier in this Report of strong cross-shelf gradients in many WQ parameters, characterised by a very rapid decline in near shore, and (2) our knowledge of the nutrient-rich large discharge rivers in the region, this finding should not be surprising. The agreement between the three maps is very strong as might be expected, since they are based on common data to degree. The exception is the far north, which as previously noted should be discounted due to the sparseness of the data.

The maps for the composite chlorophyll data and the water clarity (secchi) also show strong patterns (Figures 24). The chlorophyll risk map (Figure 25) shows strong similarities to the first three indicators in that narrow coastal band of high risk also extends from just south of the Whitsunday Islands to Port Douglas in the North, but it also shows high, though more uncertain risk, in the Pompeys. For water clarity, low values are high risk so the the 60%ile and 90%ile are correspondingly replaced by the 10%ile and 40%ile. The water clarity maps again show the coastal high risk strip, together with a moderate risk strip, but the high risk extends further north and south. In the case of the northern extension this can be explained as high sediments discharging from far northern rivers but containing lower level nutrients than the more southerly rivers.

This initial exercise in mapping risk shows great promise and the work can be further developed in many ways. There are many issues related to validation against field and laboratory experiments, temporal and spatial scales of the effectiveness, cost and ease of implementation, and new technologies, such as automated sensors and remote sensing that can perhaps gather the data necessary to assess risk more efficiently. Additional work is proceeding in order to identify indicators that can be used in the field, based on additional empirical analyses. The the major focus of this work is validation in the sense that biotic measures can be shown to correlate to the indicator values.

## ***Risk Assessment and Management of the Great Barrier Reef***

Risk maps can provide crucial information necessary for effective management of the GBR, and in this section, various ways of using risk information as a management tool are investigated. This initial foray into the use of risk assessments based on water clarity is exploratory and indicative of empirical and graphical methods that may prove useful to management. Several issues are immediately self-evident and will require collaborative efforts between science and management in order to effectively use risk information (such as the WQ predictions and maps in this Report) to better manage the GBR.

The individual zones of the Marine Park Rezoning Plan are fundamental to GBRWHA management. They determine access and activities for the whole of the GBRWHA. They greatly vary in size (three orders of magnitude), being larger away from the coast and in more remote regions (Figures 26 and 27). The biophysical constituents of large zones vary greatly, whereas small zones may be relatively homogeneous, though not universally so. For example, the predicted values of water clarity can vary 10-fold within a large zone (e.g. 4-40m). Thus classification of individual zones by typical values (e.g mean water clarity) is likely to be misleading, and any classification of zones must take this into account. A simple example of classification of zones based on the risk map is shown in Figures 26 and 27. The zones are classified according to their mean values of water clarity into high, moderate and low risk. The representation of water clarity according to the risk map is not translated in to the zone classifications: small zones (mainly Marine National Park) are classified as high risk, whereas large zones extending across the Reef (often General Use) are classified as low risk due to their extension into clearer waters across the shelf. This “naive classification” of coastal Marine National Park zones typically being “high risk” whereas coastal General

Use zones are “low risk” is clearly misleading, and is a clear example that if zones are to be classified, then it needs to be done with great care.

Zone classification is not, of course, the only option. Visual quantitative methods can be effective when dealing with spatial heterogeneity and variation in scales. In Figures 28 and 29, zone outlines are overlaid on the water clarity risk map and can provide both qualitative and quantitative information that gets lost in classification. The capacity to represent risk maps and zones at varying scales and simultaneously display empirical information is likely to prove a far more effective tool for management than zone classification. For visual quantitative methods to be effective, they need to be fully interactive and flexible, based on the best environmental - ecological knowledge and sound contemporary statistical methodologies. Potential methods vary from the simplest combining of “GIS layers” approach to graphical representation of statistical modelling of risk based on our best scientific knowledge.

An example of combining risk maps based on scientific knowledge using the chlorophyll and water clarity (secchi) data is shown in Figure 30. We know from previous and ongoing studies that both chlorophyll and water clarity affect soft coral biodiversity: high chlorophyll and low water clarity reduce generic richness. A simple index can be based on the standardised difference water quality – secchi. The resulting index and risk maps show patterns that reflect the underlying maps (Figure 30). This method however ignores the functional relationship between chlorophyll, water clarity and soft coral richness and by establishing that relationship would improve the risk maps. Such work is currently in progress.

This section has been a preliminary brief look at issues relevant to management of the GBRWHA based on risk maps. Nonetheless, it has identified several issues:

1. Geographical scale is the crucial factor, with sizes of zones varying three orders of magnitude.
2. The difficulty of classifying individual zones due to highly variable sizes.
3. Interactive visual quantitative methods, based on best science, need to be developed in conjunction with management agencies.

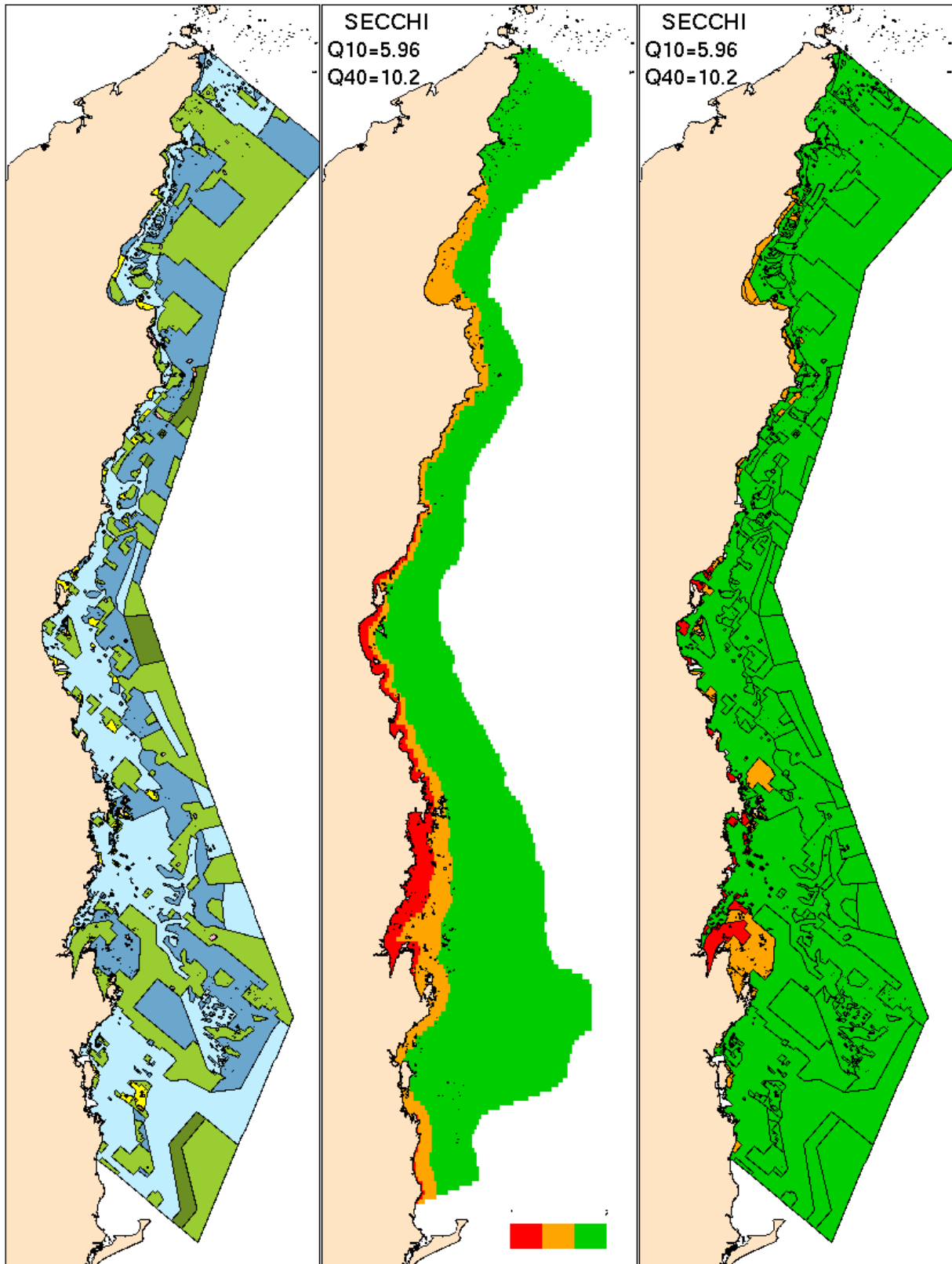


**Figure 26.** Left: the zoning of the GBRWHA. Centre: the risk map for water clarity (secchi). Right: The zones of the GBRWHA assigned to high, moderate and low risk from the risk map.

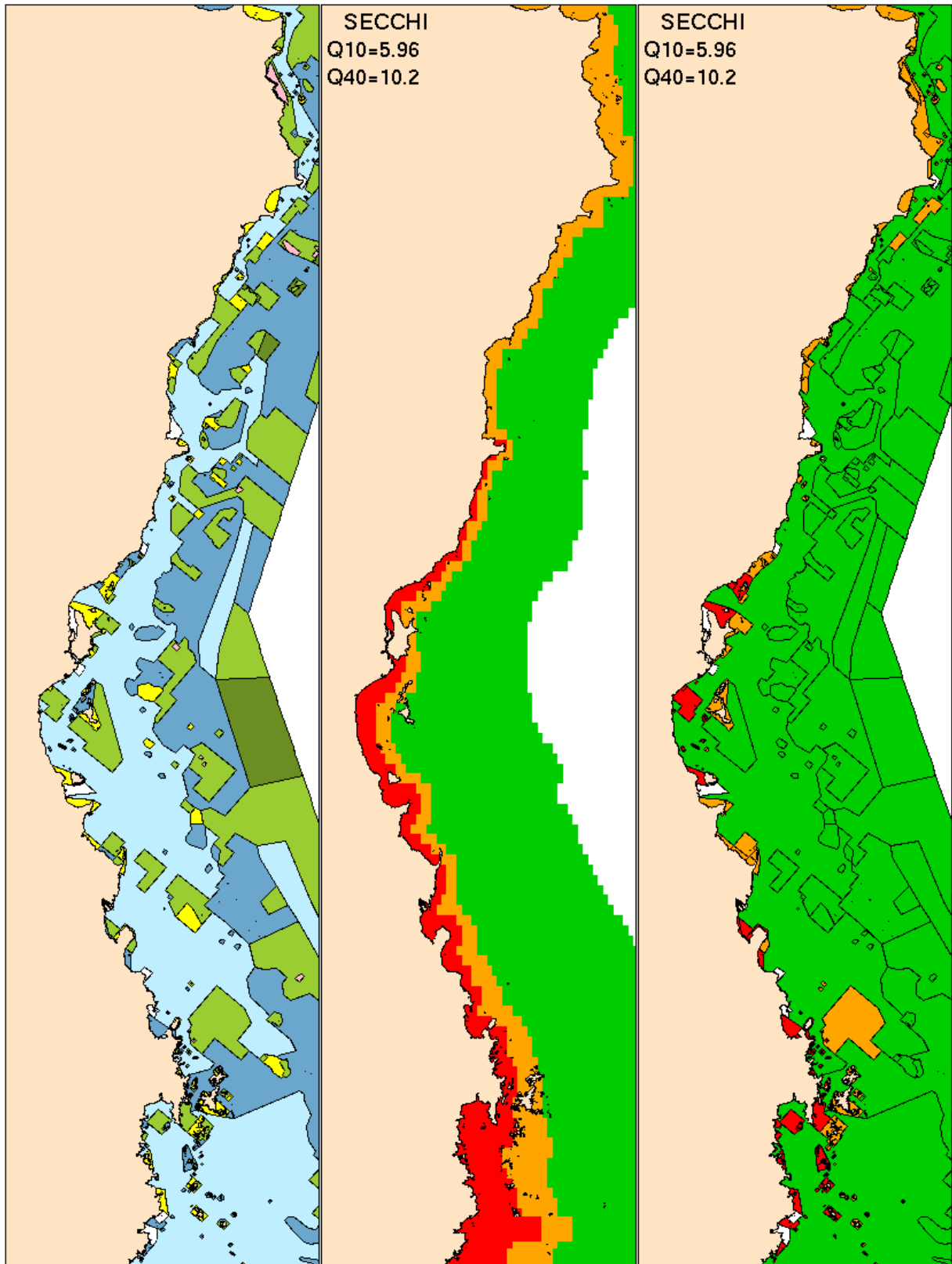


**Figure 27.** Enlargement of Figure 26 showing finer detail of zonings, reef risk map, and assignment of zones to high, moderate and low risk categories.

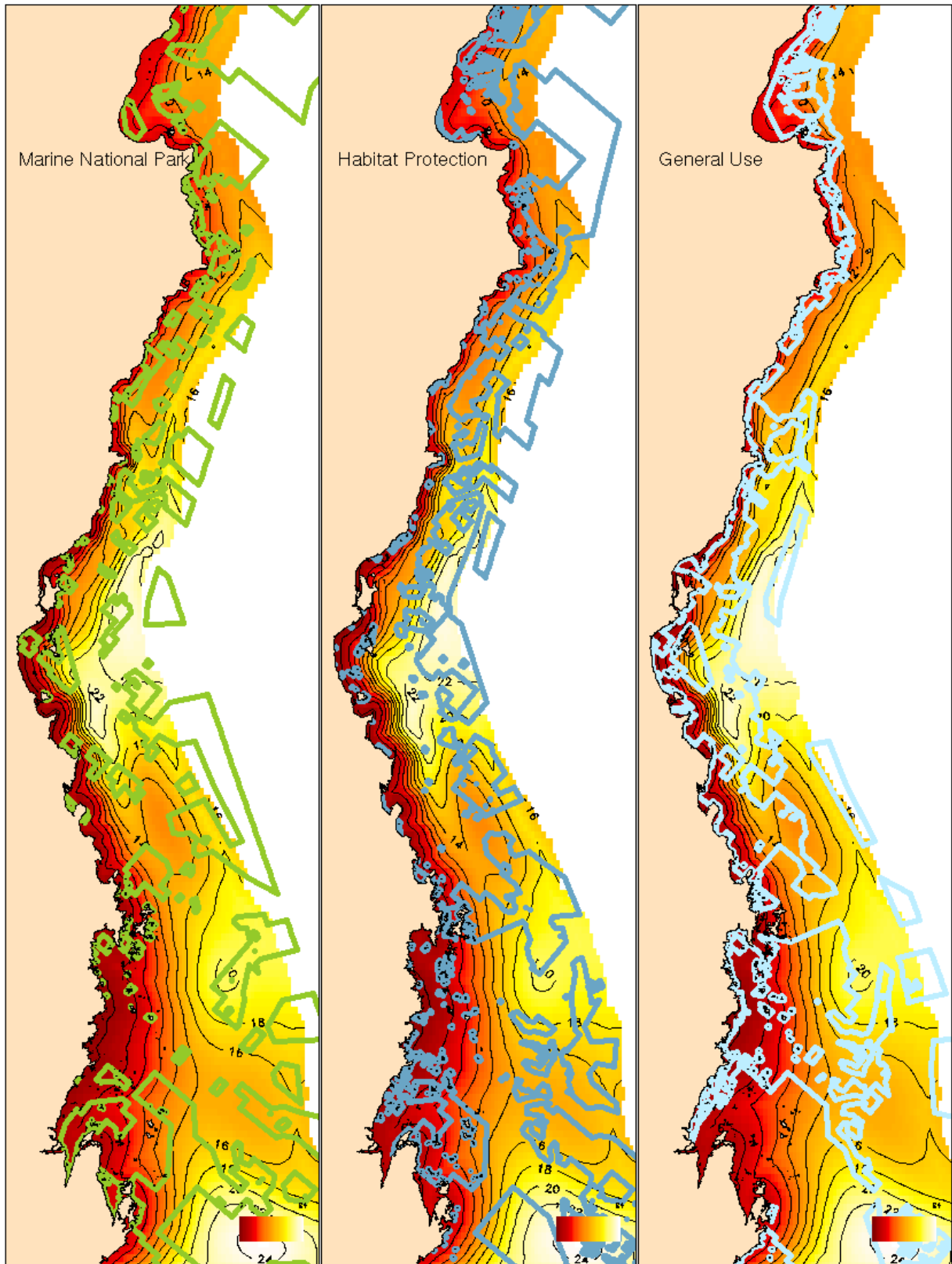


**Figure 28.** Outline of Marine National Park (green), Habitat Protection (dark blue) and General Use (light blue) zones. The large zones that extend to the outer shelf show high variation in water quality.

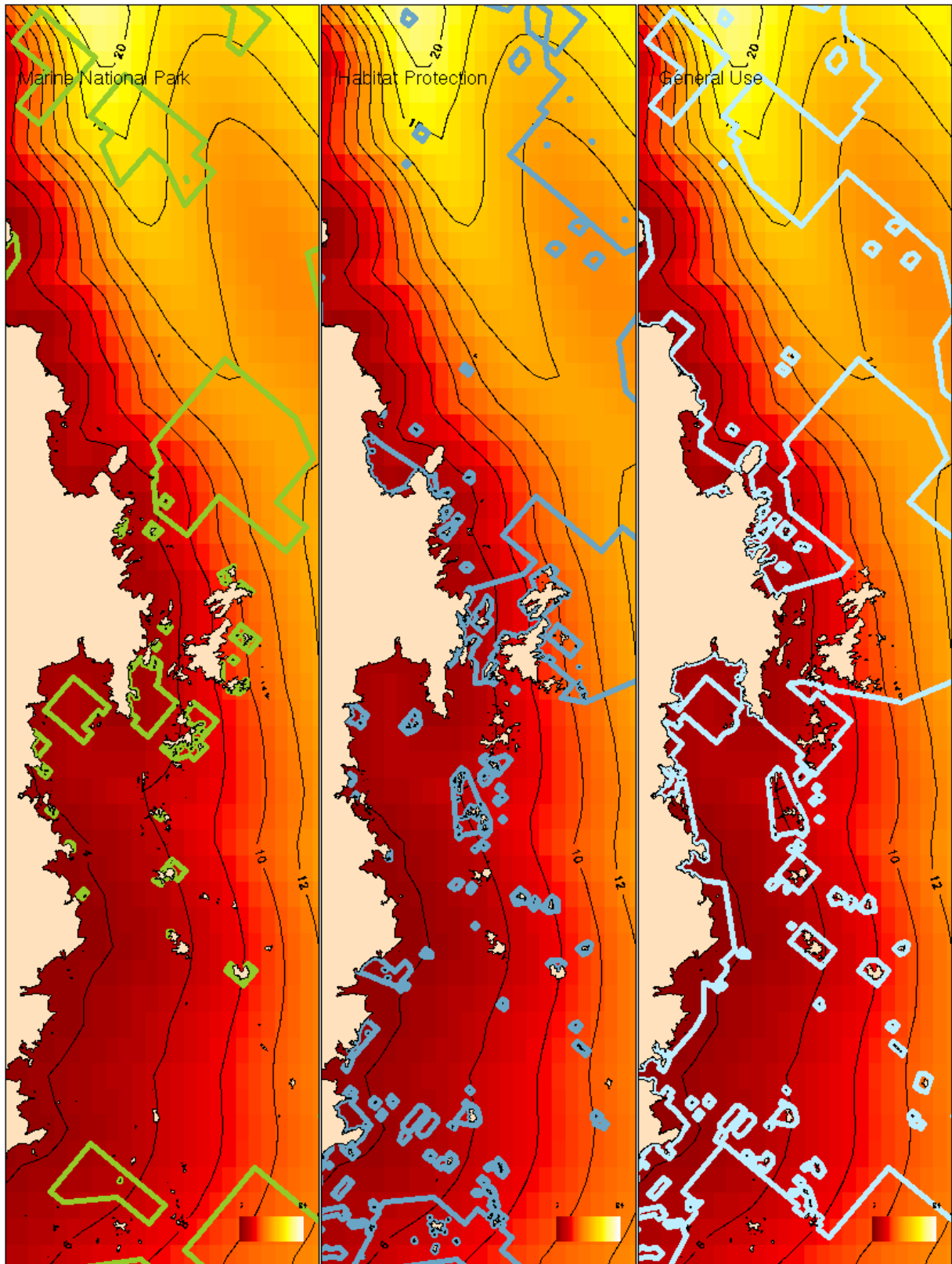


**Figure 29.** Enlarged version of Figure 28 showing inshore Marine National Park (green), Habitat Protection (dark blue) and General Use (light blue) zones. The smaller zones show low variation in water quality despite the sharp gradient in water clarity close to the coast.

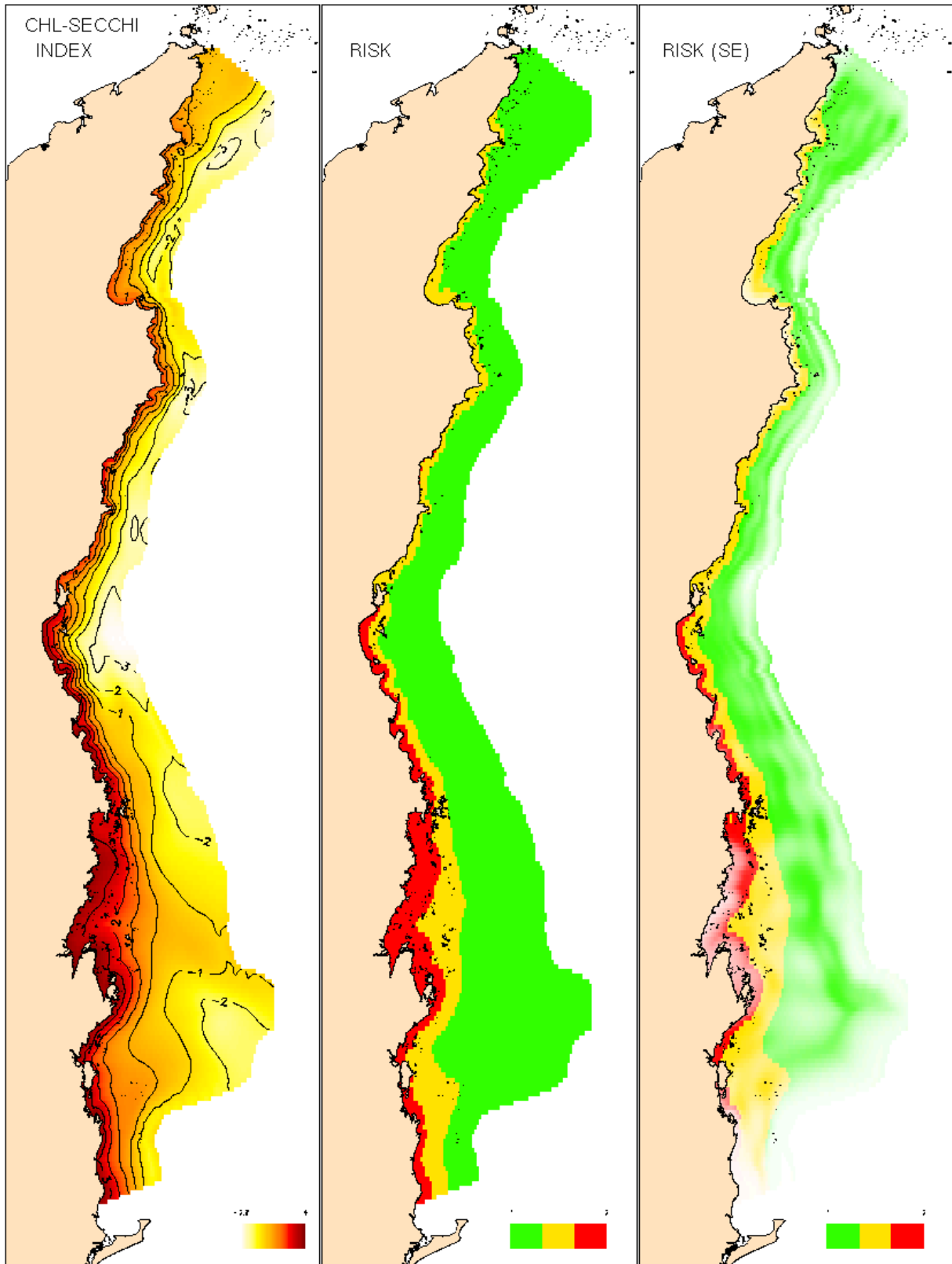


**Figure 30.** Risk for combined chlorophyll and water clarity (secchi) data. Scores for chlorophyll and secchi were predicted to the same coordinates, standardised, and differenced to give the combined index. The plots representation: the index, the 60:30:10 risk mapping, the risk map with error fading (pale=low precision).

## Summary

### Univariate Analysis

Three data sets were analysed: (1) lagoon water quality data comprising measures of 12 WQ parameters (1976-2006), (2) long-term chlorophyll monitoring data (1992-2006), and (3) a composite data set on water clarity based on secchi disks.

The principal findings were:

1. Concentrations of all WQ parameters decrease by 50-80% from the coast to 15-20% across the Reef. From 20% across to outer Reef they typically decrease by an additional 0-20%. This inner coastal strip should be the focus of future monitoring with fixed sites and automated logging of a few selected parameters; perhaps water clarity and chlorophyll. This cross-shelf pattern of strong decline in the near-shore varies along the coast for many WQ parameters, and is typically much steeper in the central third of the GBR and much flatter in the far north.
2. Synchronised cyclical seasonal variation occurs for most of the WQ parameters. Nutrients typically peak in March-April and are 10-50% lower in August-September. The seasonal variation must be accounted for in sampling programs.
3. Despite having collected extensive data on WQ for over 20 (12 WQ parameters) and 15 years (chlorophyll), we cannot make definitive statements about long-term trends in WQ on the GBR. For most of the dissolved WQ parameters the variation is such that further collection of such data should be reconsidered. The precision of the temporal trends is poorly estimated due to: (a) high variability of WQ between sampling trips and sampling locations, and (b) low precision and (likely) systematic bias of WQ measures.

### Multivariate Analysis

The correlation structure of the 12 WQ parameters its dependence on spatial and temporal variables showed that there is strong structure in the WQ data. It is dominated by a cluster of five WQ parameters (CHL, PHA, PP, PN and SS – the “solids”) and two weaker groupings (mainly dissolved). The solids vary most strongly with relative distance across the Reef, this being the best predictor of the correlation structure. The correlation structure varies systematically with the spatial and temporal covariates, but not greatly compared to the overall structure.

In terms of using composite indicators, these analyses suggest the “solids”, or a subset of them could be useful, but the concerns raised above need to be taken into account

### Mapping Risk

We have explored some potential indicators of risk and shown likely broadscale risk maps based on *relative risk* at levels of “high”, “moderate” and “low”. Regions of relative risk were mapped for the five indicators using the “60-30-10 rule” . Mapped values lower than the 60<sup>th</sup> percentile of the *observed* data are declared “low risk”, the 60<sup>th</sup>ile-90<sup>th</sup>ile are “moderate”, and >90<sup>th</sup>ile are high risk. The regions are coloured red, orange and green indicating high, moderate and low risk regions. Additionally the certainty of the predictions was displayed the colour saturation with strong shades indicating regions of low uncertainty, and pale shades indicating regions of high uncertainty.

Three potential indicators are based on the analysis of WQ structure and are strongly similar to each other. A striking feature is the narrow coastal band of high risk that extends from just

south of the Whitsunday Islands to Port Douglas in the North. The two other indicators were based on composite chlorophyll data and the water clarity. The chlorophyll risk map shows strong similarities to the first three indicators in that a narrow coastal band of high risk also extends from just south of the Whitsunday Islands to Port Douglas in the North, but it also shows high, though more uncertain risk, in the Pompeys. The water clarity maps again shows the coastal high risk strip, together with a moderate risk strip, but the high risk extends further north and south. In the case of the northern extension this can be explained as high sediments discharging from far northern rivers but containing lower level nutrients than the more southerly rivers.

This initial exercise in mapping risk shows great promise and can be further developed. There are many issues related to validation, temporal and spatial scales of the effectiveness, cost and ease of implementation, and new technologies, such as automated sensors and remote sensing that can perhaps gather the data necessary to assess risk more efficiently.

### **Risk Assessment and Management of the Great Barrier Reef**

The Marine Park Rezoning Plan determines access and activities for the whole of the GBRWHA and is fundamental to effective management. Risk maps can provide crucial information for management, but collaborative efforts between science and management are required in order to effectively use risk information in order to better manage the GBRWHA. There are (at least) three issues that require attention:

1. Geographical scale is the crucial factor; it varies over three orders of magnitude.
2. Classifying individual zones can be misleading due to their highly variable sizes.
3. Interactive visual quantitative methods, based on best science, need to be developed in conjunction with management agencies.

An example of combining risk maps based on scientific knowledge using chlorophyll and water clarity (secchi) data was presented. By determining and incorporating the functional relationship between risk factors and the environmental – biotic relationships, the risk maps can be greatly improved. Such work is in progress.

## References

- Bates, D. M. and Saikat, D. (2004) Linear mixed models and penalized least squares. *Journal of Multivariate Analysis* 91:1-17
- Breslow, N. E. and Clayton, G. D. (1993) Approximate inference in generalized linear mixed models. *Journal of the American Statistical Association* 88:9-25.
- Brodie, J, De'ath, G., Devlin, M., Furnas, M, and Wright M. (2007) Spatial and temporal patterns of near-surface chlorophyll *a* in the Great Barrier Reef lagoon. *Marine and Freshwater Research* 58:342-353.
- Fabricius K. E. and De'ath G. (2004). Identification of causes of change in complex ecosystems: Effects of terrestrial run-off on the coastal Great Barrier Reef. *Ecological Applications* 15(8):1448-1465.
- Goodall, C. R., (1991) Procrustes methods and the statistical analysis of shape (with discussion). *Journal of the Royal Statistical Soc. B* 53:285-340.
- Gower, J. C. (1975) Generalised Procrustes analysis. *Psychometrika* 40:33-50.
- R Development Core Team (2007) R: A language and environment for statistical computing. R Foundation for Statistical Computing, Vienna, Austria. ISBN 3-900051-07-0, URL <http://www.R-project.org>.
- Wood, S. N. (2003) Thin plate regression splines. *Journal of the Royal Statistical Soc. B* 67:95-114.
- Wood, S. N. (2004) Stable and efficient multiple smoothing parameter estimation for generalized additive models. *Journal of the American Statistical Association*. 99:673-686.

## Appendix One

Tensor splines (Wood 2003, 2004) are a widely used spatial smoothing technique that have the useful property that for a 2-D smooth the resulting fitted surface is invariant to a rigid rotation or translation of the axes. This is useful since we most often don't want the surface to depend on the orientation of the spatial axes. However, if we extend or shrink one axis relative to the other then the fitted surface and the degree of model fit (e.g.  $R^2$ ) can change quite dramatically.

We can take advantage of this property to include in the estimation process a parameter that represents the relative scaling of the two axes. The optimum value of this parameter will reflect the relative rate of change of the surface in the directions of the two axes.

In the example of Figure A1.1, a surface is fitted to bivariate Gaussian surface with 10% noise –

i.e.  $Z = 10 * \exp(X^2 + Y^2) + E$ , where  $E \sim N(0,1)$  and  $X$  and  $Y$  are also  $\sim N(0,1)$ .

Using a tensor spline smoother with 30 df (the left hand image), the fitted model shows the surface is recovered well ( $R^2 \sim 90\%$ ) and the error was also accurately estimated.

A simple rescaling of the  $X$  values by a factor of 10 (i.e.  $X_2 = 10 * X$ ) results in poor recovery of the surface ( $R^2 \sim 75\%$ ) and over-estimation of the error. The  $x$ -scale of change is clearly compressed to that of  $Y$  due to the rescaling.

In the context of using across-along coordinate systems we can take advantage of this characteristic of tensor splines, and choose the scaling to give the best fit and the magnitude of the rescaling should reflect the rate of change of the response across the Reef relative to along the Reef.

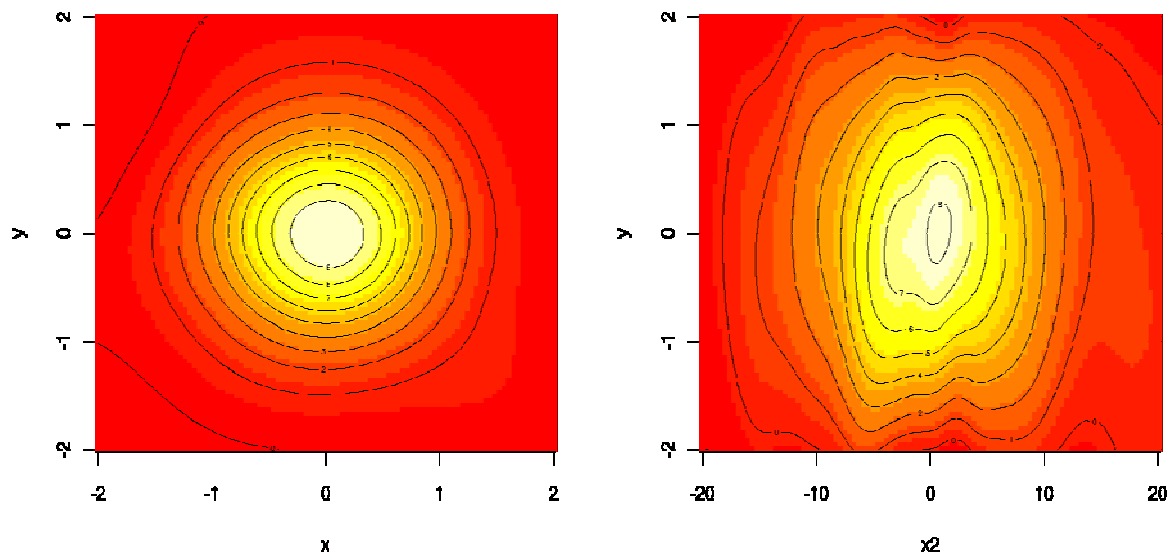


**Figure A1.1.** Demonstration of how a rescaling of one axis relative to the other can change the fitted surface and the degree of model fit (e.g.  $R^2$ ).

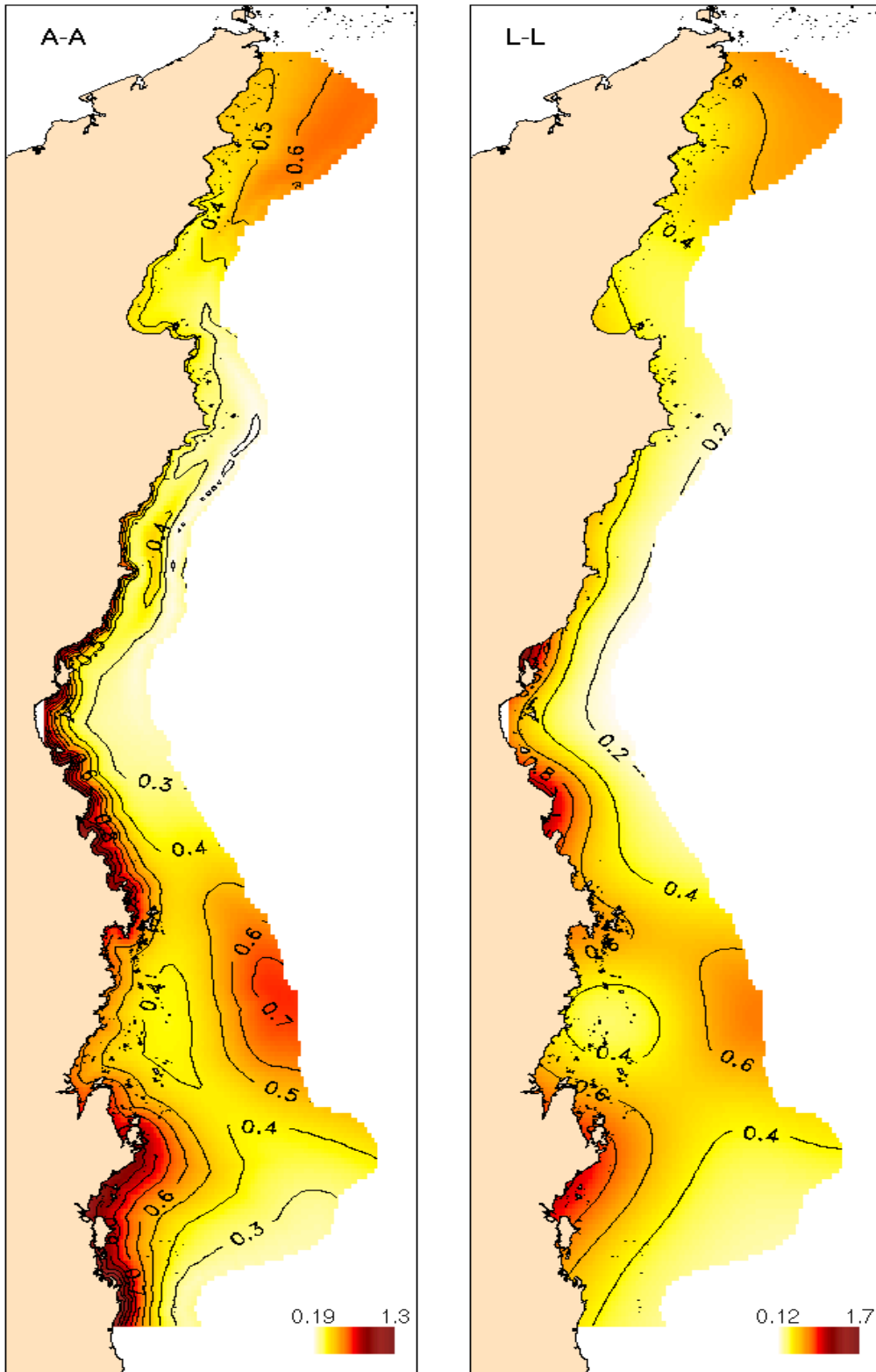


**Figure A.1.2.** Estimated spatial trends of chlorophyll based on across-along (A-A left) coordinates and latitude-longitude (L-L right). The contours of the A-A plot are more parallel to the coast when close to it. The A-A model had lower cross-validated error (75%) than L-L by 2.5%.

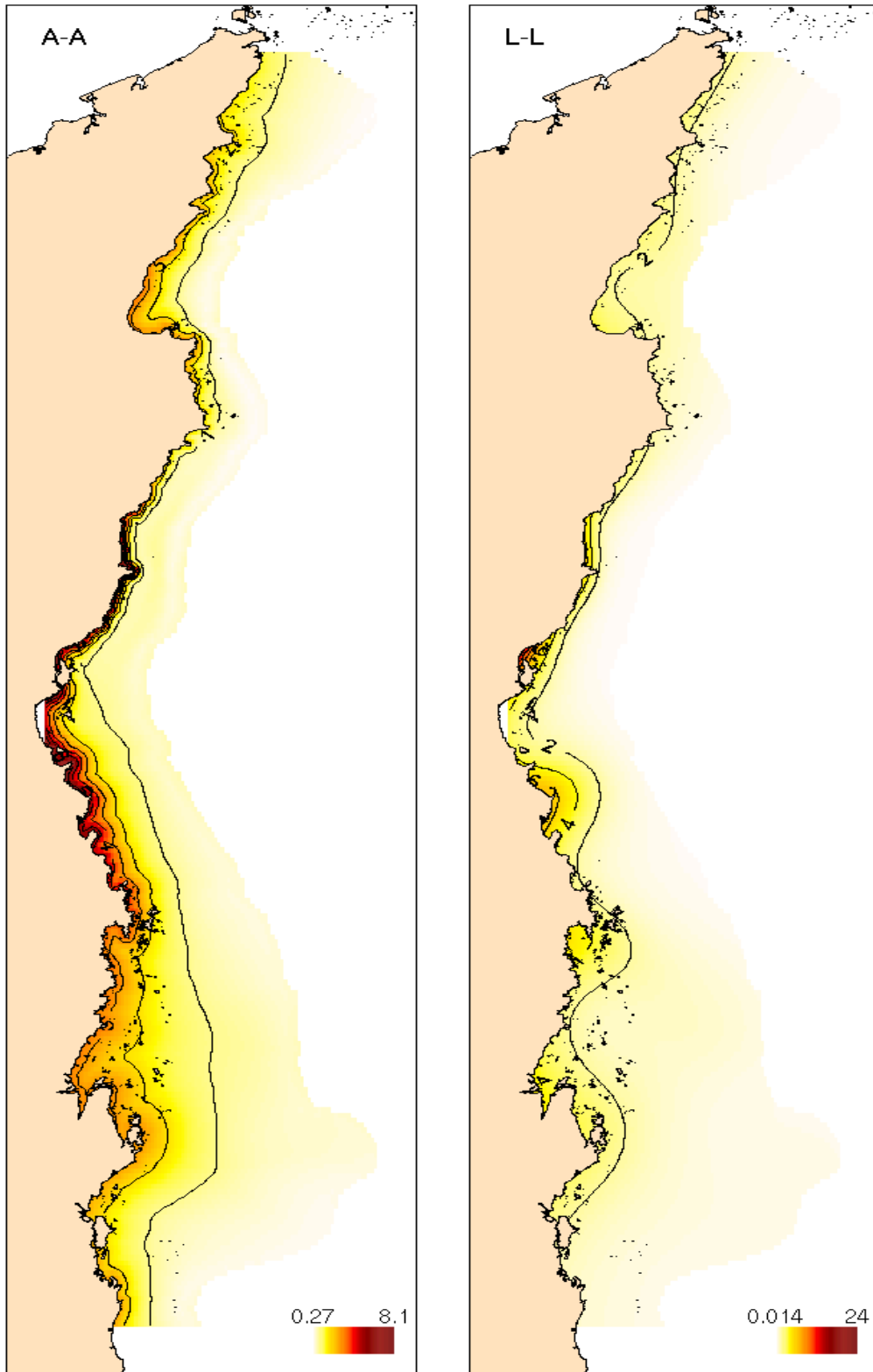


**Figure A.1.3.** Estimated spatial trends of suspended solids based on across-along (A-A left) coordinates and latitude-longitude (L-L right). The contours of the A-A plot are more parallel to the coast when close to it. The A-A model had lower cross-validated error (57.9%) than L-L by 3.4%.

R-code to illustrate the effect of axis rescaling on surface fit of thin plate splines.

```

# Generate the data

library(mgcv)
n <- 3
x <- rnorm(10^n)
y <- rnorm(10^n)
z <- 10*(exp(-(x*x+y*y))) + rnorm(10^n)
df <- data.frame(x,y,z)
ff <- gam(z~s(x,y),data=df)
print(summary(ff))
df.prd <- expand.grid(x=seq(-2,2,len=100),y=seq(-2,2,len=100))
zp <- predict(ff,newdata=df.prd)

# Scale the x-axis by a factor of 10

df$x2 <- 10*df$x
ff2 <- gam(z~s(x2,y),data=df)
print(summary(ff2))
df.prd2 <- expand.grid(x2=seq(-20,20,len=100),y=seq(-2,2,len=100))
zp2 <- predict(ff2,newdata=df.prd2)

# Plot results

x11(wid=18,hei=9)
par(mfrow=c(1,2),cex=1.75)
mzp <- matrix(zp,nrow=100)
image(x=seq(-2,2,len=100),y=seq(-2,2,len=100),mzp,xlab="x",ylab="y")
contour(x=seq(-2,2,len=100),y=seq(-2,2,len=100),mzp,add=T)
mzp2 <- matrix(zp2,nrow=100)
image(x=seq(-20,20,len=100),y=seq(-2,2,len=100),mzp2,xlab="x2",ylab="y")
contour(x=seq(-20,20,len=100),y=seq(-2,2,len=100),mzp2,add=T)

```

## Appendix Two

### *Spatial distributions of the WQ Parameters*

Plots of the spatial distributions of 12 WQ parameters. For each plot, the following information is shown across the three panels:

1. The locations of the site are shown and the size of the points are proportional to the mean value of the WQ parameter recorder at that site.
2. The estimated mean values of the specified WQ parameter.
3. The estimated standard error of the predictions shown in panel 2.

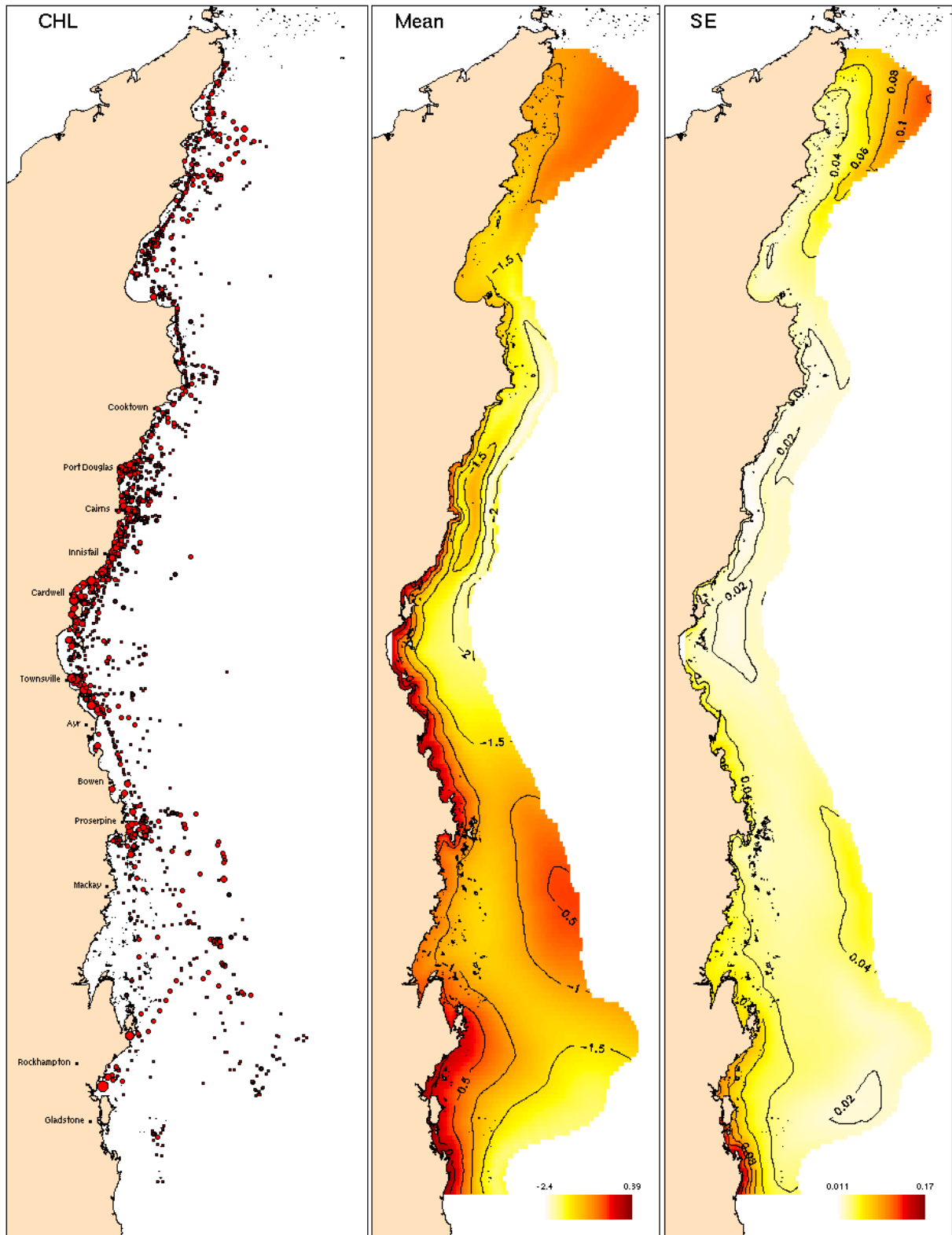


**Figure A2.1.** The three panels show (left to right): (1) the distribution of sites where chlorophyll was sampled. The dot sizes are proportional to the relative values of chlorophyll, (2) the spatially smoothed trend adjusted for temporal (month and year) effects, and (3) the precision (SE) of the smoothed surface.

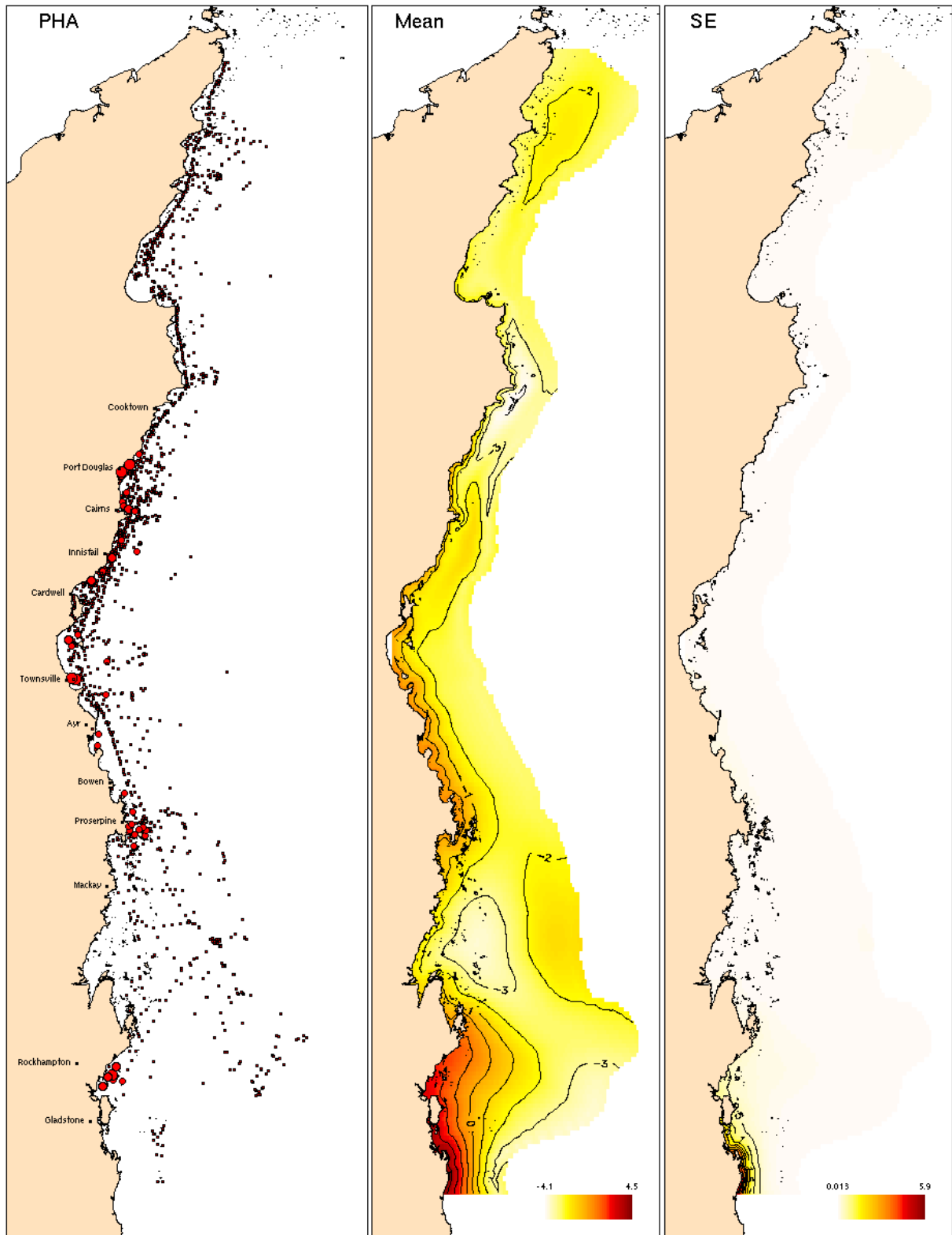


**Figure A2.2.** The three panels show (left to right): (1) the distribution of sites where phaeophytin was sampled. The dot sizes are proportional to the relative observed values, (2) the spatially smoothed trend adjusted for temporal (month and year) effects, and (3) the precision (SE) of the smoothed surface.

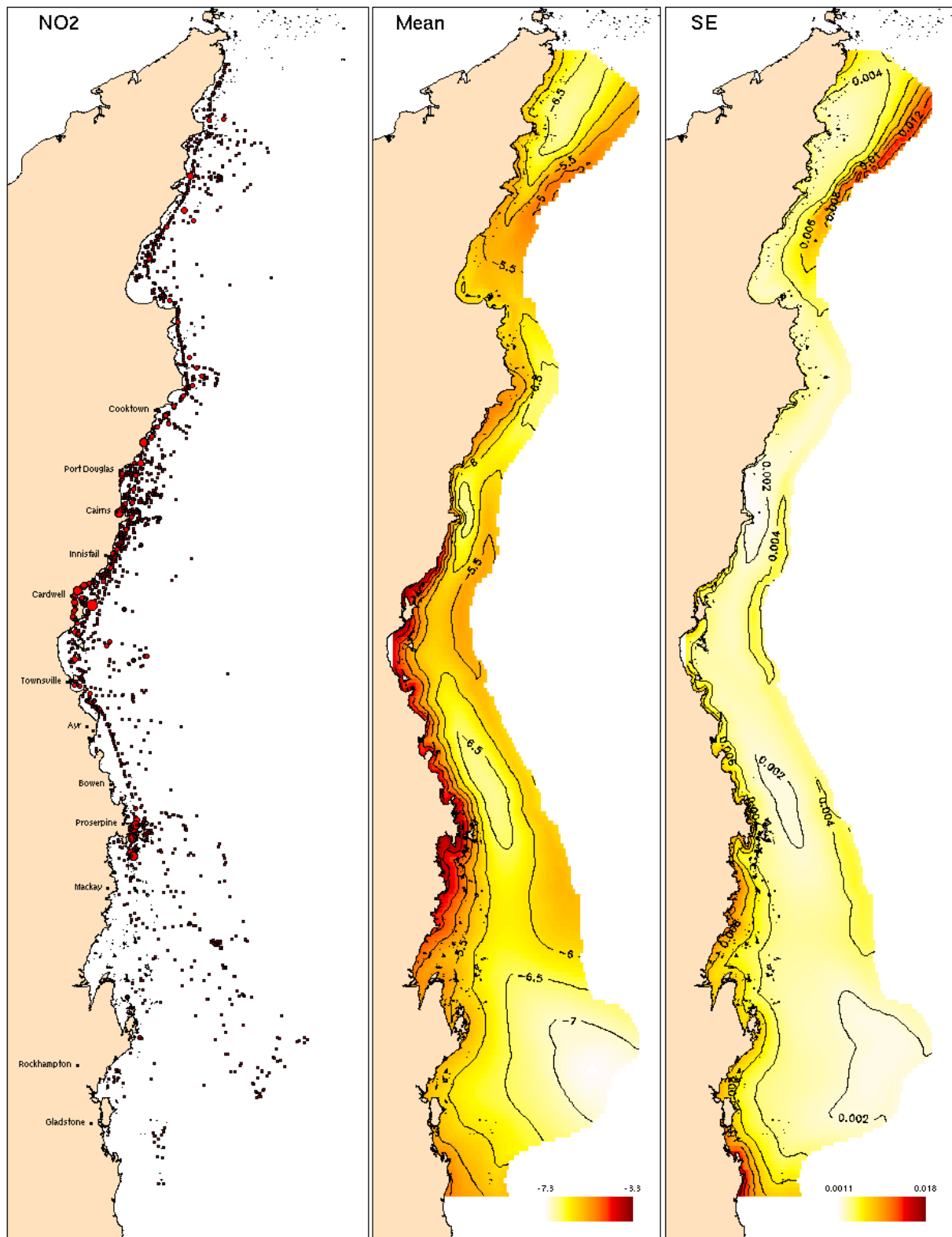


**Figure A2.3.** The three panels show (left to right): (1) the distribution of sites where nitrite was sampled. The dot sizes are proportional to the relative observed values, (2) the spatially smoothed trend adjusted for temporal (month and year) effects, and (3) the precision (SE) of the smoothed surface.

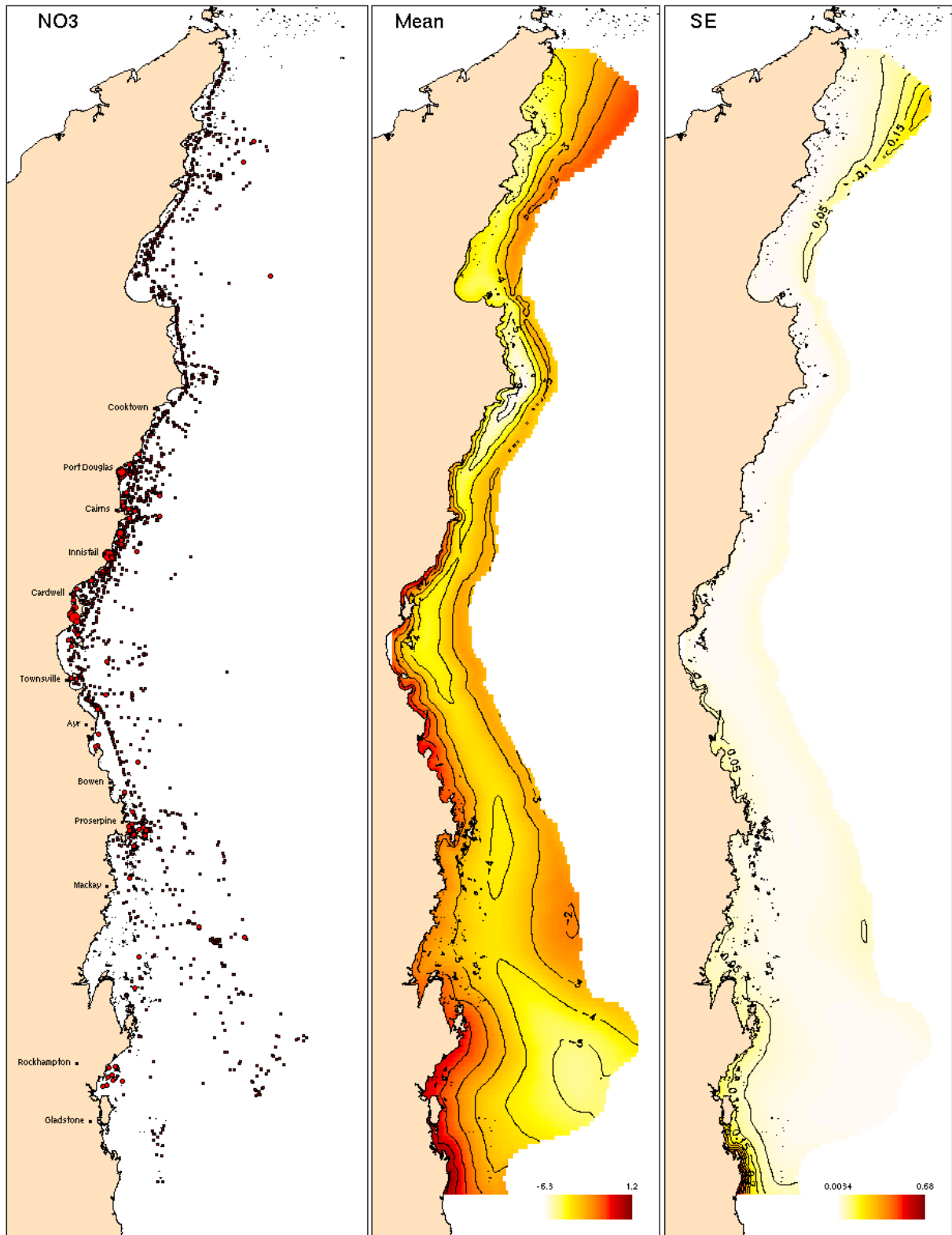


**Figure A2.4.** The three panels show (left to right): (1) the distribution of sites where nitrate was sampled. The dot sizes are proportional to the relative observed values, (2) the spatially smoothed trend adjusted for temporal (month and year) effects, and (3) the precision (SE) of the smoothed surface.

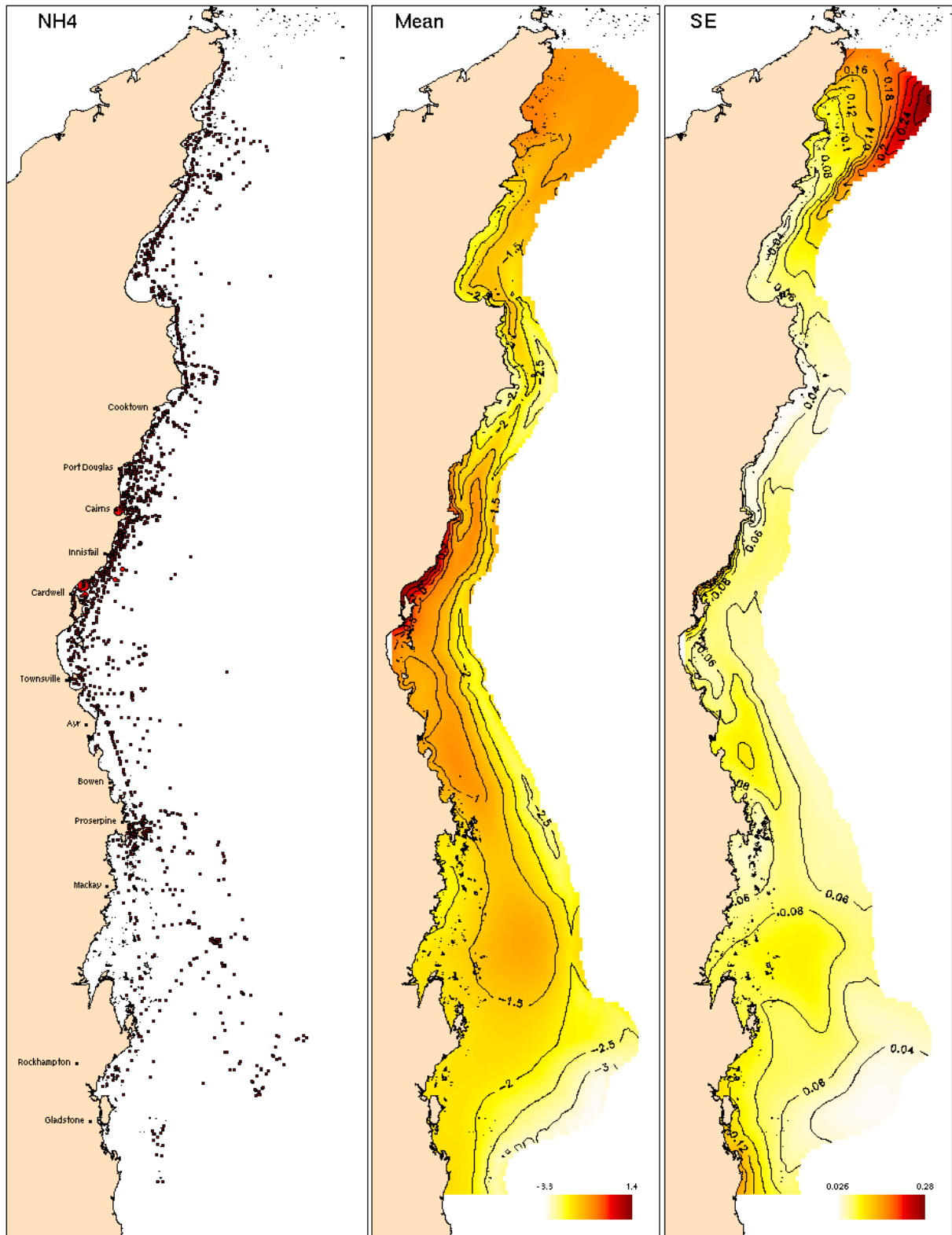


**Figure A2.5.** The three panels show (left to right): (1) the distribution of sites where ammonia was sampled. The dot sizes are proportional to the relative observed values, (2) the spatially smoothed trend adjusted for temporal (month and year) effects, and (3) the precision (SE) of the smoothed surface.

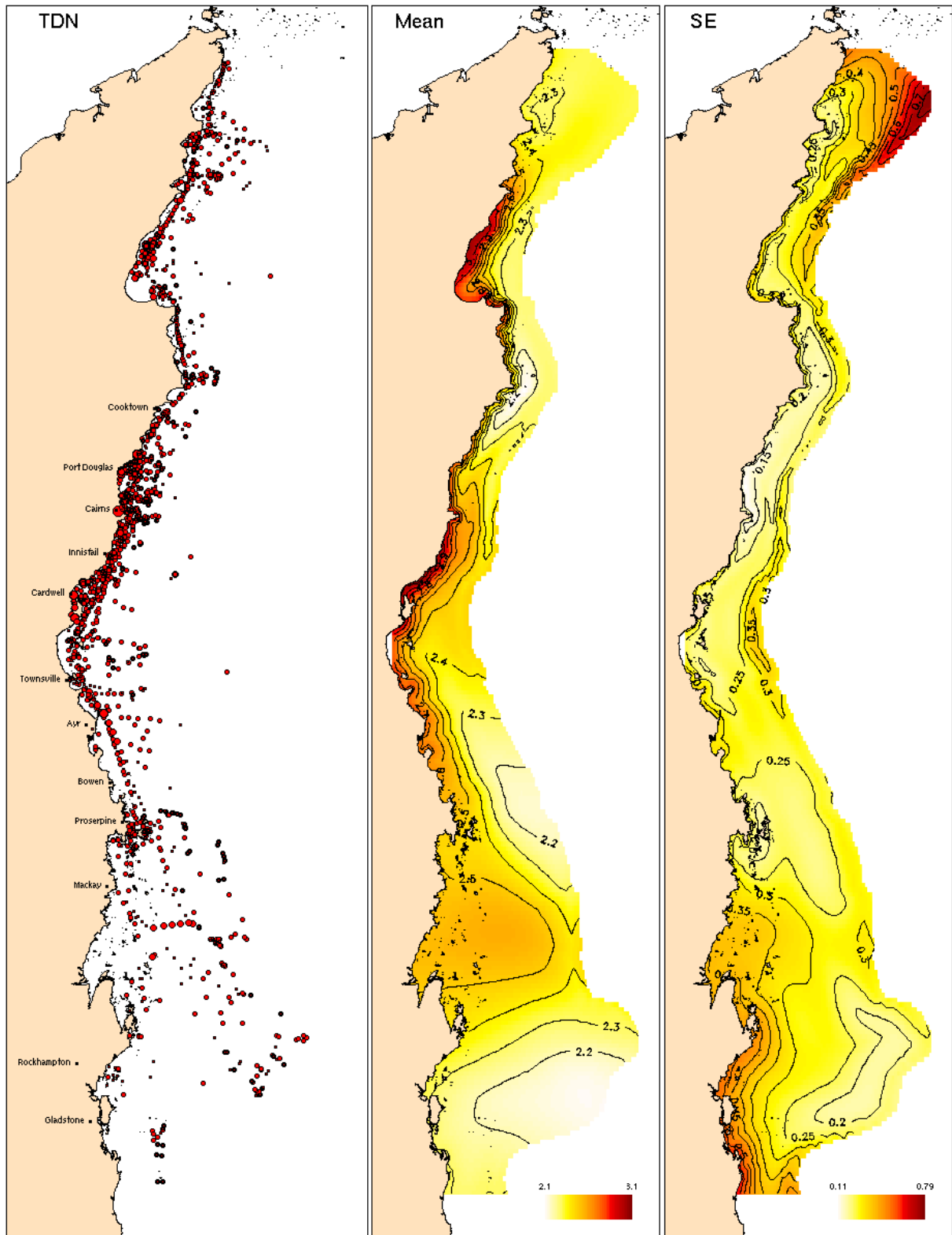


**Figure A2.6.** The three panels show (left to right): (1) the distribution of sites where total dissolved nitrogen was sampled. The dot sizes are proportional to the relative observed values, (2) the spatially smoothed trend adjusted for temporal (month and year) effects, and (3) the precision (SE) of the smoothed surface.

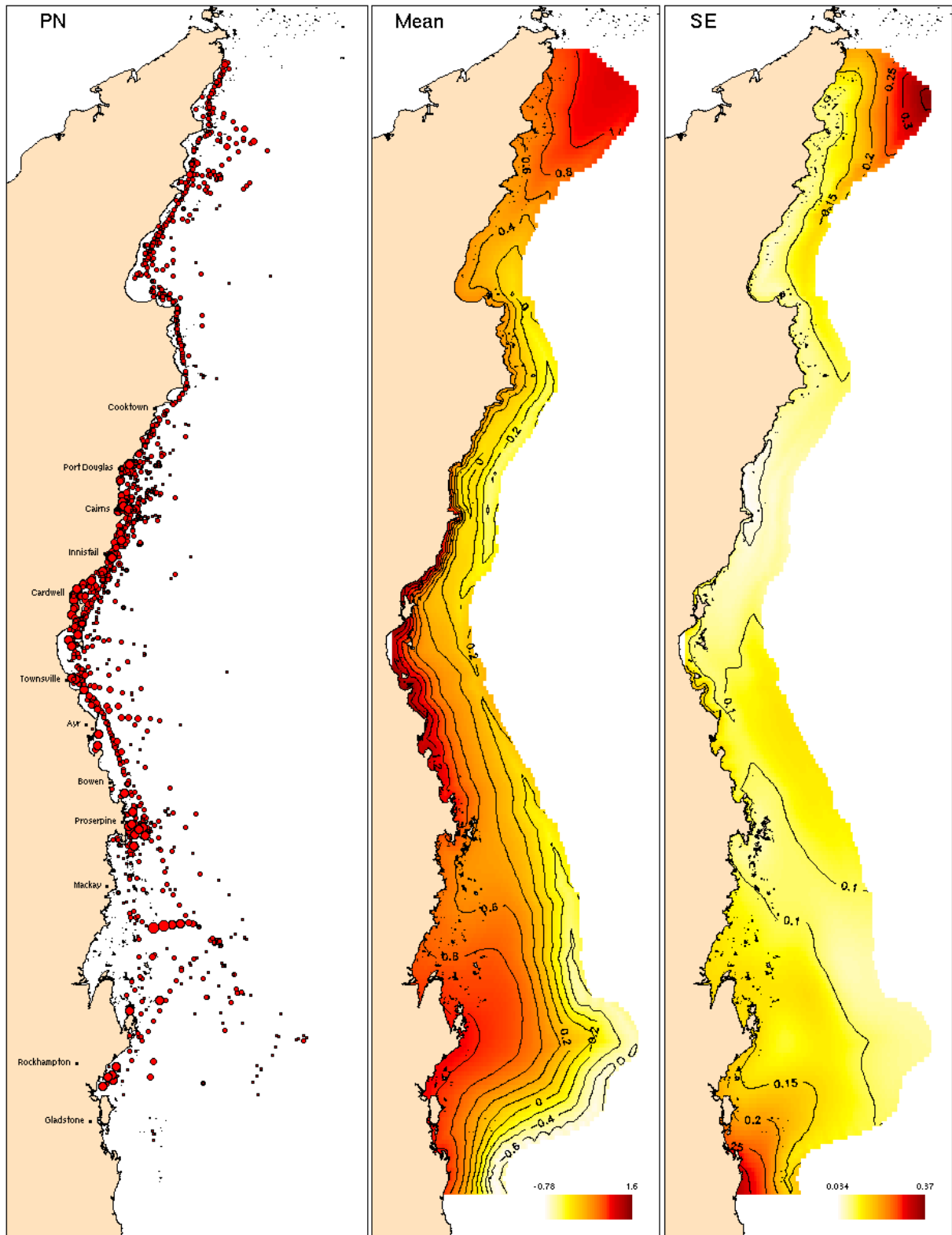


**Figure A2.7.** The three panels show (left to right): (1) the distribution of sites where particulate nitrate was sampled. The dot sizes are proportional to the relative observed values, (2) the spatially smoothed trend adjusted for temporal (month and year) effects, and (3) the precision (SE) of the smoothed surface.

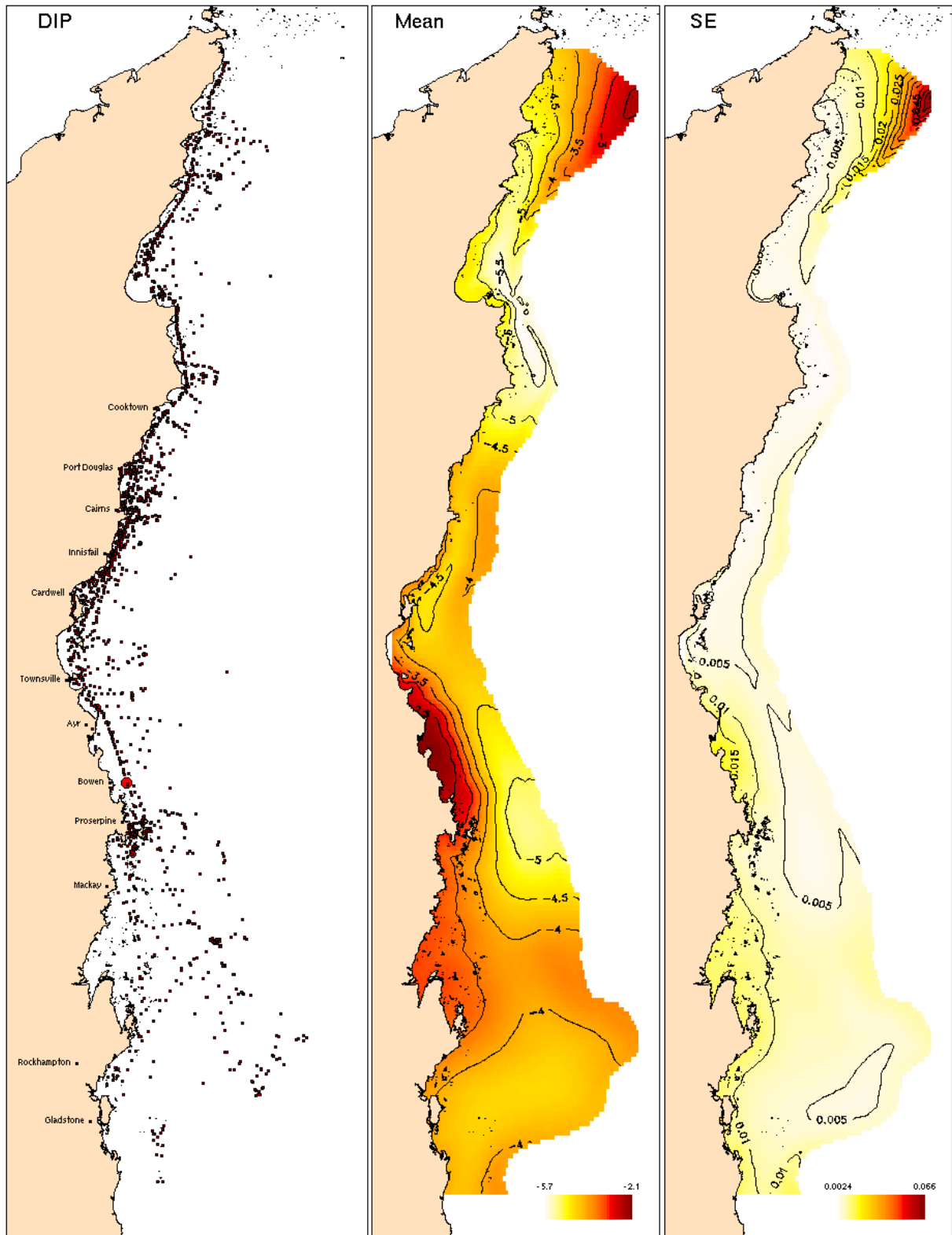


**Figure A2.8.** The three panels show (left to right): (1) the distribution of sites where dissolve inorganic phosphorous was sampled. The dot sizes are proportional to the relative observed values, (2) the spatially smoothed trend adjusted for temporal (month and year) effects, and (3) the precision (SE) of the smoothed surface.

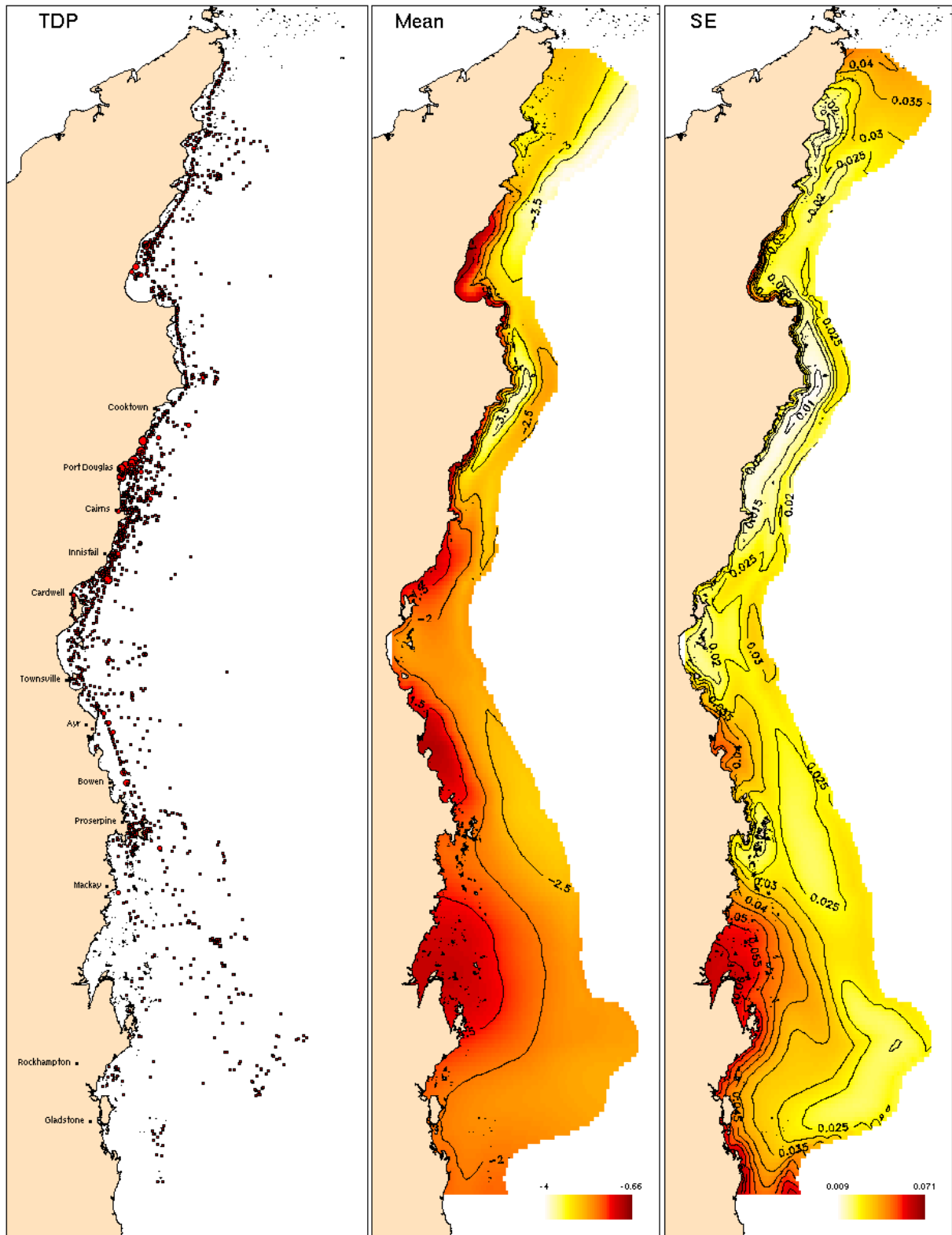


**Figure A2.9.** The three panels show (left to right): (1) the distribution of sites where total dissolved phosphorous was sampled. The dot sizes are proportional to the relative observed values, (2) the spatially smoothed trend adjusted for temporal (month and year) effects, and (3) the precision (SE) of the smoothed surface.

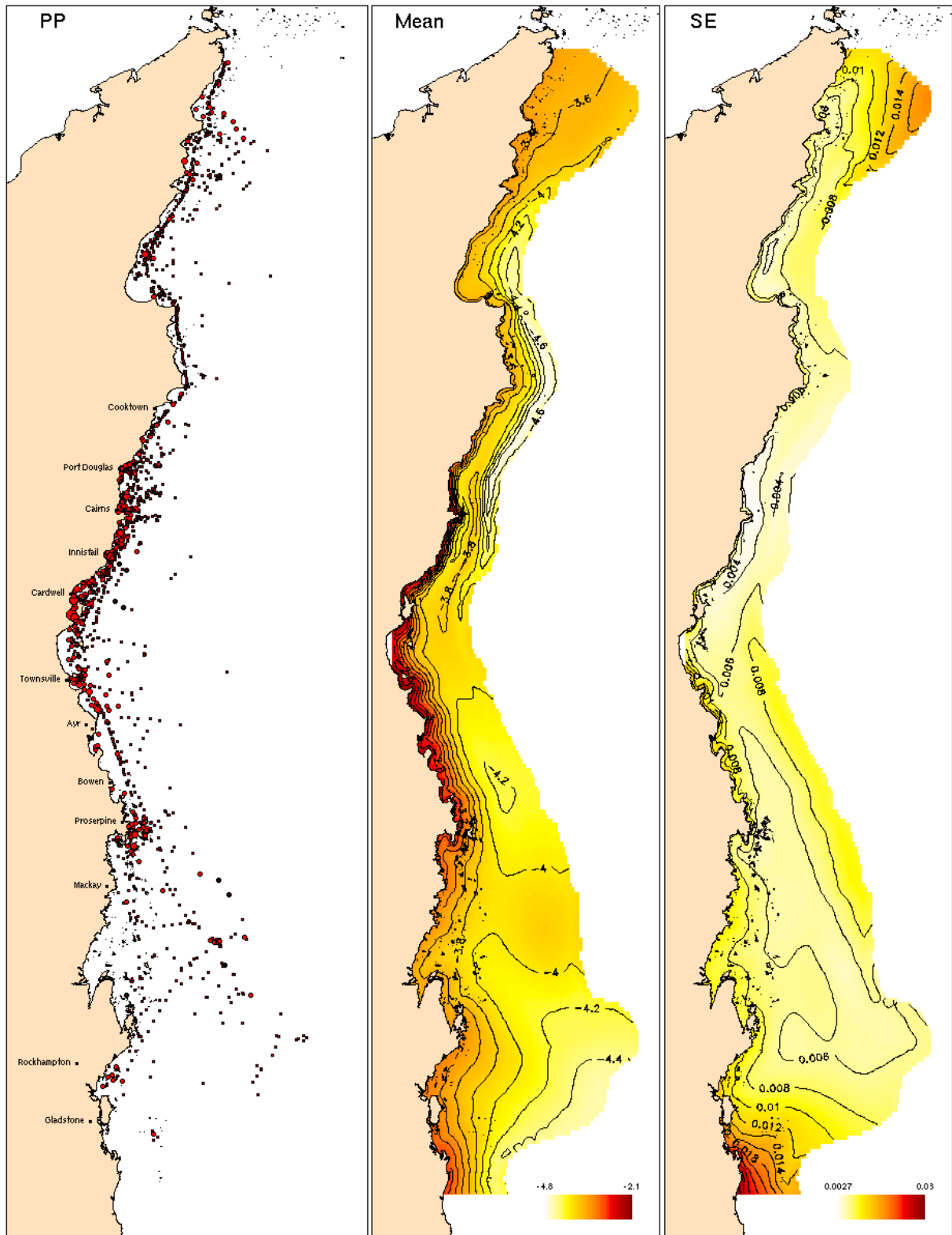


**Figure A2.10.** The three panels show (left to right): (1) the distribution of sites where particulate phosphorous was sampled. The dot sizes are proportional to the relative observed values, (2) the spatially smoothed trend adjusted for temporal (month and year) effects, and (3) the precision (SE) of the smoothed surface.

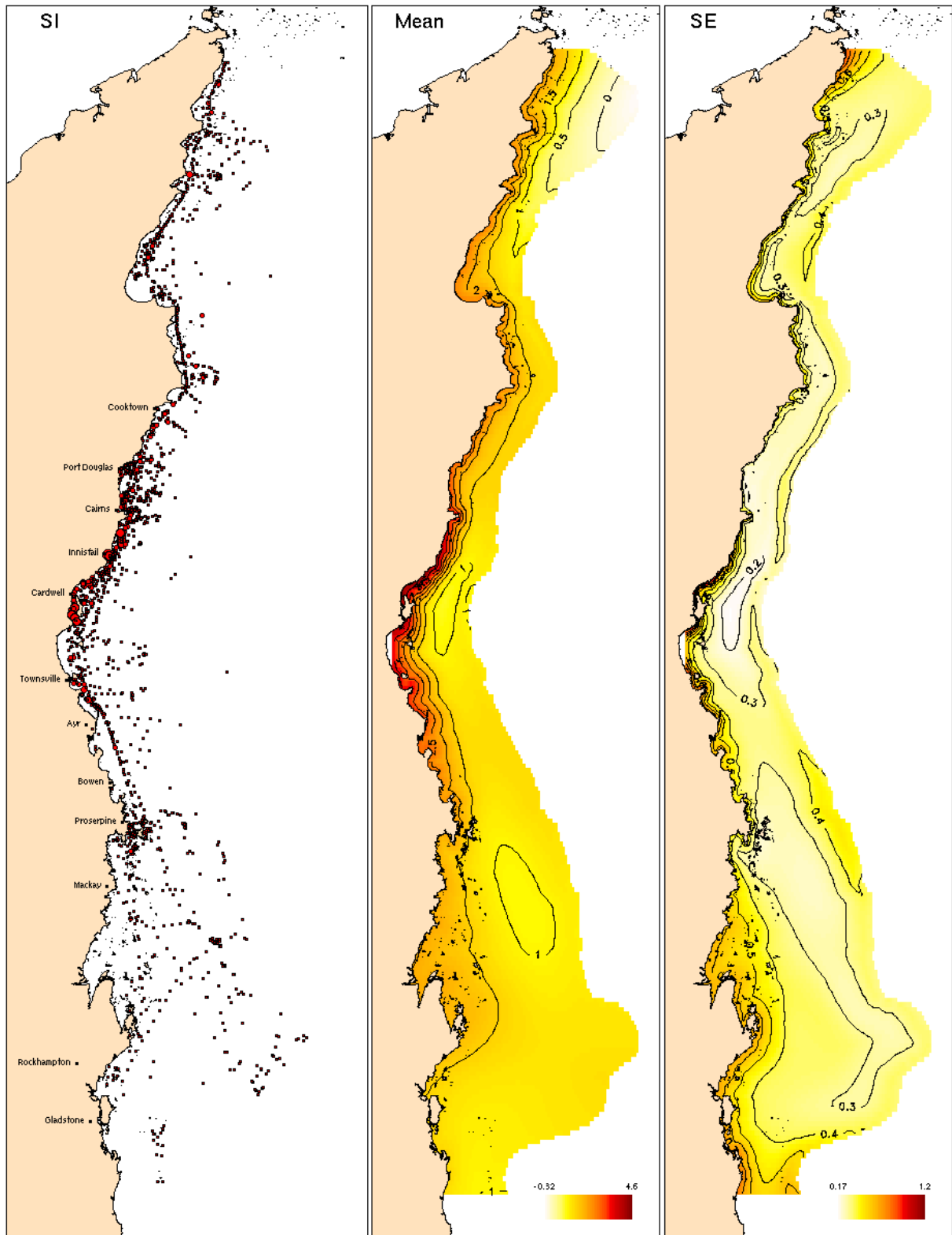


**Figure A2.11.** The three panels show (left to right): (1) the distribution of sites where silicate was sampled. The dot sizes are proportional to the relative observed values, (2) the spatially smoothed trend adjusted for temporal (month and year) effects, and (3) the precision (SE) of the smoothed surface.

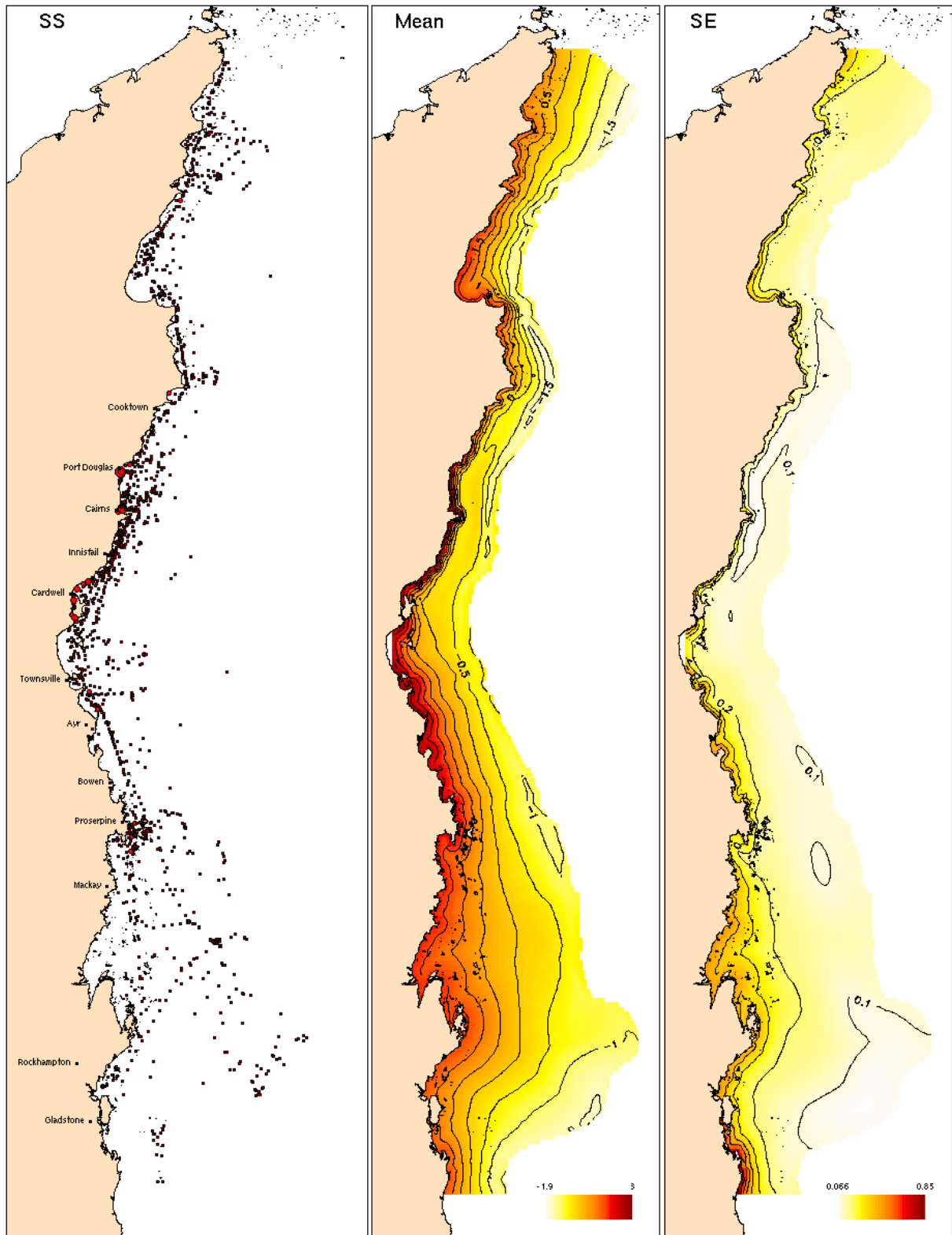


**Figure A2.12.** The three panels show (left to right): (1) the distribution of sites where suspended solids was sampled. The dot sizes are proportional to the relative observed values, (2) the spatially smoothed trend adjusted for temporal (month and year) effects, and (3) the precision (SE) of the smoothed surface.